1-1-1987

Photooxidation of polystyrene/

Paul C. Lucas
University of Massachusetts Amherst

PHOTOOXIDATION OF POLYSTYRENE

A Dissertation Presented

By

Paul C. Lucas

Submitted to the Graduate School of the
University of Massachusetts in partial fulfillment
of the requirements for the degree of

DOCTOR OF PHILOSOPHY

February, 1987

Polymer Science and Engineering

PHOTOOXIDATION OF POLYSTYRENE

A Dissertation Presented

By

Paul C. Lucas

Approved as to style and content by:

Roger S. Porter, Chairman of Committee

Shaw Ling Hsu, Member

James C.W. Chien, Member

Edwin L. Thomas, Department Head
Polymer Science and Engineering

ACKNOWLEDGEMENTS

I would like to thank my advisor, Prof. Roger Porter, for both the freedom and support he has given me during the course of this project. I would also like to thank my dissertation committee, Prof. Shaw Hsu and Prof. James Chien, for their help and cooperation in completing this work. The many helpful comments and suggestions of Dr. Edward Otocka are also greatly appreciated.

I would like to thank the Center for UMass-Industry Research on Polymers (CUMIRP) for the generous financial support of this project.

A special thanks is offered to William Dickstein for his friendship and for preparing the deuterated polystyrene used in this study. The efforts of Dr. Charles Dickinson and Jerry Parmer in the use of NMR are also greatly appreciated.

A warm and heart-felt thanks is offered to my wife, Sue, for her love and patience, and for her efforts in preparing this manuscript.

Finally, I would like to recognize God for His faithfulness in making this and far greater things possible.

Romans 3:21-28 John 1:11-14

ABSTRACT

Photooxidation of Polystyrene

February 1987

Paul C. Lucas, B.S., University of Massachusetts

M.S., SUNY/College ESF, Ph.D., University of Massachusetts

Directed by: Professor Roger S. Porter .

Much disagreement is found in the literature regarding the mechanism of polystyrene (PS) photooxidation. This is due, in large part, to the difficulties in characterizing the reaction products. In the present study, the products of PS photooxidation have been characterized, primarily using Fourier-transform infrared spectroscopy (FTIR). Both absorbance and reflectance (ATR) techniques were employed. Infrared band assignments have been made on the basis of absorption frequency and the changes in the spectrum caused by exposing the film to reactive vapors.

As PS films were photooxidized in air with 254nm UV, several types of functional groups were produced. Free and H-bonded hydroperoxides were detected, along with carboxylic acids and simple ketones. Other carbonyl-containing products include a low molecular weight compound (perhaps a perester), a structure that undergoes ammoniolysis and a minor component that reacts with methyl amine (perhaps an aldehyde). A weak absorption band was

detected at a frequency appropriate for trisubstituted olefins. The use of chain deuterated PS showed that the hydroperoxides detected had formed by reaction of the phenyl ring.

The 254nm UV is strongly absorbed by PS. The ATR technique has shown that the degradation products are distributed along a concentration profile that is consistent with the UV absorption profile. At high UV dosages, a highly oxidized surface layer is formed. This highly oxidized layer is more photostable than the original PS and acts as a protective layer, preventing further photooxidation.

A preliminary investigation was made to see if these results could apply to solar region (300 to 400nm UV) photooxidation of PS containing sensitizers. Photooxidized PS containing acetophenone produced IR bands similar to those described above. Likewise, chain deuterated PS plus trideuteroacetophenone showed that the phenyl ring also reacts in solar region photooxidation. It can be concluded from these results and those obtained using 254nm UV that reaction mechanisms in the literature that include phenyl ring reactions should be given further consideration. These mechanisms have been cited and discussed in this work.

TABLE OF CONTENTS

LIST OF TABLES

LIST OF FIGURES

Figure

Figure

C H A P T E R I

PHOTOOXIDATION OF POLYSTYRENE: REVIEW OF LITERATURE

Introduction

Polystyrene is rapidly oxidized by ultraviolet light in the presence of oxygen, and this process has been the subject of many investigations. Considerable progress has been made toward understanding the complex processes that occur, both in terms of understanding the mechanism of photooxidation and the effects that various environmental factors have on these reactions. The photooxidation reactions are a complicated series of photochemical and photophysical processes which depend on the chemistry of the polymer (including any impurities), along with the environmental parameters such as temperature, atmospheric composition and UV radiation wavelength.

Since the initiation mechanism for the photooxidation process depends strongly on the wavelength of the UV radiation, the following discussion is divided into two sections according to the wavelength being considered. In the first section, shorter wavelengths of UV are discussed and this generally centers on 254nm UV. This radiation can be absorbed directly by any of the normal polymer repeat units. In the second section, longer wavelengths are

considered, and these are generally longer than 300nm. These wavelengths correspond to the region of the UV spectrum that reaches the earth's surface from the sun. This solar radiation is not absorbed directly by the polystyrene repeat unit, and it is therefore considered separately.

Photooxidation at 254nm

Initiation

The mechanism of photooxidation of polystyrene (PS) with 254nm UV has been extensively investigated at early stages of exposure. The initial reaction of highly purified PS is generally agreed to be absorption of light by the phenyl group, followed by energy transfer to and the subsequent scission of the tertiary C-H bond. This reaction occurs fairly slowly, with photophysical energy dissipation being more likely. This mechanism has been deduced from the vacuum photolysis of PS during which crosslinking was observed (1), along with the production of molecular hydrogen (2,3) and the development of an ESR spectrum felt to be consistent with that of a benzylic radical (4,23) (Fig. 1.1). The high absorptivity of polystyrene at 254nm causes this reaction to take place on the surface of the polymer film, with about 99% of the radiation being

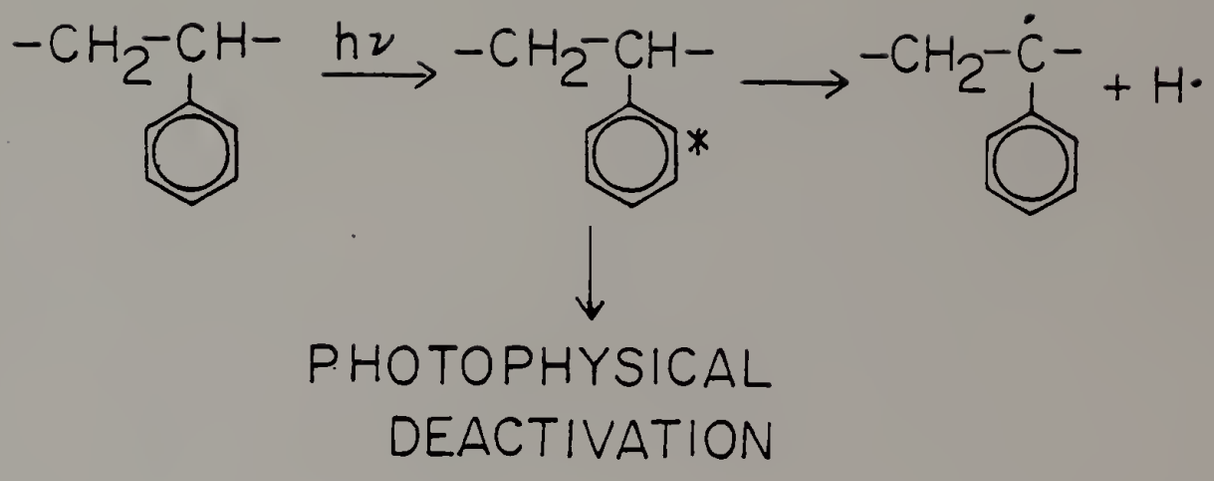

Figure 1.1

Primary photolysis process of PS with 254nm UV.

absorbed in the top 10 micrometers (58).

In the presence of oxygen, the macroradical quickly adds oxygen to form a peroxy radical, which abstracts a hydrogen atom from the surrounding polymer to form a hydroperoxide (Fig. 1.2). Polystyrene fluorescence is dominated by phenyl ring excimers (22) but as the hydroperoxide concentration increases, fluorescence intensity reportedly decreases (2) as energy is transferred to the hydroperoxide where scission occurs. The products of this scission reaction are thought to be a terminal aromatic ketone, analogous to acetophenone, water and a terminal unsaturation (5,6,7) (Fig. 1.3).

The existence of this ketone is supported by infrared absorption at about 1685cm^{-1} where acetophenone absorbs (8,9). It has been suggested that these chain end groups (aromatic ketone and terminal vinyl) may continue to photooxidize to diones and dienes (6). The broad carbonyl absorption in the 1720 to 1780cm^{-1} region has been attributed to a variety of aliphatic ketones, aldehydes, acids, peracids, and peresters (10,11,17). The assignment of IR bands to functional groups has generally been done by a comparison between the spectra of the photooxidized polymer and either low molecular weight analogs or the photooxidation products of low M.W. analogs. The IR band at 3540cm^{-1} for PS irradiated in air has been assigned by

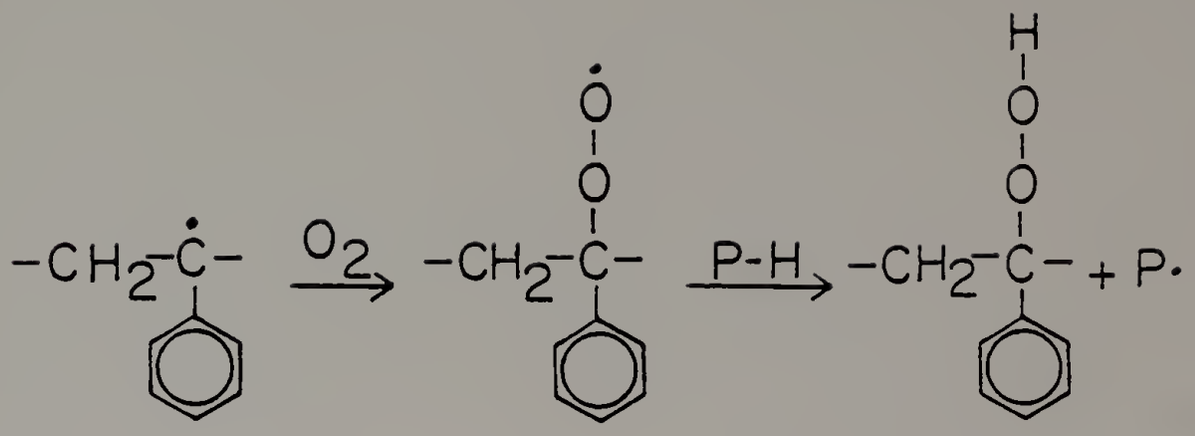

Figure 1.2

Hydroperoxide formation from the tertiary radical.

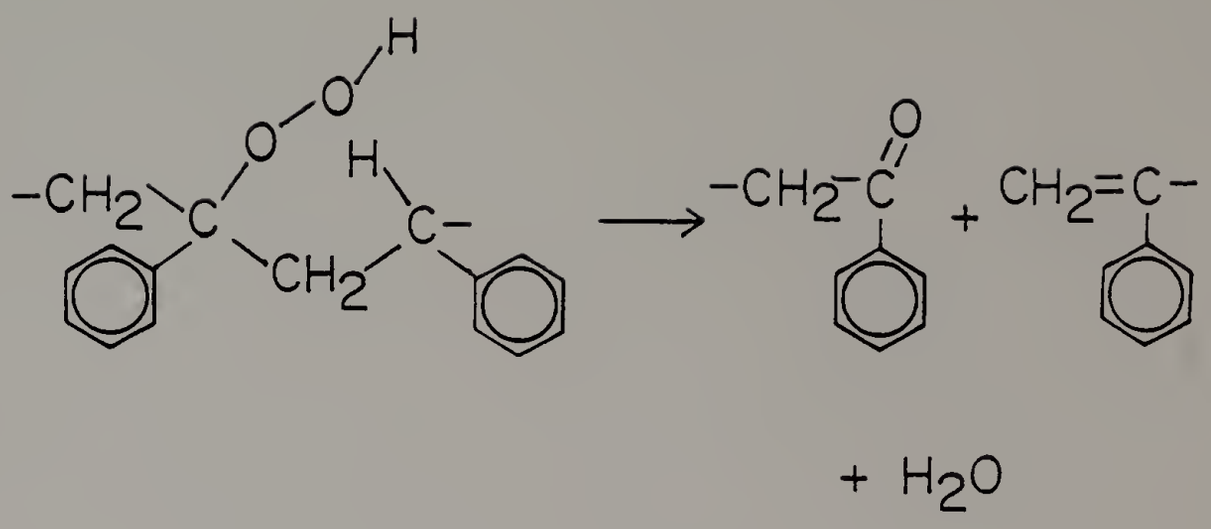

Figure 1.3

Hydroperoxide decomposition leading to chain scission with the formation of acetophenone- and terminal olefin- endgroups.

heating the photooxidized polymer to 120°C, which reduced in peak intensity, indicating that the peak corresponded to a hydroperoxide structure (4). This same study reported that such heating at 120°C did not affect the carbonyl band, suggesting that peracids, and presumably peresters, are not extensively formed. Evidence used to support the idea of perester formation was obtained by the photolysis of previously photooxidized (in 600 torr O_2) polystyrene, where CO_2 was evolved and the 1760cm^{-1} band became weaker (10). The mechanism proposed for the production of peresters and their photolytic decomposition is based on a Norrish type-I scission, followed by the addition of oxygen and a cage recombination (Fig. 1.4). The elimination of CO_2 from peresters proceeds quantitatively, according to information cited by the authors.

It should be noted that the proposed reaction in Figure 1.4 begins with an aliphatic ketone. The production of such ketones can only occur if hydrogen abstraction occurs from the parent methylene group in the original repeat unit. This leads to the formation of a secondary radical, which should not be favored on the basis of C-H bond reactivities. An explanation of these structures has been suggested in statements made concerning the reactivity of C-H bonds along the chain (19), where it is suggested that reactivity is determined more by proximity with the

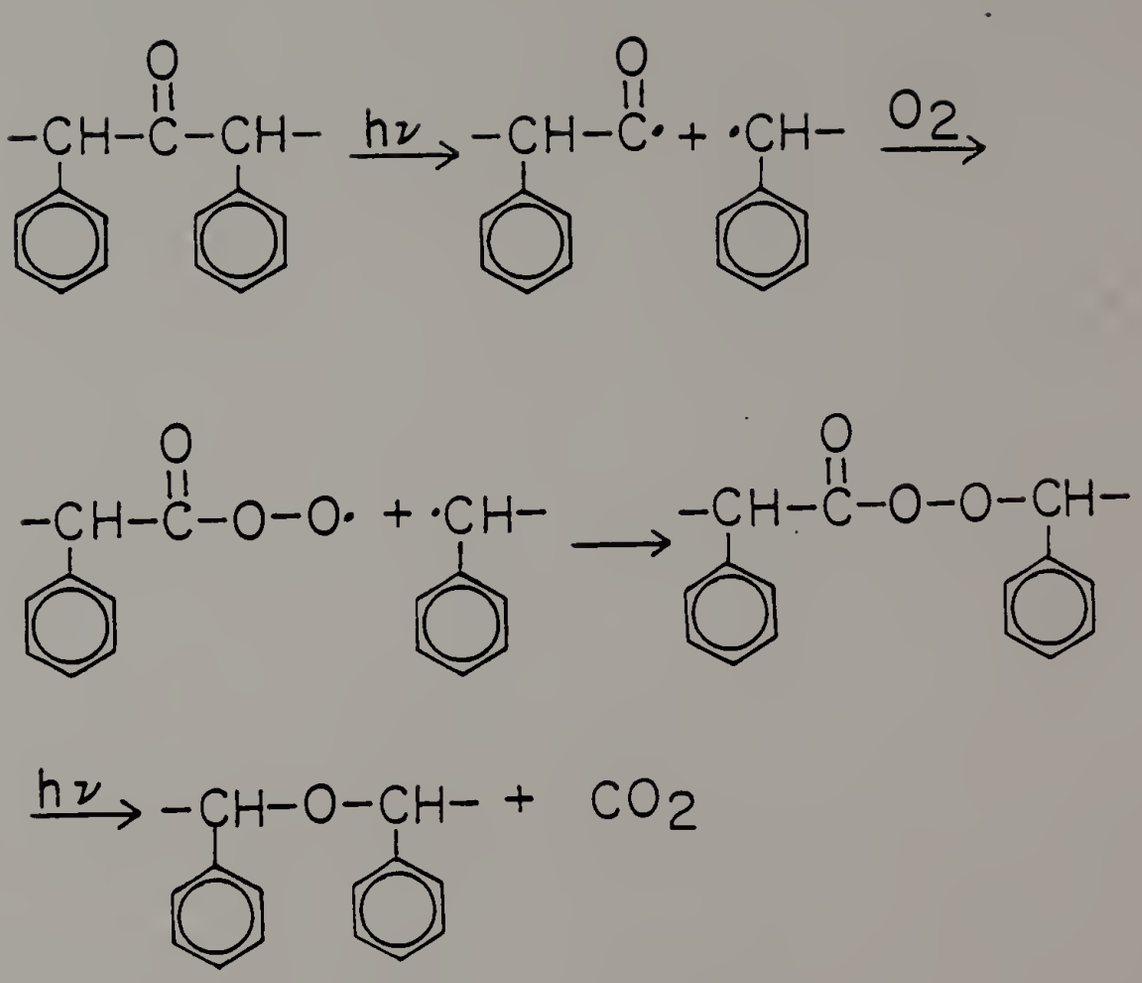

Figure 1.4

Perester formation and its subsequent photolysis in the polymer backbone.

glassy "cage" rather than on the basis of C-H bond strength. These authors thereby account for the formation of secondary radicals which they feel lead to the formation of such aliphatic ketones. Thus reactions within a glassy matrix may proceed by mechanisms that would not be expected from the knowledge of chemical reactivity learned from liquid solution chemistry.

It should be noted that there is disagreement in the evidence discussed in the above paragraphs over the formation of peracids and peresters. In one case these products are not thought to be present since heating the photooxidized polymer did not change the carbonyl band shape (4), while in the other case photolysis of previously photooxidized PS produced CO_2 and the 1760cm^{-1} band became weaker. Perhaps exposure at different oxygen pressures contributed to these contradictory results, although this may be indicating that decarboxylation is not a thermally activated process, but proceeds much more readily photochemically.

Color Formation

After prolonged photooxidation, polystyrene becomes yellow in color. The chemical structures that produce the yellow color are not known with certainty, and, in fact, at least two very different mechanisms of color formation have

been proposed. According to one mechanism, yellowing results from the formation of conjugated sequences of double bonds in the polymer backbone. The vacuum photolysis of PS has reportedly led to the formation of yellow coloration as quickly as did photooxidation, as judged by changes in absorbance at 440nm (5). Other studies support the idea that conjugated double bonds lead to yellowing, although yellowing occurred more quickly in the presence of oxygen (6,7). Evidence for the existence of these conjugated polyene structures is from ultraviolet absorption and fluorescence spectra.

Yellowing has also been explained in terms of reactions involving the phenyl rings on the polymer. Using 2-phenylbutane as a model compound, photooxidation produced a variety of dialdehydes, diketones, lactones, etc., which included some very yellow compounds (12). These products were the result of ring opening reactions occurring on the phenyl group. The photoisomerization of benzene to fulvene, along with other compounds, is cited to account for the yellowing observed during vacuum photolysis (Fig. 1.5). The photooxidative ring opening of benzene is well known (13), and has also been proposed by other workers to account for the behavior of polystyrene during photooxidation (14,15). Certainly such an explanation of yellowing in PS would explain why the polymer turns yellow but fails to turn red

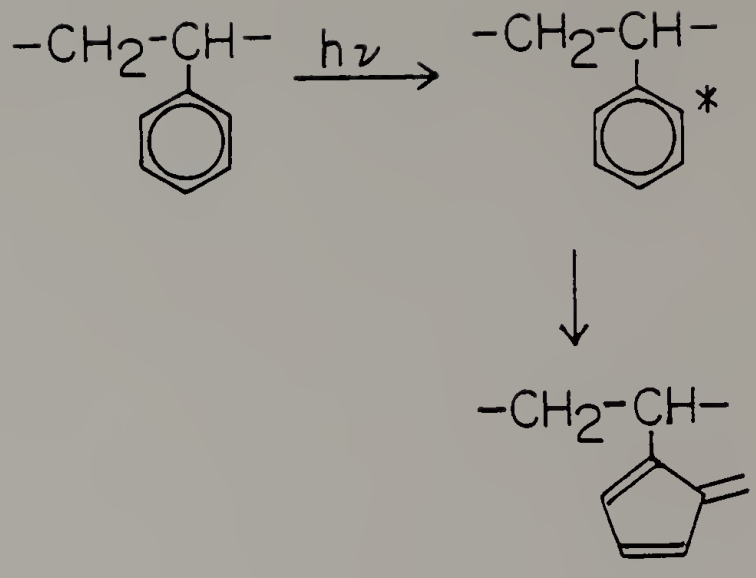

Figure 1.5

Photoisomerization of the phenyl group to fulvene, which is yellow in color.

at long exposure times. Whereas PVC produces long sequences of conjugation on photooxidation, such extensive conjugation causes absorption to move farther into the visible region with exposure and the polymer becomes yellow, and then red, and finally black. Yellow-colored products in PS could increase in concentration, causing the yellow color to become more intense, but without leading to the development of red or black coloring.

The reason for the lack of red coloring in PS given by some proponents of the conjugation theory of yellowing is the lack of chain mobility and flexibility within the glassy matrix (5), with these steric restrictions preventing extensive pi-bond overlap. Heating the photolyzed polymer above Tg leads to a rapid darkening, and this is explained in terms of pi-bond coplanarity becoming possible as chain mobility increases. These authors suggest that three conjugated double bonds along a PS chain should move the absorption into the visible range. This has been criticized by the proponents of the fulvene/ring-opening chromophores (12) who cited work showing that as many as eight double bonds needed to be conjugated in order to move absorptions into the visible region. The work cited (16), however, was based on linear hydrocarbons not possessing phenyl pendant groups, and this should be a contributing factor. Oligomers of phenyl acetylene having an average

degree of polymerization of five are yellow-orange (20), but these materials were not fractionated, and may contain some higher molecular weight components. Terminal diphenyl polyenes reportedly absorb in the blue region when they contain four conjugated double bonds (24).

Ring-Opening Reactions

The importance of ring-opening reactions during polystyrene photooxidation is not universally accepted. Evidence that supports this idea that these reactions occur in polystyrene includes model compound studies (11), a decrease in the aromatic carbon content at the polymer surface as detected by ESCA (15) and the observation that more CO_2 was produced than could be accounted for if ring opening did not occur (14). Presumably the small amounts of phenol (14), acetophenone and benzaldehyde (10) could not account for the loss of aromatic content from the polymer.

One route proposed for ring-opening involves the attack of the ring by peroxy radicals on the chain (11). In this case, the peroxy radical reacts with the phenyl group in an excited triplet state so that the attack at the ring is a radical coupling reaction (Fig. 1.6).

Another mechanism proposed for ring-opening reactions is the reaction of the ring with singlet oxygen (12). Singlet oxygen is thought to be produced by energy transfer

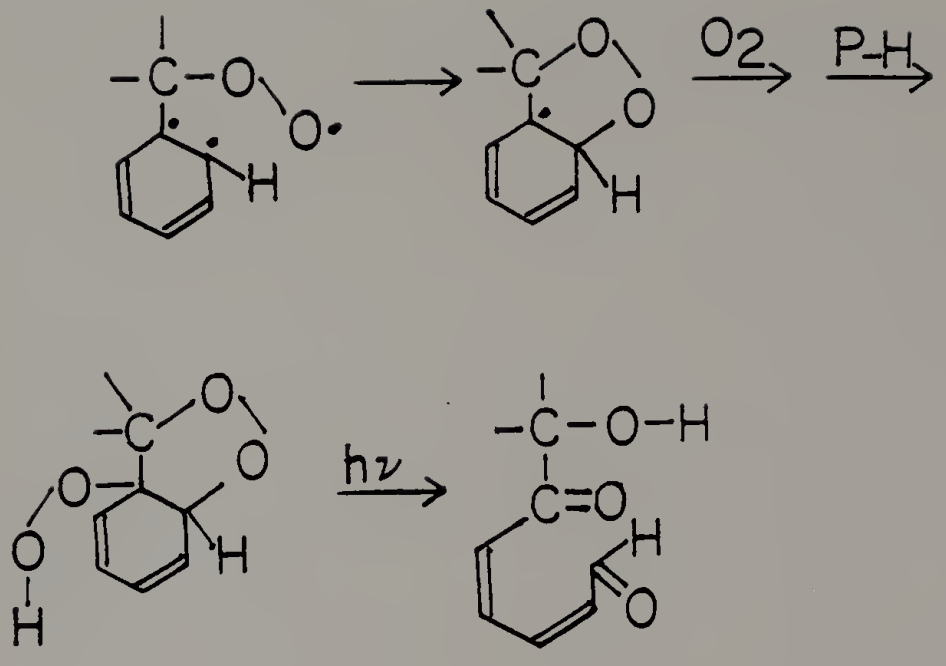

Figure 1.6

Ring opening reaction starting from a tertiary peroxy radical and a triplet state phenyl ring.

from excited phenyl groups. Subsequent reactions include the addition of oxygen as shown in Fig. 1.6 for one possible structure. Further absorption of $h\nu$ leads to ring-opening, and production of aldehyde groups (absorption at $1740cm^{-1}$).

The importance of singlet oxygen in PS photooxidation has not been conclusively shown, according to some (18), who feel that the evidence supplied, i.e. $^1O_2$ quenchers inhibit photooxidation, could be more definitive. Others suggest that the quenchers might also be quenching other structures besides singlet oxygen (42).

In spite of the objections to these ring-opening reactions, they do provide an appealing explanation of the yellow (and not red) color formation that develops with prolonged exposure. Perhaps the need for long exposure times to cause yellowing would also be consistent with the idea that the yellow coloration is caused by the products of these multi-photon, low overall quantum yield reactions. Certainly any contribution to the yellow color formation by conjugated polyenes would also be the result of many photons being absorbed since the kinetic chain length of reactions is thought to be limited to about five (18), and intermolecular abstraction reactions are commonly suggested. In addition to these theories of color formation, several other structures have been proposed to

account for the yellowing process. These structures were suggested on the basis of work done using longer wavelength UV, and will be considered later.

Low Molecular Weight Products

The production of water vapor, CO_2 and other low molecular weight products at long exposure times has been reported. Such products include acetophenone, benzaldehyde (10), oxalic acid, formic acid, phenol (14) and several other highly oxidized products. The loss of CO_2 and other volatile compounds from the surface suggests an erosion process, and it has been reported that eventually a steady-state surface concentration of photooxidation products is reached (15,21).

Molecular Weight Changes

Changes occur in the molecular weight of the polymer during photooxidation. Crosslinking has been reported (14) for powdered polystyrene exposed to 185nm and 254nm UV, but it was suggested by the authors that the crosslinking may be largely the result of ozone generated by the 185nm band in the UV. Ozone is reported to react with polystyrene to produce crosslinked structures (25), but gel structures have also been reported for 254nm photooxidation, as will be seen. This indicates that crosslinking reactions are

occurring along with chain scission reactions.

The photooxidation rate is reported to increase linearly with oxygen pressure (27) and also with light intensity at 600 torr oxygen (27). The quantum yields of scission and crosslinking are found to be independent of intensity at 600 torr oxygen over the range of 5.9×10^{-8} to 4.44×10^{-7} $E/cm^2 \cdot min.$ (52), which is consistent with an intensity exponent of one, i.e. rate linear in intensity. The dosage required to produce a gel was also independent of intensity, although the magnitude of this dosage was five times greater in vacuum photolysis than in photooxidation at 600 torr oxygen (52). This is probably the result of energy transfer mechanisms that operate during photooxidation, such as the transfer of energy from excited phenyl rings to hydroperoxides. As already mentioned, hydroperoxides quench excimer fluorescence, and this leads to the production of radicals which can lead to crosslinking instead of allowing for a radiative dissipation of energy.

Temperature

A zero temperature coefficient was found by monitoring absorbance at $1725cm^{-1}$ (59) while a positive temperature coefficient has been reported for oxygen uptake by polystyrene during photooxidation at 254nm (27). It would

seem that since the absorption of light is nearly independent of temperature in this range (42), a positive temperature coefficient here would indicate that activation energies are being overcome for reactions leading to more highly oxidized products, or that a longer kinetic chain length is produced. Although this implies that oxidative yellowing should proceed more rapidly at higher temperatures, the photoisomerization of benzene is also reported to have a positive temperature coefficient (55), as does the production of hydrogen during photolysis (3). Thus both ring isomerization and the production of unsaturation are also enhanced at higher temperatures. Both chain scission and crosslinking reactions are also favored at higher temperatures until the glass transition temperature is approached, where both drop (56). The crosslinking reaction quantum yield, however, drops more than the scission quantum yield, and this is explained in terms of a more facile diffusion of radicals away from each other near Tg which inhibits radical combination reactions.

Photooxidation at Solar Wavelengths

Initiation

The photooxidation of polystyrene by ultraviolet light in the solar region (wavelengths >300nm) proceeds much more

slowly than at shorter wavelengths because of the low absorptivity of the polymer to solar UV. This low absorptivity is the result of the fact that pure polystyrene, as described by the repeat unit, possesses an electronic transition due to the phenyl group at about 260nm. This band corresponds to the longest wavelength transition of pure polystyrene, and it does not extend beyond about 280nm. Thus, the initiation of photooxidation in polystyrene by solar UV is the result of absorption by structures other than the ideal repeat unit. This point is brought out by results obtained during vacuum photolysis at wavelengths greater than 300nm. Unlike the photolysis process at short wavelengths, photolysis in the solar region produced no hydrogen gas (26,3). This was taken as proof that the initiation step during photooxidation is not absorption by a phenyl group followed by energy transfer and scission of the tertiary C-H bond for solar UV.

A variety of possible structures have been suggested as chromophores for the initiation of photooxidation in the solar region of the UV spectrum. Since these structures tend to be present as impurities or in trace amounts. considerable controversy persists as to the exact nature of the initial chromophore. Several reasonable possibilities, however, are considered here.

The most common impurity in commercial polystyrene

seems to be styrene monomer, although ethyl benzene may be present in similar quantity, along with other hydrocarbons (28). Styrene monomer extends the absorption spectrum from about 280nm to about 293nm (29), but monomer alone cannot account for the absorption by certain commercial polymers that extends well beyond 340nm. The presence of monomer, however, led to more rapid photooxidation, especially when it is present in moderate quantities, i.e. > 1.5% (26).

Other likely impurities in commercial polystyrene are oxidation products that formed during polymerization or during melt processing. During a free radical polymerization oxygen can be added to the growing chain, and this can lead to the production of carbonyl compounds as polymerization proceeds or subsequently during melt processing if oxygen is not excluded (30). The most commonly mentioned product of such oxidation processes is the acetophenone-type end group, which reportedly forms from styrene polymerized in the presence of oxygen (31,32) and during processing in air (30). The band that forms at 1685cm^{-1} in the IR has been assigned to this structure, with supporting evidence from UV absorption and phosphorescence spectra (30,31,32,33). Although acetophenone-type end groups may be present, their absorption extends only weakly to wavelength above 300nm, as judged by data on acetophenone itself (34). Such end

groups are, nonetheless, thought to be significant in the initiation of photooxidation since the pure polymer does not absorb above 300nm.

The idea that in-chain peroxides could form during the radical polymerization of styrene in the presence of oxygen has been long held. Styrene/oxygen copolymers can be made, which are thought to be in the form of an in-chain peroxide (34). Although such peroxides should decompose during melt processing, they should be photolabile and decompose rapidly by UV light. Peroxides absorb UV at about 313nm, and this wavelength is reported to be the most destructive to a styrene/oxygen copolymer (35). This wavelength is quite close to that given by Hirt et al. (36) of 318.5nm, which was found to be the most destructive wavelength for polystyrene in the solar region, but the source and history of the polystyrene used here was not specified.

It is interesting to note that the presence of in-chain peroxides in styrene/oxygen copolymers is itself controversial. The lack of an appropriate absorbance in the IR in the 1000-1100cm^{-1} region, along with an apparent lack of variation in the number of chain scission with oxygen partial pressure during polymerization led some authors to conclude that the styrene/oxygen copolymer does contain "weak links" but not in-chain peroxides (37). It is reported, however, that acetophenone-type end groups are

formed to a greater extent in vacuum-photolyzed poly(styrene-co-oxygen) that had been prepared at higher oxygen partial pressures than at lower pressures (38), and this behavior was different from that of "hydroperoxidized" polystyrene (i.e. PS reacted with AIBN with oxygen present). This suggested that in-chain peroxides are more likely to explain the behavior of sytrene/oxygen copolymers than hydroperoxide structures, although in-chain peroxides are still not proven.

Finally, another "structure" proposed to be the initiating chromophore for polystyrene in the solar region is the polymer/oxygen charge transfer complex (CTC). It is proposed by some (12,39) that the absorbing species is a complex between the phenyl ring and molecular oxygen, with the excited state being formed with the transfer of one electron to the oxygen molecule from the ring. It is, thus, an ionic excited state (40) and its formation in polystyrene has been supported by data showing an increase in absorption above 320nm by polystyrene with increased oxygen pressure in the surrounding atmosphere (41). It is proposed (12) that the CTC dissociates to form singlet oxygen plus a phenyl group in its ground state, with the singlet oxygen molecule proceeding to attack the ring to produce a variety of oxidation products.

Possibly conflicting evidence against the involvement

of singlet oxygen in the photooxidation of polystyrene in the solar region was brought out be examining polystyrene containing benzophenone (19). Excited triplet benzophenone is able to transfer energy to molecular oxygen to produce an excited singlet oxygen molecule, and it was supposed that this could be the reason for the sensitization caused by benzophenone. However, the addition of naphthalene to the system quenched the benzophenone and also quenched the photooxidative process. Since excited naphthalene can also transfer energy to oxygen to form an excited singlet, it was concluded that the benzophenone, and not singlet oxygen, reacts with polystyrene. Since these results were obtained at 600 torr oxygen, the observations are probably valid under atmospheric conditions where the concentration of oxygen is lower and the probability of transfer to oxygen should also be lower. Finally it should be mentioned that the absorption caused by the polymer/oxygen CTC is extremely weak in an environment of air at one atmosphere pressure, suggesting that this mechanism may be significant only in highly purified polystyrene, if at all.

Photooxidation Reactions

A variety of reactions have been proposed to account for the complex assortment of products formed during polystyrene photooxidation. It is generally accepted that

the acetophenone-type end groups play a prominent part in the oxidation reactions that follow their introduction, although the process that produces these end groups may not be known. This is borne out first of all by the observation that their phosphorescence spectrum decreases during the vacuum photolysis of previously photooxidized polystyrene (43). This indicates that the acetophenone-type end groups are being consumed by the photolytic reactions occurring in the absence of oxygen, indicating that they are active as chromophores and as reactive species (44).

In order to study the behavior of aromatic ketones in polystyrene, Geuskens et al. (9) introduced various aromatic ketones (e.g. benzophenone) into polystyrene films in known quantities. This was done in order to be able to calculate quantum yields based on the known concentrations and absorptivities of the aromatic ketones used. It is reported that the first reaction is, generally, the abstraction of the tertiary hydrogen from PS by the excited triplet state of the aromatic ketone. This idea is in general agreement with the observation that α-deutero PS photooxidizes much more slowly than the purely hydrogenous polymer (45). The abstraction of hydrogen by the aromatic ketones is affirmed by the production of the corresponding pinacols, seemingly by radical coupling reaction of the ketyl radicals. Once the polystyryl radical is formed, it

can quickly add molecular oxygen, which leads to a hydroperoxide group via hydrogen abstraction. Once formed, the hydroperoxides can decompose thermally, or by a reaction with an excited triplet-state aromatic ketone. These ketones are thought to abstract the hydrogen atom from the hydroperoxide, rather than to cause homolysis of the O-O bond by some energy transfer process (18). Scission of the O-O bond can also occur, and a tertiary alcohol group is produced (Fig. 1.7). Another reaction of the hydroperoxide group is the decomposition that leads to chain scission (7,38) (Fig. 1.8). In the absence of aromatic ketones, cumene hydroperoxide was found to decompose too slowly to account for the observed rate of PS photooxidation. Thus, the idea of a sensitized decomposition of hydroperoxides by aromatic ketones is further supported.

The presence of common pollutant gases also affects the photostability of polystyrene. Kambe (57) describes the effect of sulfur dioxide on the photooxidation of polystyrene with solar UV. It was found that the amount of carbon dioxide released during photooxidation was proportional to the amount of sulfur dioxide present. A similar effect was observed when ozone was present along with solar-region UV. The chain scission of polystyrene exposed to nitrogen dioxide proceeded five times faster

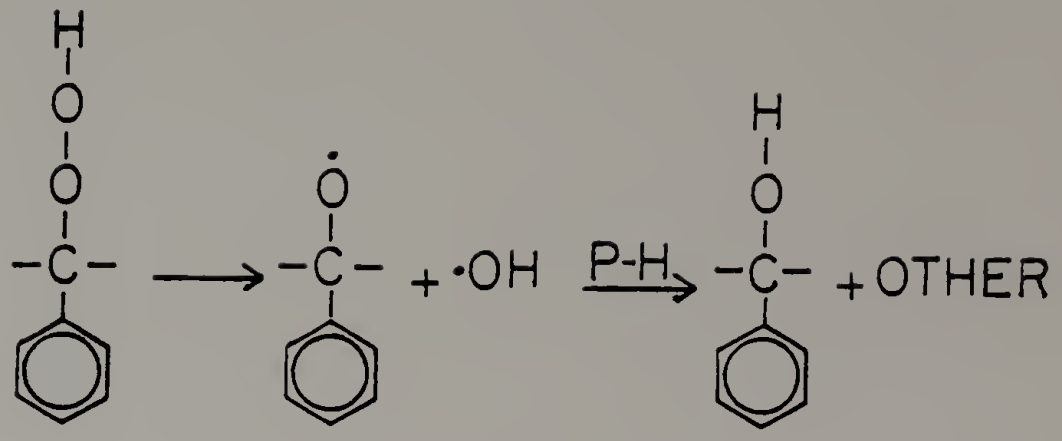

Figure 1.7

Reaction path for hydroperoxides which leads to alcohol formation along the main chain.

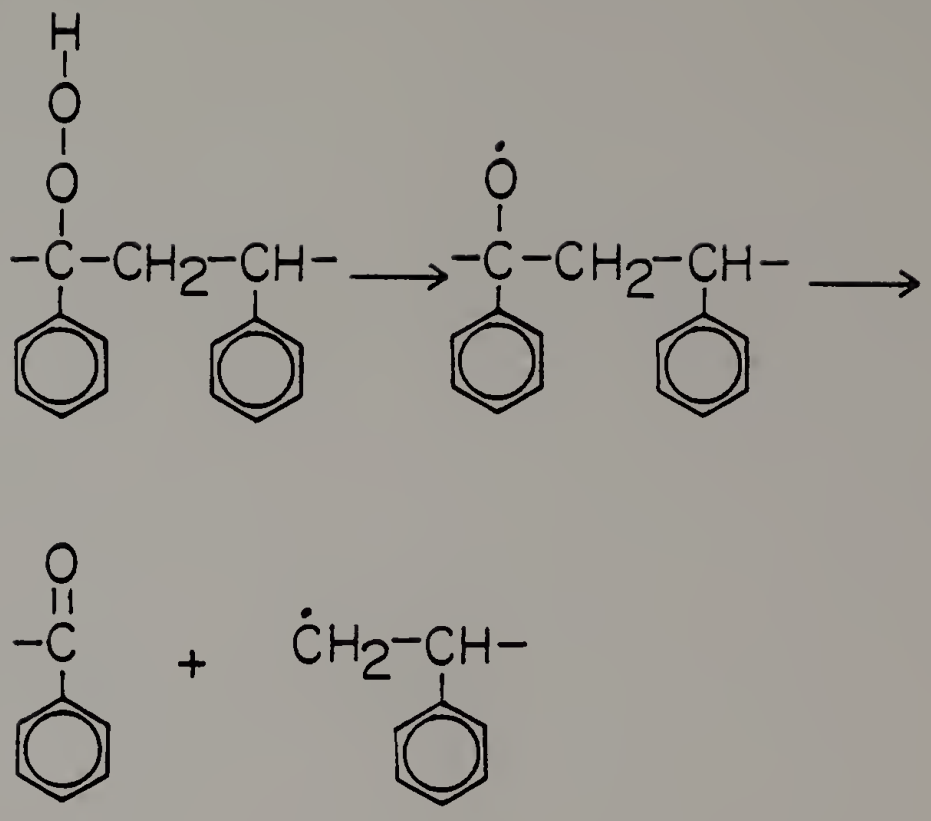

Figure 1.8

Decomposition of hydroperoxides and the formation of acetophenone- endgroups and an alkyl radical.

when solar UV was introduced.

A number of other carbonyl-containing products have been reported including acid functional groups (46), ketone compounds (47), benzalacetophenone structures (48) (Fig. 1.9) and a variety of ring-opening reaction products. While it has been suggested that ring-opening reactions start with some form of molecular oxygen attacking the ring (12), such reactions are also reported to begin with hydroxyl radicals attacking the ring (49). It is reported that attack of the ring by a hydroxyl radical may be energetically more favorable than tertiary hydrogen abstraction. The products believed to form during ring-opening reactions include dialdehydes, hydroxy dialdeydes and phenolic structures.

Low Molecular Weight Products

Low molecular weight products are also produced during photooxidation. Extraction of the surface of photooxidized polystyrene films show that the products formed include a variety of acids (26,5Ø) which may include formic and acetic acids (51). Other carbonyl-containing compounds have also been reported, such as formaldehyde, methyl formate (51), α,β-enones and diketones (44). Water also forms, presumably as a result of hydroperoxide decomposition. The production of acetophenone was used to explain the somewhat

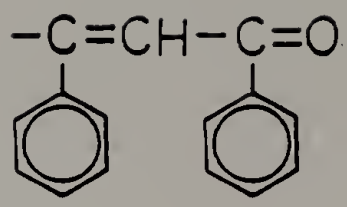

Figure 1.9

Structure of benzalacetophenone.

higher yield of acetophenone-type groups than chain scissions, which are usually thought to form together in a one to one ratio (38). The reaction sequence believed to be responsible for acetophenone production is given in Figure 1.10. Certainly any acetophenone produced would act as a photosensitizer capable of migrating throughout the polymer, but as long as it remained in the polymer, it would be detected along with the acetophenone-type chain end groups.

Molecular Weight Changes

The photodecomposition of hydroperoxides in polystyrene can lead to chain scission, with an acetophenone-type end group and terminal unsaturation produced on either side of the point of scission. Chain scission proceeded linearly with exposure time, as judged by changes in molecular weight (35,38). Some cross-linking reactions also occur, along with scission, and this is seen by the production of an insoluble gel (47). Quantum yields for scission and crosslinking have been estimated for polystyrene containing a known amount of benzophenone after exposure to a broad band UV source (365nm maximum) (52). Values for the quantum yields were 0.0013 and 0.00025 for scission and crosslinking respectively. Both values increased with increasing oxygen pressure, although

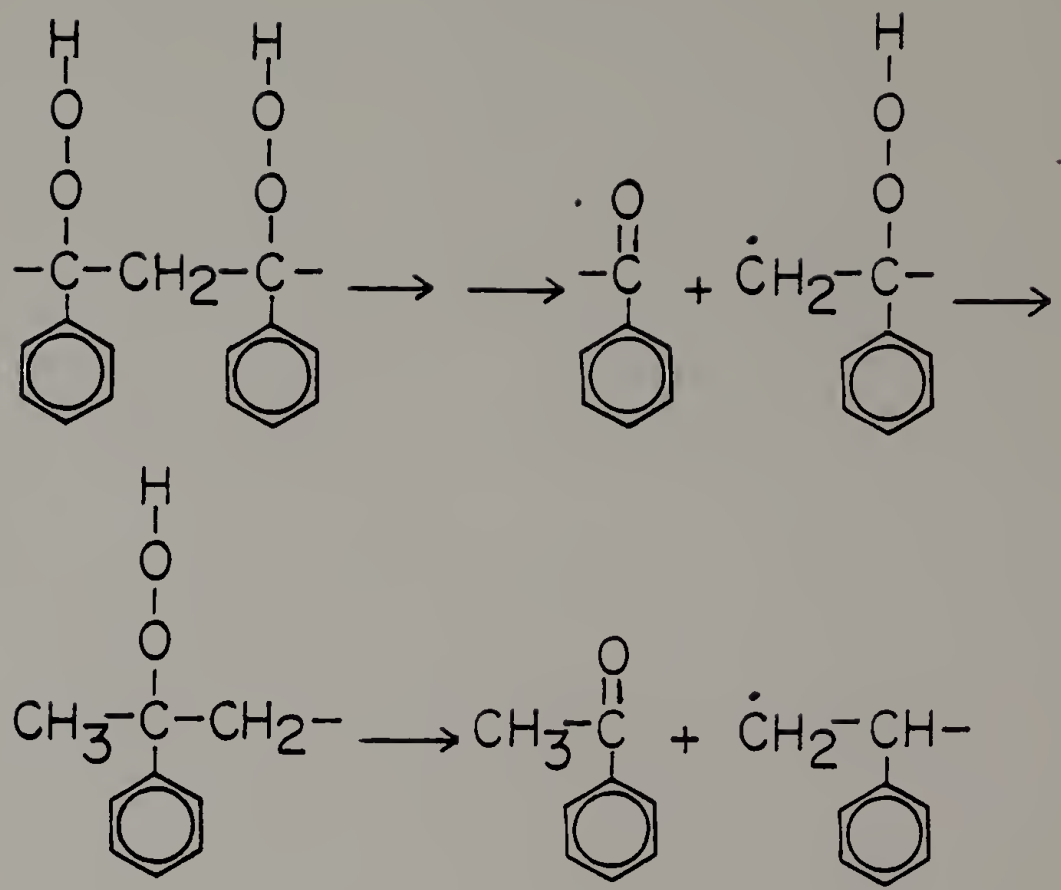

Figure 1.10

A reaction sequence that could lead to the formation of acetophenone itself.

scission reactions always remained more efficient than crosslinking. Interestingly, the overall rate of photooxidation at 365nm may decrease as oxygen pressure is increased from 400 to 760 torr (9).

Color Formation

Polystyrene eventually turns yellow during photooxidation in the solar region of the UV spectrum, and a number of different structures have been proposed as being the cause of this color. As with photooxidation at short wavelengths, ring-opening reaction products have been indicated as possible sources of the yellow coloration (12). Conjugated unsaturation as well as carbonyl-containing groups were thought to be responsible for yellowing when it was observed that chemical reduction of the carbonyl groups did not eliminate the yellow color from the polymer film (53). These authors argue against the idea that quinone (47) or benzalacetophenone (29) structures could be responsible on the basis of IR, UV, and NMR data of model compounds, while these structures were originally proposed on the basis of having appropriate IR and UV bands along with appropriate absorptivities. The yellow colorants are, in part, thought to be oxidation products, with the point of agreement based on vacuum photolysis experiments in which no yellow coloration

developed (26,51). This is, of course, quite different from the results obtained during the vacuum photolysis of polystyrene at short wavelength (254nm) UV although conjugated unsaturation has been reported to form during photooxidation here as well (52). Low molecular weight compounds seem to contribute to the observed color because washing the surface of a photooxidized polystyrene film removes some of the coloring (54). Low molecular weight oxidation products are also thought to contribute to an increase in surface hydrophilicity, as judged by contact angle (50).

Temperature

A positive temperature coefficient has been reported for chain scission of polystyrene during photooxidation at 310nm (19). This has been attributed to an increasing importance of a chain scission reaction, which is favored as chain mobility increases (Fig. 1.8). Another series of reactions found to have positive temperature coefficients are collectively referred to as the post-irradiation effect. These are reactions which occur after the UV source has been shut off. This effect has been explained in terms of two reactions occurring simultaneously, one being the thermal decomposition of hydroperoxides and the other being the cis-trans isomerization of benzalacetophenone

structures (48). The possibility of a cis-trans isomerization was demonstrated by adding benzalacetophenone itself to polystyrene and noting the change in absorbance at 340nm caused by raising the temperature. The trans isomer has a higher absorptivity than the cis isomer, and it is formed by thermal isomerization while the cis isomer is formed on photoisomerization. Reactions that follow the hydroperoxide decomposition reaction are thought to include tertiary hydrogen abstraction since there is a strong isotope effect noticed upon deuteration of the tertiary position.

Conclusions

The photooxidation of polystyrene proceeds by a complicated sequence of reactions. As it has been shown, the photooxidation process quickly changes from being a process determined by the chemistry of polystyrene into one dominated by interactions of the photooxidation products. Energy enters the system through a chromophore, which may become insignificant as the reaction proceeds due to the production of more efficient chromophores. Once absorbed, the energy from the photon may be dissipated photophysically or it may lead to a chemical reaction at

the chromophore or after migration to a remote site. The importance of these mechanisms change as the chemistry of the polymer is modified during photooxidation, with the relative importance of the different mechanisms being determined by the environmental conditions present during photooxidation as well as the presence of photo-active impurities.

C H A P T E R II

CARBONYL FUNCTIONAL GROUPS

Introduction

Many reaction mechanisms have been proposed to account for the formation of various carbonyl and OH-containing (hydroxy,hydroperoxy) groups during PS photooxidation (see Chapter I). The examination of any of these mechanisms in detail is quite difficult because of our limited knowledge of chemistry within a glassy matrix, and perhaps more importantly, because the reaction products continue to react to form more highly oxidized products. In fact, a principle limitation in our understanding of PS photooxidation is our ability to identify the reaction products present in the film. The ultimate products of photooxidation are water and carbon dioxide, and although they are formed in fairly high quantum yields (1Ø), they do not lead to further reactions of the polymer but are lost as volatile products. Therefore, attention in the present study is given to identifying the reaction products that remain in the PS film.

The use of 254nm UV to investigate PS photooxidation offers many advantages over solar UV. First, this

wavelength of light is absorbed directly by the polymer repeat unit (phenyl ring) and so the production of primary radicals is dominated by the photochemistry of the repeat unit. This stands in contrast to solar UV, where the presence of fortuitous impurities can dominate PS photostability. Second, because the UV light is strongly absorbed by PS, films can be used that are thick enough to absorb all (99+%) of the incoming light so that the total photon dosage is known. This only requires a knowledge of the UV intensity reaching the film and the total exposure time.

Identification of the functional groups that form during PS photooxidation is best accomplished using infrared spectroscopy because of the large quantity of information contained in a given spectrum and because analysis can be performed on a solid polymer film. The ability to analyze solid films is of great importance since it allows photooxidation to occur in the solid (glassy) polymer. This is significant because PS becomes partially insoluble with photooxidation. Fourier-transform spectrometry is the preferred choice of instrumental techniques because of the high resolution and high signal to noise ratio obtainable. This instrument also allows both scale expansion and computer-aided data manipulations (e.g. spectral subtraction) to be easily performed.

When PS is photooxidized using 254nm UV, most of the light is absorbed within the top 4 to 6 μm of the film (see Appendix A). This means that the functional groups that form will be located near the film surface. Advantage can be taken of this fact by using attenuated total reflectance (ATR), which samples only the top few micrometers of the PS film. Since the sampling depth can be controlled by choosing different angles of incidence or ATR crystals of different refractive index, it is possible to obtain some information about the location of functional groups within the photooxidized film. Only two studies have been reported in which ATR was used to examine PS photooxidation (59,60), but the low signal to noise ratio obtained using a conventional grating instrument limited the amount of information obtained. A third paper mentions the use of ATR to analyze PS photooxidized using a medium pressure mercury arc lamp (λ max > 300nm) (50), but only limited spectral information was reported.

This chapter deals with the development of carbonyl functional groups as PS is photooxidized at constant temperatures from 30° to 75°C. The general features of the infrared carbonyl bands are described along with the response of these carbonyl functional groups to reactive gas-phase reagents. The identity of the functional groups is determined by the infrared absorption frequency and the

response seen on exposure to reactive vapors. Their depth within the PS film is described using ATR.

Experimental

A narrow molecular weight distribution, anionic polystyrene (Pressure Chemical Co., Lot 5Ø124; $\bar{M}_W$=233,ØØØ; $\bar{M}_W/\bar{M}_n \leq$1.Ø6) was used throughout this study. Polystyrene films were cast from dilute solutions in distilled chloroform into glass dishes. The solvent was allowed to evaporate under a nitrogen atmosphere until "dry" ($\sim$6 hours). The films were then placed in a vacuum desiccator, purged three times with nitrogen and evacuated to 3 millitorr. The temperature of the desiccator was then raised to 8Ø°C for 24 hours and then raised again to 1Ø7°C for at least six hours. Films were cooled slowly under nitrogen, followed by equilibration in air for at least three days before being used. The final thickness of the films was 1Ø-15 μm. Certain films were also prepared having a wedge-shaped cross-section by casting the chloroform solutions into tilted dishes. This procedure produced films with thicknesses ranging from 1Øμm at the thin edge to 2Ø μm at the thick edge of a two inch wide film.

Photooxidation involved the use of a low pressure mercury arc lamp combined with a 1Ønm bandpass interference

filter which isolated the 254nm UV line. This arrangement provided a stable source of UV radiation with an intensity of 1.95×10^{-6} E/cm^2.hr, as measured by potassium ferrioxalate actinometry (61) (see Appendix B). Irradiation of the films took place in a glass chamber under a slow, continuous flow of air from a compressed air cylinder (Merriam-Graves Co., 19.5-23.5% oxygen, balance nitrogen, 3ppm H_2O). The temperature of the chamber could be controlled at a constant value between 30° and 75°±0.5°C.

Infrared spectra were recorded using an IBM IR-98 Fourier-transform infrared (FTIR) spectrometer. Both absorbance and reflectance (ATR) spectra were recorded using wedge-shaped and flat films respectively. All spectra were recorded at 2cm^{-1} resolution with absorbance single beam spectra produced with 500 scans and reflectance spectra from 1000 scans. The ATR spectra were obtained using 50x20x2mm trapezoid crystals, and all were used with 45° incident illumination relative to the sample normal. The depth of penetration decay constant, dp (62), for each crystal is given in Table 2.1. An order-of-magnitude measure of the carbonyl concentration profile is made from spectra collected using the KRS-5,45° and the Ge,45° crystals. These results are compared to those predicted from published oxygen uptake data and from the UV absorption profile.

Table 2.1

ATR Depth of Penetration Constants, dp

Crystal	1725cm^{-1}	1950cm^{-1}
KRS-5,45°	1.67μm	1.48μm
KRS-5,60°	0.86μm	0.76μm
Ge,45°	0.40μm	0.35μm

To describe the distribution of UV light in the PS film, the absorptivity at 254nm was determined using films of different thicknesses. UV absorption was recorded using a Beckman ACTA MVI UV/Vis spectrophotometer. Infrared absorptivities were determined with the IBM FTIR for polystyrene bands and for the carbonyl band of acetone dissolved in chloroform. These results are given in Appendix C.

Immediately following irradiation, the photooxidized films were subjected to a variety of post-irradiation treatments that would selectively affect the different carbonyl products. The first treatment involved heating the free-standing film in argon at 87°C for 15hrs., with infrared spectra recorded before and after heating. Another film was heated to 90°C in a modified ATR attachment for 15 hours. Other films were exposed to the vapors from ammonium hydroxide, methyl amine or pyridine in a covered Petri dish

for 30 minutes. Films exposed to the ammonia or methyl amine vapors were subsequently stored over ferric chloride for 3 or 12 days respectively, to absorb amine vapors coming from the films.

Results

Infrared Band Shape

The photooxidation of PS in air at 254nm produces subtle changes in its infrared spectrum, with these changes being most noticeable as increases in absorption in the regions of 3600-2600cm^{-1} (OH stretch region), 1800-1650cm^{-1} (carbonyl region) and a region around 1200cm^{-1} (C-O stretch). These bands are actually composed of numerous overlapping absorption bands which are detected as maxima or shoulders in the OH stretch and carbonyl regions.

The qualitative features produced in the carbonyl region are best illustrated with spectra obtained using ATR. Figure 2.1 shows the growth of the carbonyl band as a function of UV dosage at 30°C. Figure 2.1 shows that the carbonyl absorption band is broad (>100cm^{-1}) even at low UV dosages. At larger dosages, at least three overlapping bands can be seen at 1775, 1725, and 1690cm^{-1}. After $5.15 \times 10^{-5} E/cm^2$, (1E = 1 einstein = 1 mole photons), an increase in absorption at 1300cm^{-1} is seen that is part of

Figure 2.1

Carbonyl growth as a function of UV dosage at 30°C using a KRS-5,45° ATR crystal.

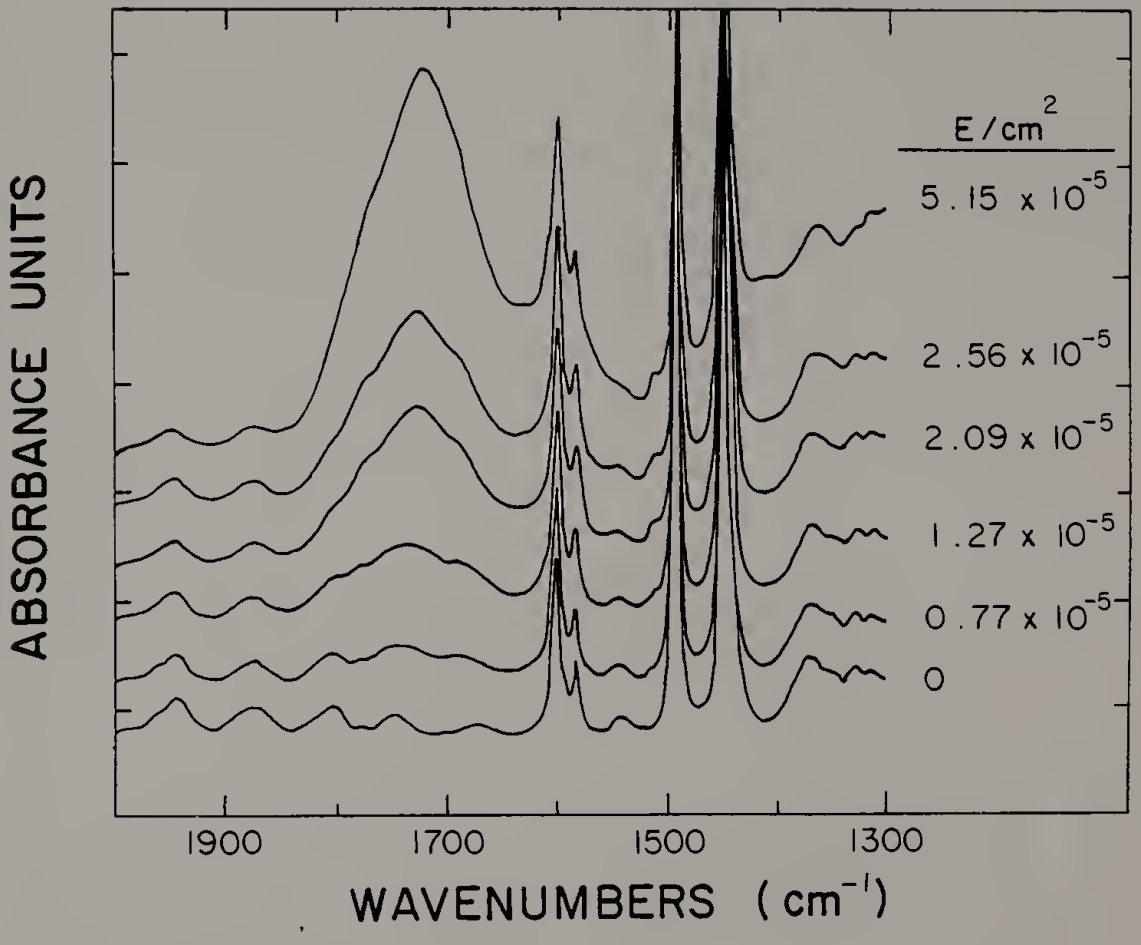
ABSORBANCE UNITS
E / cm²
5.15 x 10⁻⁵
2.56 x 10⁻⁵
2.09 x 10⁻⁵
1.27 x 10⁻⁵
0.77 x 10⁻⁵
0
1900
1700
1500
1300
WAVENUMBERS (cm⁻¹)

a broad, strong band centered at about 1200cm^{-1}.

The shape of the carbonyl band depends on the temperature of the film during irradiation. This is seen in Figure 2.2 for PS irradiated at 30° to 75°C for similar UV dosages. At 30°C, the 1690cm^{-1} shoulder is higher than the shoulder at 1775cm^{-1}, but this relationship is reversed for films exposed at 75°C. This same result can be seen using transmittance spectra, but the effect is much less obvious.

Carbonyl Location

The use of ATR crystals of different refractive index and/or different angles of incidence provides some insight into the depth distribution of the carbonyl products relative to the PS film surface. This is illustrated in Figure 2.3, where it is seen that the carbonyl band is much stronger relative to the 1601cm^{-1} band in the top 1μm than it is in the top 4.5μm (sampling depth is about equal to 3dp (63)). If it is assumed that the carbonyl products are distributed along an exponential profile, then their distribution can be described in terms of an exponential function characterized by a surface layer concentration in the top monolayer, C_o, and a decay constant, d_c. These values can be calculated using published equations (64,65) and infrared absorptivity values from Appendix C. The results are given in Table 2.2, along with results

Figure 2.2

Carbonyl band shape vs. exposure temperature. ATR spectra of the carbonyl region after $\sim 2 \times 10^{-5}$ E/cm^2. The band at 1775cm^{-1} is found to develop more quickly at higher temperatures: (A) 30°, (B) 45°, (C) 60° and (D) 75°C.

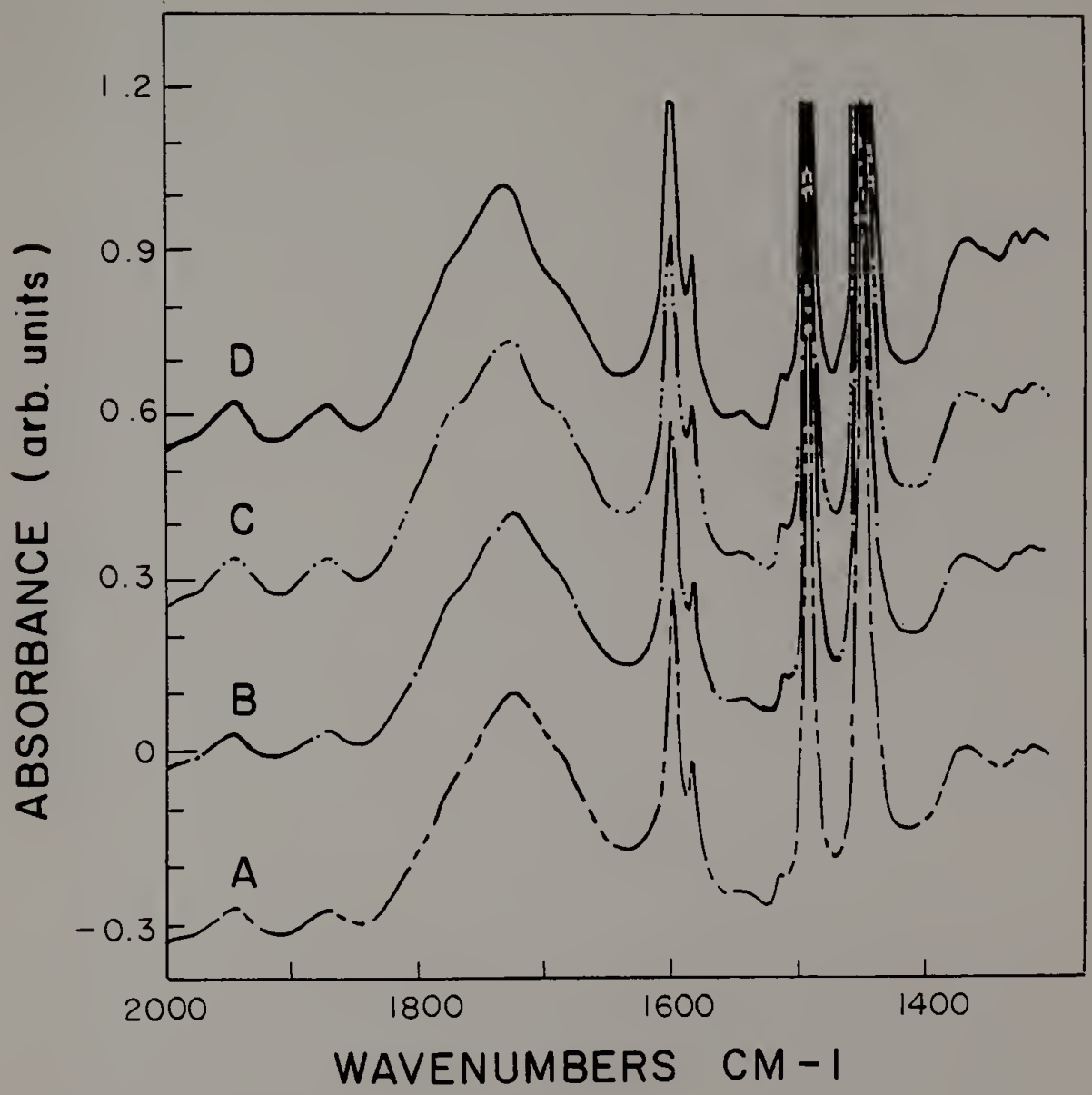
1.2
0.9
0.6
0.3
0
-0.3
ABSORBANCE (arb. units)
D
C
B
A
2000
1800
1600
1400
WAVENUMBERS CM-1

Figure 2.3

Carbonyl band vs. depth. Carbonyl intensity vs. depth into the PS film after $2.6x10^{-5}E/cm^2$. Note that the carbonyl intensity increased relative to the $1601cm^{-1}$ band from A (KRS-5,45°) to B (KRS-5,60°) to C (Ge,45°) as the IR sampling depth was decreased.

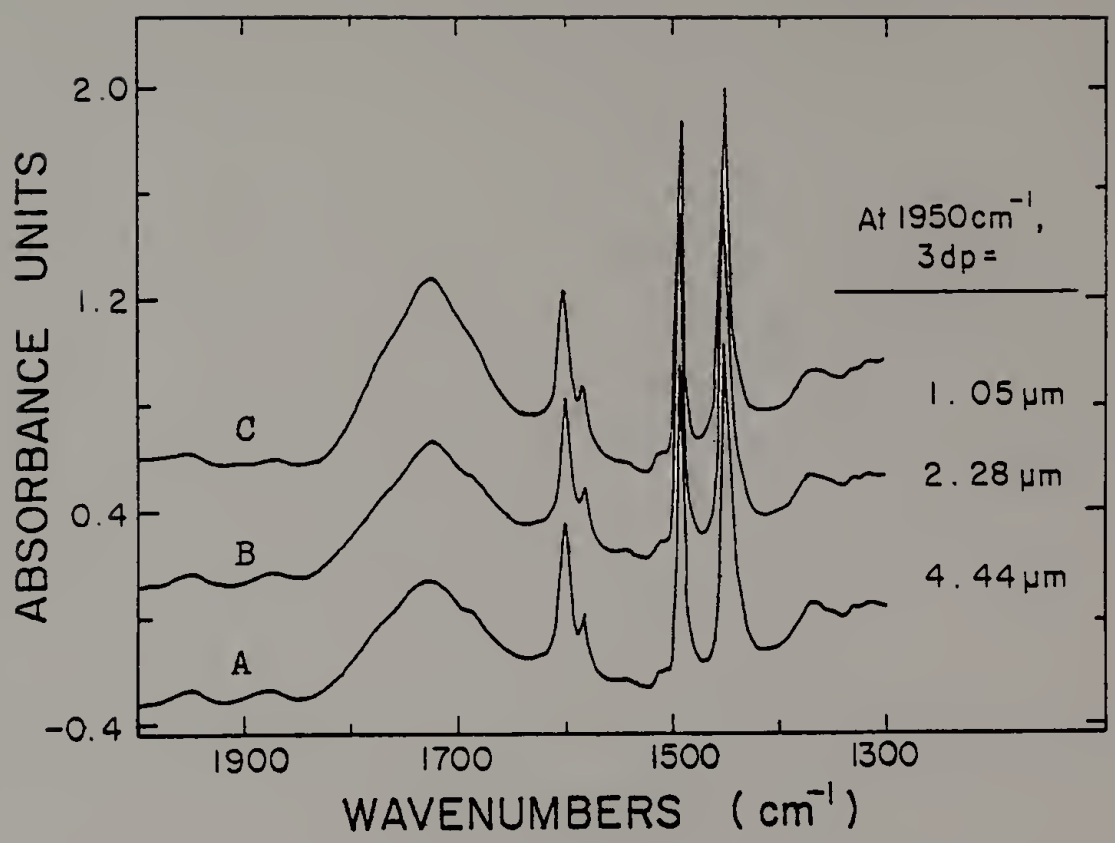
ABSORBANCE UNITS
2.0
1.2
0.4
-0.4
1900
1700
1500
1300
WAVENUMBERS (cm⁻¹)
C
B
A
At 1950cm⁻¹,
3dp=
1.05 μm
2.28 μm
4.44 μm

calculated a priori from published oxygen uptake data (10).

Table 2.2

Total Carbonyl Concentration Gradient Constants

	A Priori		Experimental	
UV Dosage($E/cm^2 x 10^5$)	C_o(mol/l)	d_c(μm)	C_o(mol/l)	d_c(μm)
0.77	0.24	1.95	0.4	0.7
1.27	0.39	1.95	0.9	0.7
2.09	0.66	1.95	2.4	0.6
2.56	0.80	1.95	2.9	0.4

In addition to the assumptions made in deriving the equations, the experimental values were obtained by: 1) assuming the phenyl ring concentration to be constant, so that the $1950cm^{-1}$ combination band could be used as a reference peak, and 2) that the absorptivity of the carbonyl functional groups from 1800 to $1650cm^{-1}$ is approximately that of acetone (Appendix C).

A priori values are based on the assumption that the carbonyl products are located on the UV absorption profile, which is assumed to be constant. In addition, an estimate of the quantum yield of carbonyl formation is obtained from the data of Geuskens et al. (10), where

$$\phi_{C=O} = 1/2 \left(\phi_{O_2} - \phi_{CO_2} - 1/2 \, \phi_{H_2O} \right)$$

Here, $\phi_{C=O}$ represents the quantum yield of carbonyl groups

present in the film. The total quantity inside the parenthesis is one half the quantum yield of oxygen atoms present in the film, since oxygen atoms are lost from the film through the evaporation of carbon dioxide and water vapor. The factor of 1/2 outside the parenthesis is used because only about one quarter of the oxygen atoms in the film are carbonyl oxygen atoms, with the rest being in hydroxyl, hydroperoxyl or other groups. This value of $\phi_{C=O}$ is used to calculate C_o in the a priori data.

Post-Irradiation Treatments

Exposing photooxidized PS to ammonia vapor for 10 minutes changed the carbonyl band shape. Figure 2.4 shows difference spectra obtained by subtracting the pure PS spectrum from the photooxidized PS spectrum. The initial band, 2.4A, is partially consumed on exposure to ammonia and bands appropriate for carboxylate anions (1560 and 1380cm^{-1}) form. No additional changes were observed after further exposure to ammonia. The band at 1690cm^{-1} was not changed, nor were a number of weaker bands centered around 1710-1740cm^{-1}.

Figure 2.4C shows that the ammonia vapor could be removed by storing the film with $FeCl_3$. This appears to have partially regenerated the carbonyl band at 1725cm^{-1}, eliminating the carboxylate anion form. Some elimination of

Figure 2.4

Reversibility of ammonia treatment. Difference spectrum of PS after $1.6 \times 10^{-4} E/cm^2$ at 45°C minus the unoxidized PS (Spectrum A). Spectrum B represents the same film after 10 minutes exposure to NH_3 vapor, showing the carboxylate asymmetric and symmetric stretch bands. Spectrum C was recorded after storing the film from B over $FeCl_3$ for 3 days, which regenerated the carboxylic acid band.

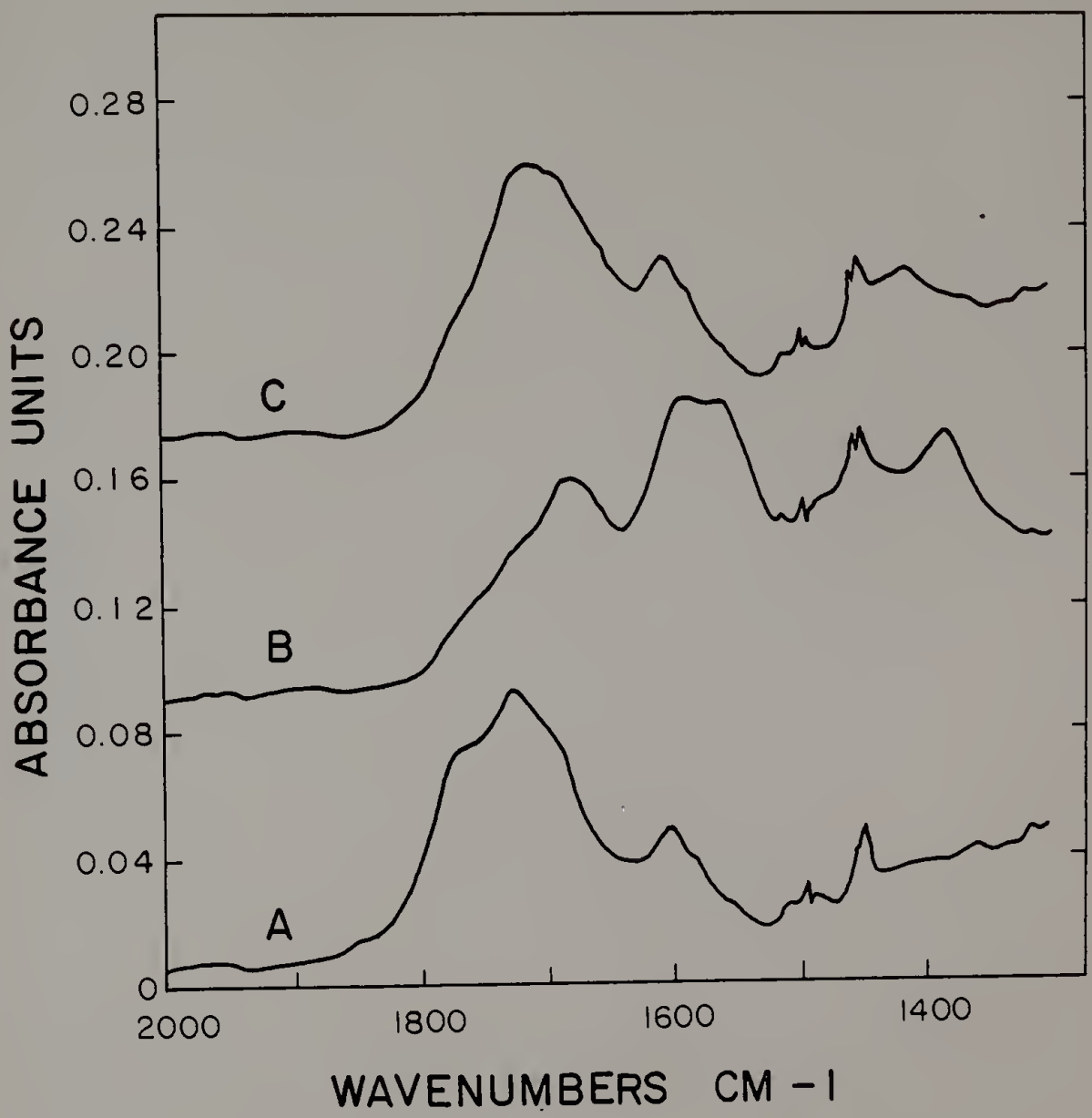
0.28
0.24
0.20
0.16
0.12
0.08
0.04
0
ABSORBANCE UNITS
C
B
A
2000
1800
1600
1400
WAVENUMBERS CM -1

the 1725cm^{-1} band is evident, however, along with the complete loss of the 1775cm^{-1} band. A new, weak band is found at 1405cm^{-1} which is not affected by a second exposure to ammonia vapor, and which may be associated with ammoniolysis products. The second exposure to ammonia regenerated spectrum 2.4B (plus the 1405cm^{-1} band) and removing the ammonia with $FeCl_3$ regenerated 2.4C. This shows that part of the observed reaction with ammonia is reversible.

Exposing photooxidized PS to methyl amine vapor for 30 minutes caused a change similar to that seen with ammonia, but with several differences. Figure 2.5 shows that methyl amine caused the disappearance of nearly all carbonyl bands from 1700 to 1780cm^{-1}. Storage over $FeCl_3$ eliminates the carboxylate anion bands, revealing a new band near 1660cm^{-1}. Subsequent exposure to ammonia, followed by storage over $FeCl_3$ for three days, produced a strong band at 1405cm^{-1} (Figure 2.6).

In a separate test, exposing photooxidized PS to pyridine vapor reduced the absorption at 1775 and 1725cm^{-1} slightly, but did not produce carboxylate anion bands.

The results obtained from heating photooxidized PS in argon at 87°C are shown in Figure 2.7. Although not as clearly resolved as the spectra in 2.4 the absorbance difference spectra in Figure 2.7 are from a PS film

Figure 2.5

Reversibility of methyl amine treatment. ATR spectra of photooxidized PS (A) showing the effect of exposure to methyl amine (B). Storing the film over $FeCl_3$ (C) partially regenerated the 1725cm^{-1} band and revealed a new band at 1660cm^{-1}.

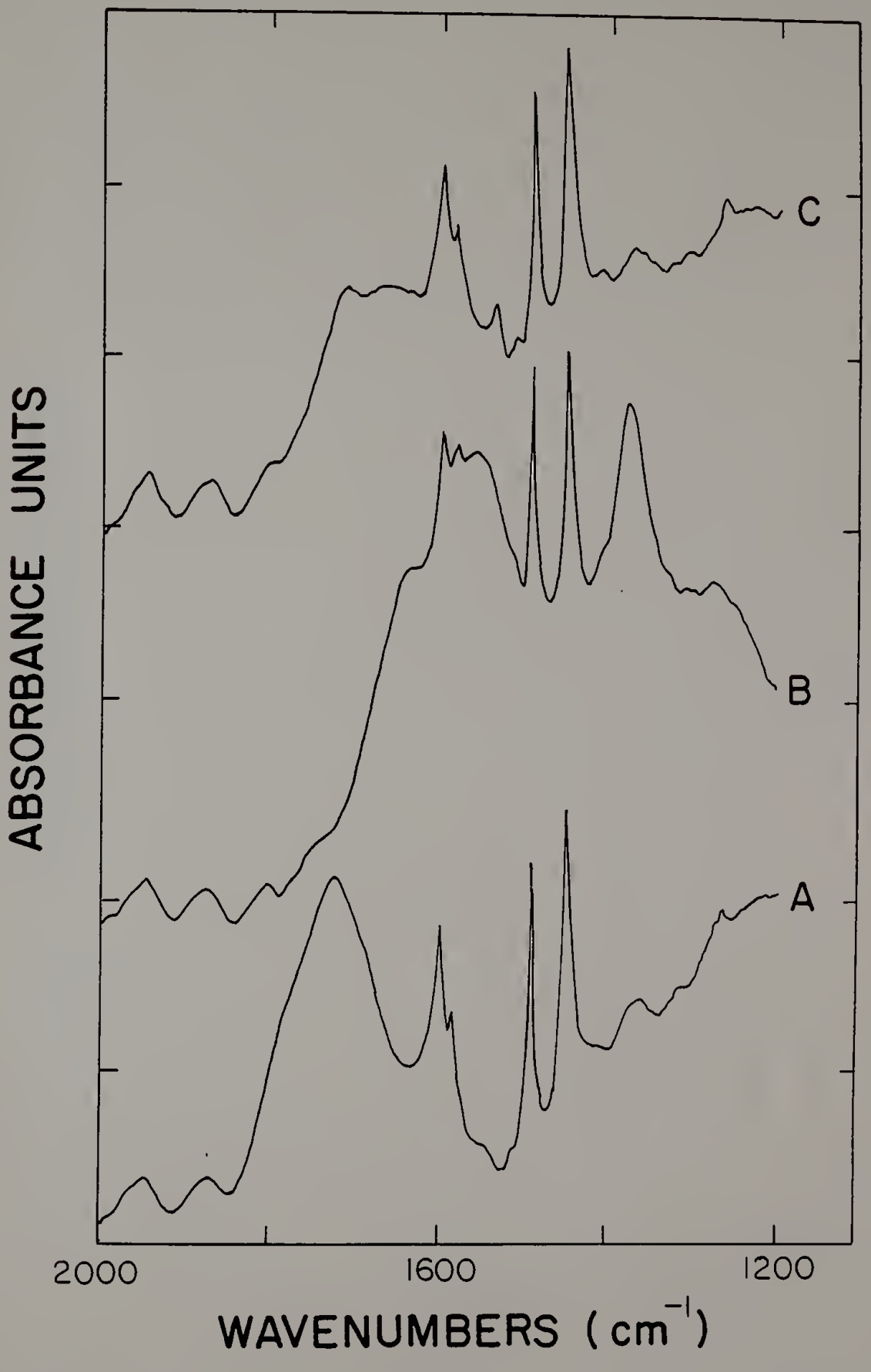
ABSORBANCE UNITS
C
B
A
2000
1600
1200
WAVENUMBERS (cm⁻¹)

Figure 2.6

Methyl amine/ammonia treatment. Exposing the film from Figure 2.5C to ammonia followed by storage over $FeCl_3$ produced a strong band at 1405cm^{-1}.

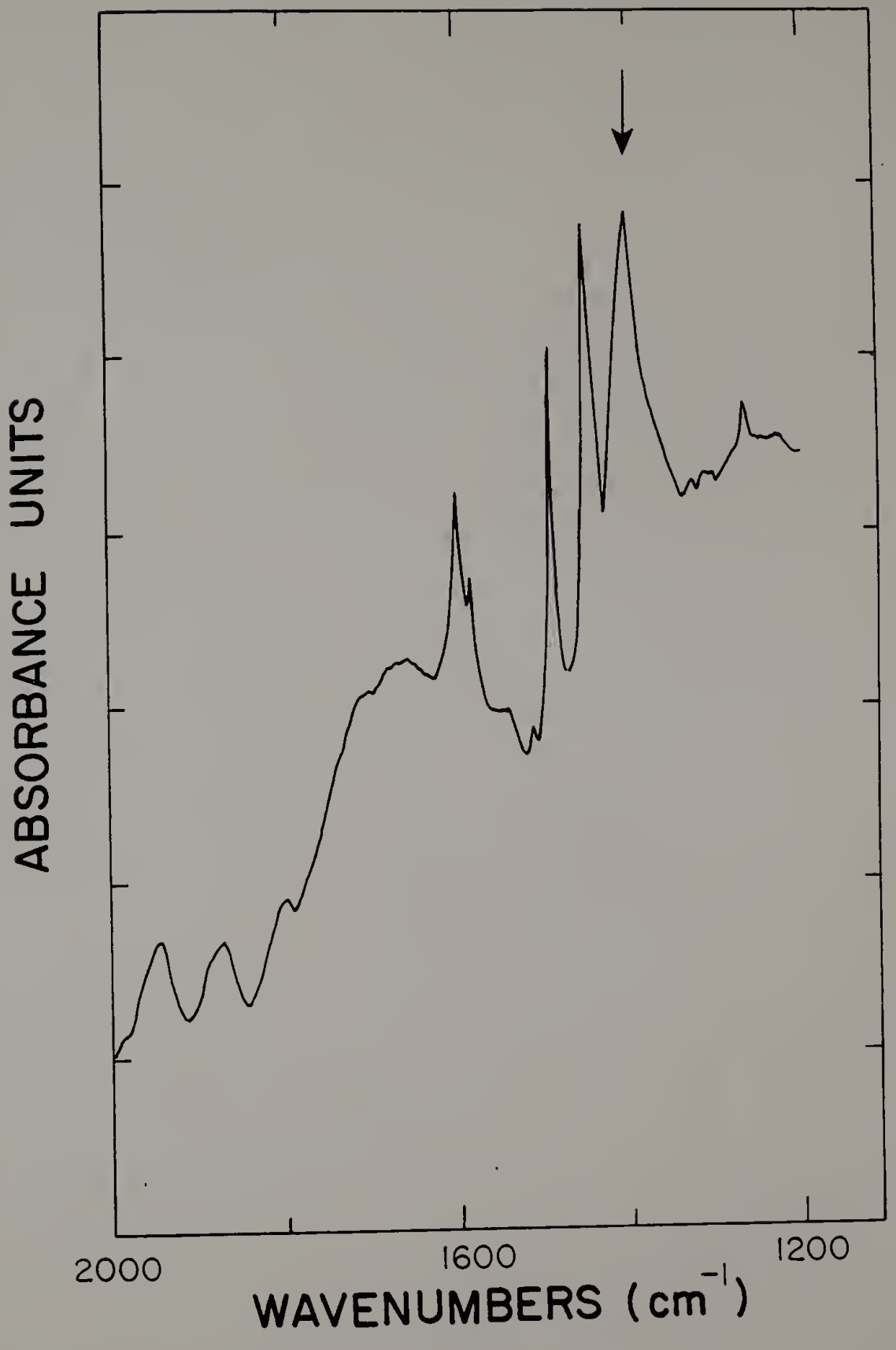
ABSORBANCE UNITS
2000
1600
1200
WAVENUMBERS (cm⁻¹)

Figure 2.7

Volatilization of 1775cm^{-1} product. Difference spectrum of photooxidized PS (6.5x1Ø$^{-5}$E/cm^{2},75°C) minus the unoxidized PS (spectrum A). Spectrum B is the same film after heating in argon for 15 hrs. at 87°C which revealed a decrease at 1775cm^{-1}.

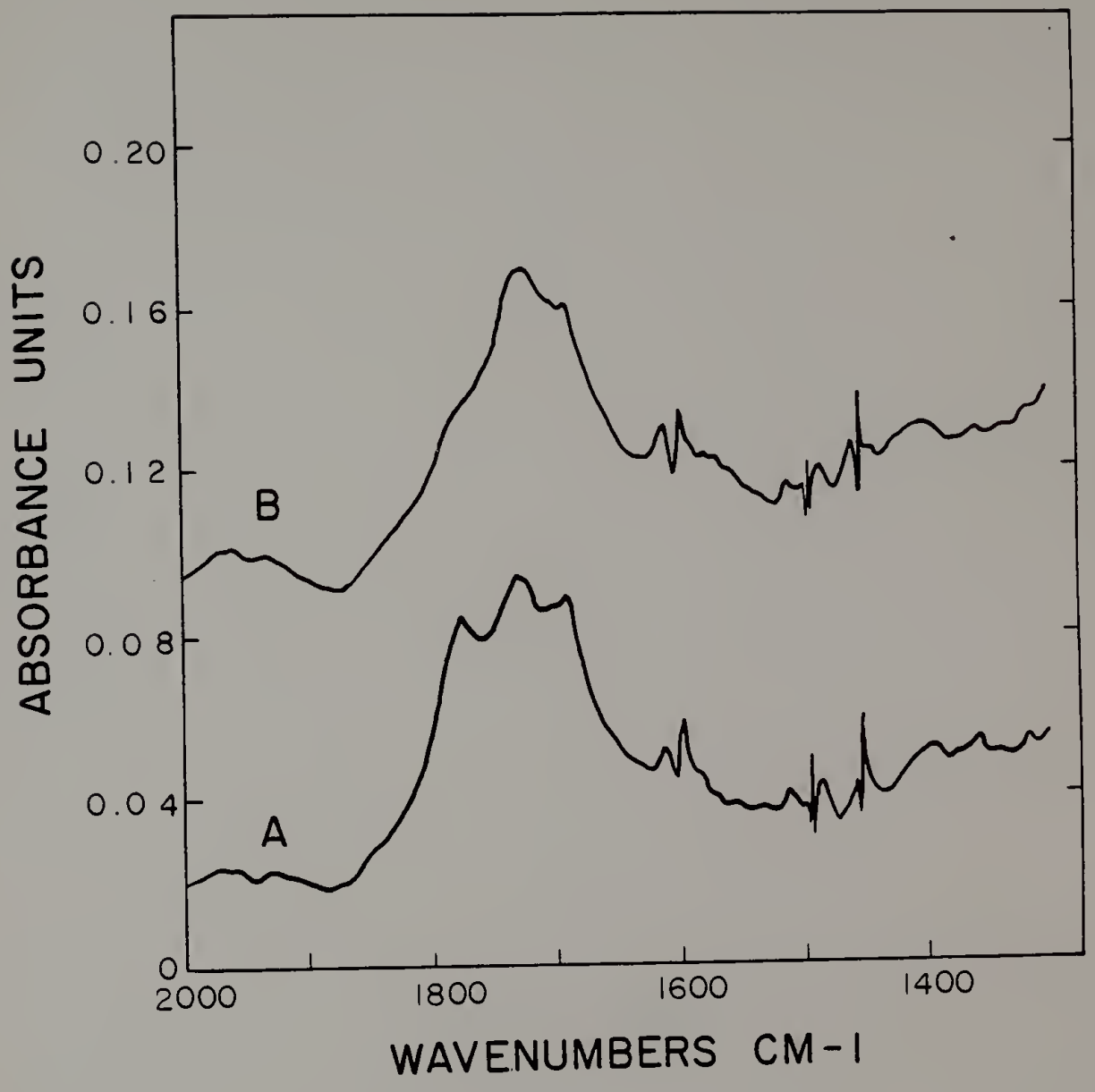
ABSORBANCE UNITS
0.20
0.16
0.12
0.08
0.04
0
B
A
2000
1800
1600
1400
WAVENUMBERS CM-1

irradiated at 75°C and show that the component at 1775cm^{-1} was eliminated upon heating in argon. A similar but less dramatic result was obtained on heating a film irradiated at 30°C (less dramatic because the 1775cm^{-1} product was initially present at a lower concentration). Figure 2.7 also shows that the 1775cm^{-1} product was lost independently of the other carbonyl products, although a minor loss at 1690cm^{-1} may have occurred. Heating a film photooxidized at 60°C to 91°C for 15hrs in the heated ATR attachment (Figure 2.8) produced no change in the carbonyl region (Figure 2.9), indicating that in this case the 1775cm^{-1} product was not lost.

Discussion

Infrared Band Shape

As seen in Figure 2.1, the infrared spectrum of the carbonyl products formed during PS photooxidation is clearly revealed using FTIR-ATR. The existence of three shoulders and maxima (1775, 1725 and 1690cm^{-1}) suggests that there are at least three types of carbonyl groups responsible for this absorption. As the film temperature during photooxidation was raised from 30° to 75°C, there was a change in the relative shoulder heights at 1775 and 1690cm^{-1} (Figure 2.2). This indicates that the processes

Figure 2.8

Design of the heated ATR attachment.

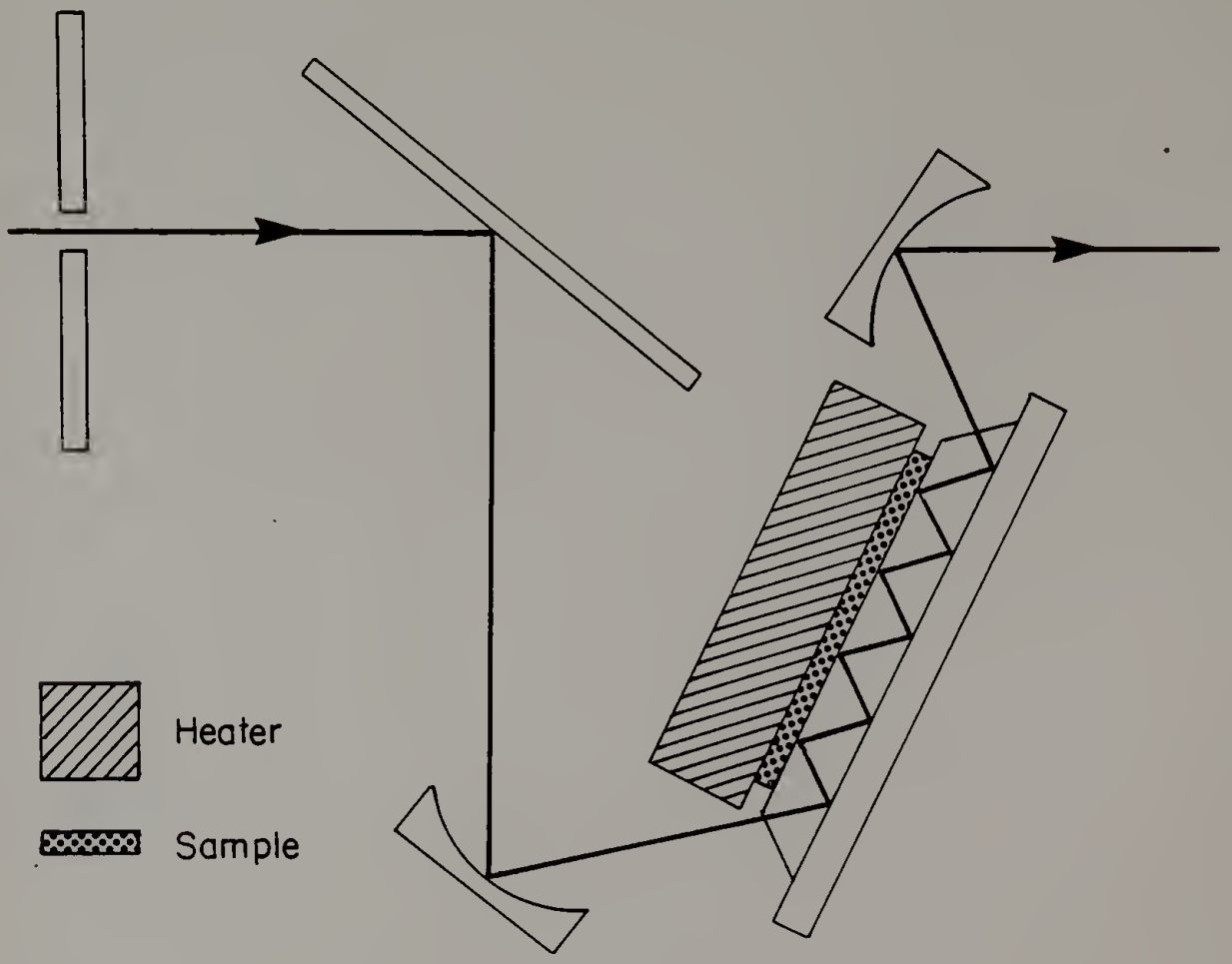
Heater
Sample

Figure 2.9

Heated ATR results. ATR spectra of photooxidized PS before (A) and after (B) heating against the ATR crystal for 15 hrs. at 91°C. No changes were detected.

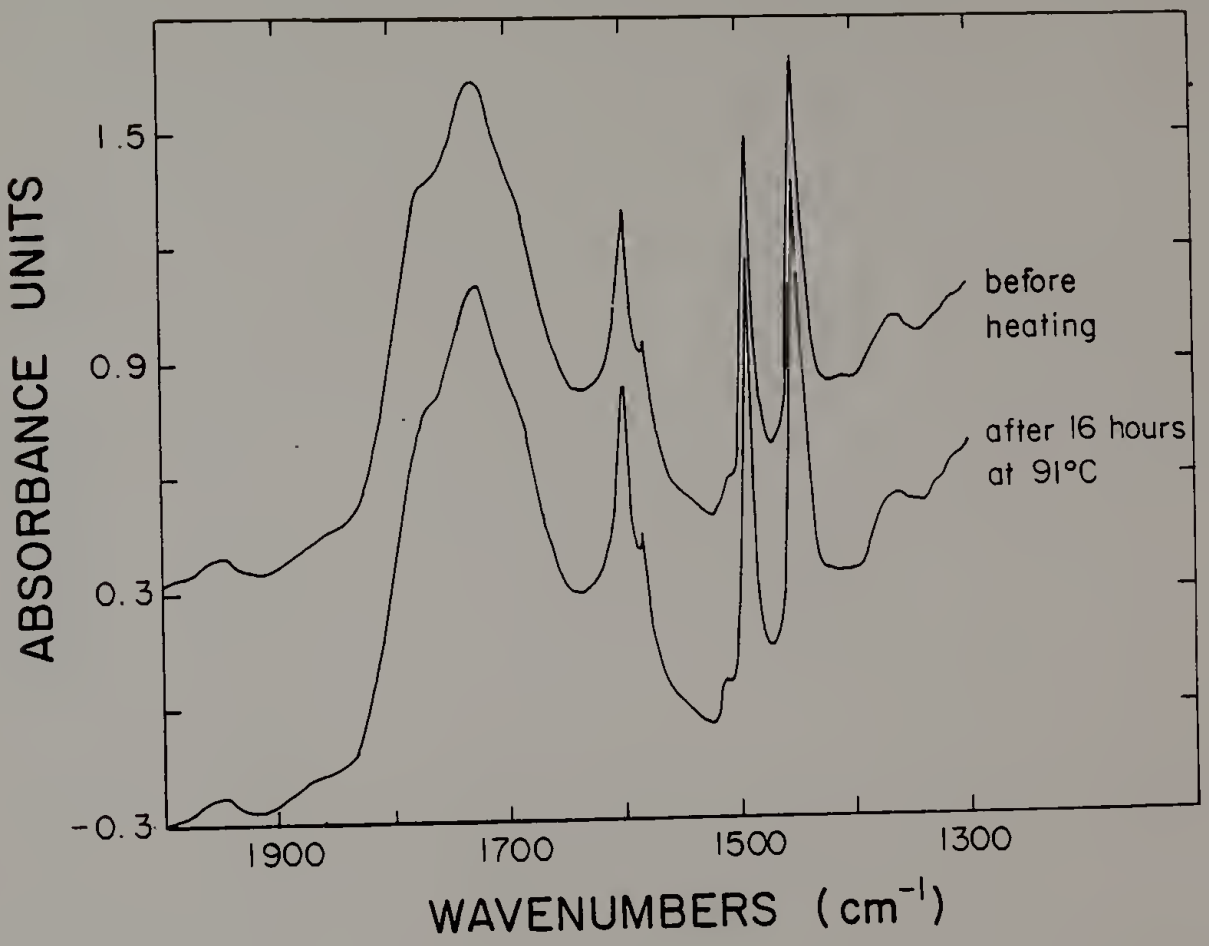
ABSORBANCE UNITS
1.5
0.9
0.3
-0.3
1900
1700
1500
1300
WAVENUMBERS (cm⁻¹)
before heating
after 16 hours at 91°C

that lead to the formation of these two absorptions have different activation energies. Although it is not clear which processes represent the rate determining step (e.g. changes in oxygen permeability, energy transfer to hydroperoxides, etc.), it is plain that these two absorptions represent different carbonyl products. It was noted that the carbonyl absorption is quite broad, even at low UV dosages. This indicates that lightly oxidized carbonyl products continue to react to form highly oxidized groups even at a low overall reaction conversion.

Carbonyl Location

As seen in Table 2.1, the carbonyl concentration gradient constants obtained experimentally are in reasonable agreement with those calculated from published oxygen uptake data. This indicates that the photooxidation products produced in PS are located where they would be expected on the basis of the UV absorption profile.

There are many possible reasons for the lack of quantitative agreement between the calculated and experimentally observed C_o and d_c values. The experimental C_o value depends on the molar absorptivity chosen for the carbonyl products. In the present case, the absorptivity of acetone was used, but this value may not accurately represent the photooxidation products since there is a

broad range of absorptivities for different types of carbonyl groups (66). Another concern is that the quantum yield of oxygen uptake is not accurately known (compare references 10 and 27). Both C_o and d_c are also affected by experimental uncertainty in the angle of incidence of the IR beam. This uncertainty is compounded by the focusing mirrors of the Perkin-Elmer ATR attachment. Finally, possible changes in the refractive index of the PS with reaction conversion were not taken into account. Accuracy in the data in Table 2.1 may be no better than a factor of three.

One interesting feature of the experimental values of C_o and d_c is that there is a trend toward larger C_o and smaller d_c values with increased UV dosage than is predicted a priori. Two possible explanations for this are immediately evident. First, it is known that the UV absorptivity of PS photooxidation products is greater than that of pure PS. This leads to an increase in the fraction of UV absorbed by the top few micrometers of the film as irradiation proceeds. It is therefore possible that the surface layers react more extensively (larger C_o) and the reaction occurs less deeply (smaller d_c) than expected at long exposure times. A second explanation is, of course, that the phenyl ring concentration is not constant with respect to depth into the film or UV dosage. It was assumed

that the phenyl ring absorption at 1950cm^{-1} was a constant so that it could serve as an internal standard to compare with the carbonyl band. It may be, however, that ring opening reactions occur which consume the phenyl rings. This possibility will be explored in Chapter IV.

Post-Irradiation Treatments

Post-irradiation treatments have been used to assign the infrared bands to specific functional groups. This approach has generally involved the use of gas phase reagents because of the problems that can be caused by solvents (e.g. introduction of solvent IR bands, solvolysis, etc.).

The infrared absorption at 1690cm^{-1} has long been associated with the presence of acetophenone-type end groups that result from chain scission. This assignment is consistent with our observation that this product does not react with ammonia vapor, nor was it destroyed by heating. The small decrease that may have occurred in the band upon heating in argon to 87°C (Fig. 2.7) is consistent with the reported production of small quantities of acetophenone itself (10).

Carboxylic acid functional groups appear to be responsible for part of the absorption band at 1725cm^{-1}. The presence of carboxylic acids in photooxidized PS has

previously been proposed on the basis of reaction with ammonia (60). In this study, their presence is confirmed by absorption bands typical of carboxylic acids (ν_{OH} at 3300-2500cm^{-1}, $\nu_{C=O}$ at 1725cm^{-1}, ν_{C-O} at 1265-1230cm^{-1} and δ_{OH} at $\sim$1000cm^{-1}) (67). All of these bands were initially present in the photooxidized PS and were found to react reversibly with ammonia.

Also detectable at 1725cm^{-1} is another product that, like the carboxylic acid, was not lost upon heating. This component, however, was lost upon exposure to ammonia since it did not react reversibly, but seemed to undergo an ammoniolysis reaction. A decrease in the absorption near 1300 and 1190cm^{-1} was also observed which may be associated with the changes in the 1725 or 1775cm^{-1} bands because these bands also showed an irreversible decrease in intensity with ammonia treatment. Esters, peresters and certain carbonates absorb in this general region (68) and all react irreversibly with ammonia (ammoniolysis). The reaction of peresters (69) and aromatic carbonates with ammonia, however, is extremely rapid, so that these structures could be associated with the 1775cm^{-1} band.

Carbonates (15), peresters (10), and ring-opening reaction products such as 2,3-furandione structures (11) have all been reported as possible structures found in photooxidized PS. While all can absorb near 1775cm^{-1}, none

of these structures can be accepted as the major product found at 1775cm^{-1} without some reservation. For example, the 2,3-furandione structure possesses two carbonyl absorption bands (1770 and 1740cm^{-1}), whereas it was seen that the 1775cm^{-1} band can be eliminated by heating in argon without affecting the intensity at 1740cm^{-1}.

Exposing a thin layer of diethyl carbonate to ammonia vapor in a Petri dish for 30 minutes did not cause any detectable reaction. Polycarbonate, which served as a model for aromatic carbonates, reacted rapidly but produced a new, strong band at $\sim$2200cm^{-1}. Since no such band was found in photooxidized PS after exposure to ammonia vapor, it would seem that aromatic carbonates are not present.

Peresters are thermolabile and could be decomposed upon heating in argon. However, the results of the heated ATR experiment indicate that the product absorbing at 1775cm^{-1} was lost by volatilization rather than thermal decomposition. In this experiment, it was seen that holding the PS film firmly against the heated ATR crystal reduced volatilization, and no loss of the 1775cm^{-1} product occurred. This product is therefore a low molecular weight fragment from the PS chain. In lieu of the slow decomposition rate of some peresters at 90°C (70), it is possible that the major product that absorbs at 1775cm^{-1} is a perester that is not bonded to the polymer chain. Since

heating in argon did not diminish the OH stretch peak intensities, a peracid is not an appropriate assignment of this band.

As seen in Figure 2.4, ammonia reacts with most carbonyl products absorbing from 1690 to 1800cm^{-1}. Many weak bands persist, however, and they probably represent a variety of minor products. Exposure to methyl amine led to a rapid reaction with these products that did not prove to be reversible in the same way as ammonia. Instead, a new band formed near 1660cm^{-1}, and a strong band formed at 1405cm^{-1} on subsequent exposure to ammonia and $FeCl_3$. As with the film treated solely with ammonia, the 1405cm^{-1} band may be due to the formation of amide groups (67), but in this case it is a very significant reaction. The new band at 1660cm^{-1} appears to be a new carbonyl product (perhaps a conjugated ketone) which did not react on exposure to ammonia vapor, although if imines formed they would also absorb at this frequency (71). Clearly it is difficult to reconstruct all of the different carbonyl functional groups present in photooxidized PS from their reactivity toward amines. It is plain, however, that much of the structureless absorption extending up to nearly 1800cm^{-1} in ammonia-treated photooxidized PS is not due to simple ketones, as they were found to react rapidly with methyl amine.

The products that absorb at 1775 and 1725cm^{-1} must be very reactive since pyridine vapor seems to have caused the slow decomposition of these functional groups. No carboxylate anion bands were detected, seemingly because of the weak basicity of pyridine and perhaps also because of its high solubility in the unoxidized PS (pyridine dissolves unoxidized PS). The usefulness of pyridine will be considered further in Chapter III.

Conclusions

It has been seen in this chapter that a number of different carbonyl functional groups form in PS as it is photooxidized with 254nm UV in air. FTIR-ATR reveals that these functional groups are distributed along a concentration profile that is consistent with the profile expected from the UV absorptivity of PS at 254nm. The composition of the carbonyl products formed was found to be dependent on the temperature during photooxidation. The different products appear to be present together, even at early times of exposure, although there may be some change in the product distribution at long exposures (see Chapter III).

At least four major carbonyl products form in photooxidized PS. These include a simple ketone at 1690cm^{-1}

such as an acetophenone-type end group, carboxylic acids ($1725cm^{-1}$), another product at $1725cm^{-1}$ and a volatile product at $1775cm^{-1}$. Both unknown carbonyl structures (1725 and $1775cm^{-1}$) react rapidly and irreversibly with ammonia. Several minor constituents of unknown structure were also detected in the 1700 to $1780cm^{-1}$ region.

C H A P T E R III

OH-CONTAINING FUNCTIONAL GROUPS

Introduction

In Chapter II, carbonyl-containing functional groups in photooxidized PS were considered. Another region of the infrared spectrum that provides considerable information about PS photooxidation is the OH stretch region (3600-2600cm^{-1}). Functional groups that could absorb in this region of the spectrum include alcohols, phenols, hydroperoxides, carboxylic acids and peracids.

Little information has been published regarding the OH stretch region of the spectrum of photooxidized PS. The presence of hydroperoxides has long been assumed because they represent primary photooxidation products. Iodometric analysis of photooxidized PS reveals that peroxides, in general, are present (10). An attempt was made to label hydroperoxides for analysis using ESCA by reacting them with sulfur dioxide (72). This treatment was thought to cause the formation of a sulfate half ester, $ROSO_2OH$, by inserting the sulfur dioxide into the O-O bond. Such groups were reportedly found, and this supported the idea that hydroperoxides will form during photooxidation.

Assignment of infrared bands in the OH stretch region has been limited to one study in which photooxidized PS was heated in a nitrogen atmosphere to decompose the hydroperoxides (4). A decrease in the peak intensity at 3540cm^{-1} was noticed and this peak was thus assigned to hydroperoxides.

In the present study FTIR was used to provide clearly resolved spectra of the OH stretch region of photooxidized PS. As in Chapter II, several post-irradiation treatments were employed to aid in band assignment. Most of these post-irradiation treatments were designed to bring about the thermal or chemically-induced decomposition of hydroperoxides, since these products should be distinguishable from other functional groups that absorb in this region.

Experimental

PS film preparation, photooxidation conditions and infrared spectrometry are described in Chapter II. After irradiation, photooxidized PS was exposed to a number of reactive vapor phase reagents under the following conditions. One PS film was exposed to ammonia vapor from ammonium hydroxide and another was exposed to pyridine vapor for 30 minutes in covered Petri dishes. Another

treatment involved exposing photooxidized PS to acetyl chloride vapors in argon at room temperature for 3 hours.

A photooxidized PS film was exposed to sulfur dioxide at one atmosphere and room temperature for four hours. This was accomplished by placing the film in a vacuum desiccator, evacuating the desiccator and then filling it with one atmosphere SO_2. Another film was exposed to the mixed acid vapors from hydriodic and hydrochloric acids at room temperature in argon for two hours. The final post-irradiation treatment was to heat a photooxidized PS film on a NaCl infrared plate to 145°C for two hours in a nitrogen atmosphere.

Iodometry

In addition to observing changes in the infrared spectrum caused by exposure to ammonia, the total peroxide content of ammonia-treated films was determined iodometrically. In this experiment, two large PS films (2"x3") were irradiated simultaneously. After exposure, the films were cut in half, and one half from either film was exposed to ammonia vapor for 30 minutes in a Petri dish followed by storage over $FeCl_3$ for three days. The other halves were stored with $FeCl_3$ for 3 days without exposure to ammonia. After 3 days, the films were analyzed iodometrically to determine the total peroxide content of

each sample by the method of Banerjee and Budke (73). Results for the calibration curve are given in Appendix D.

Results

Infrared Band Shape

An increase in absorbance in the OH stretch region of the infrared spectrum was observed as PS was photooxidized. This result is shown qualitatively in Figure 3.1. It is seen here that the first sign of photooxidation in this region is the appearance of a weak absorption at 3540cm^{-1}. This is followed by an increase at 3540cm^{-1} and the appearance of a band at 3440cm^{-1}. Both of these peaks continue to grow with UV dosage. Finally a peak becomes visible at 3250cm^{-1} and this occurs at the same time that absorption below 2800cm^{-1} can be detected. Absorption eventually extends to about 2500cm^{-1}.

The quantitative aspects of peak height growth with UV dosage are best measured by transmittance rather than reflectance since such an experiment samples through the entire film thickness. Increases in peak height as a function of UV dosage are shown in Figure 3.2 for the 3540cm^{-1} band. It is seen here that the peak growth is faster at higher temperatures, but that the peak height reaches a limiting value that is greater at lower

Figure 3.1

Increase in absorption in the OH stretch region as PS is photooxidized (KRS-5,45°).

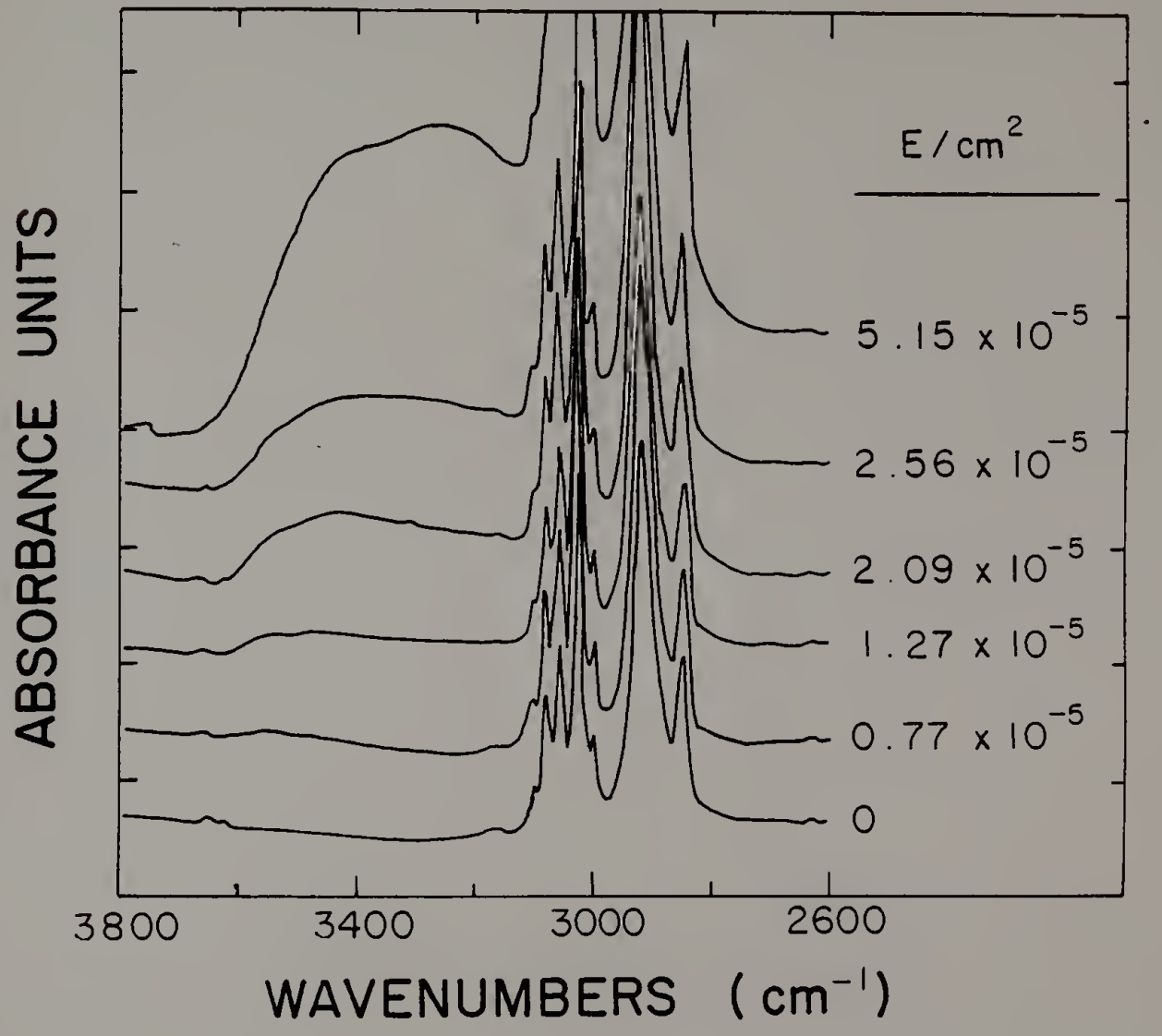
ABSORBANCE UNITS
E / cm^2
5.15 x 10^{-5}
2.56 x 10^{-5}
2.09 x 10^{-5}
1.27 x 10^{-5}
0.77 x 10^{-5}
0
3800
3400
3000
2600
WAVENUMBERS (cm^{-1})

Figure 3.2

3540cm^{-1} band intensity vs. temperature. Peak intensity of the 3540cm^{-1} band as a function of UV dosage and film temperature during irradiation.

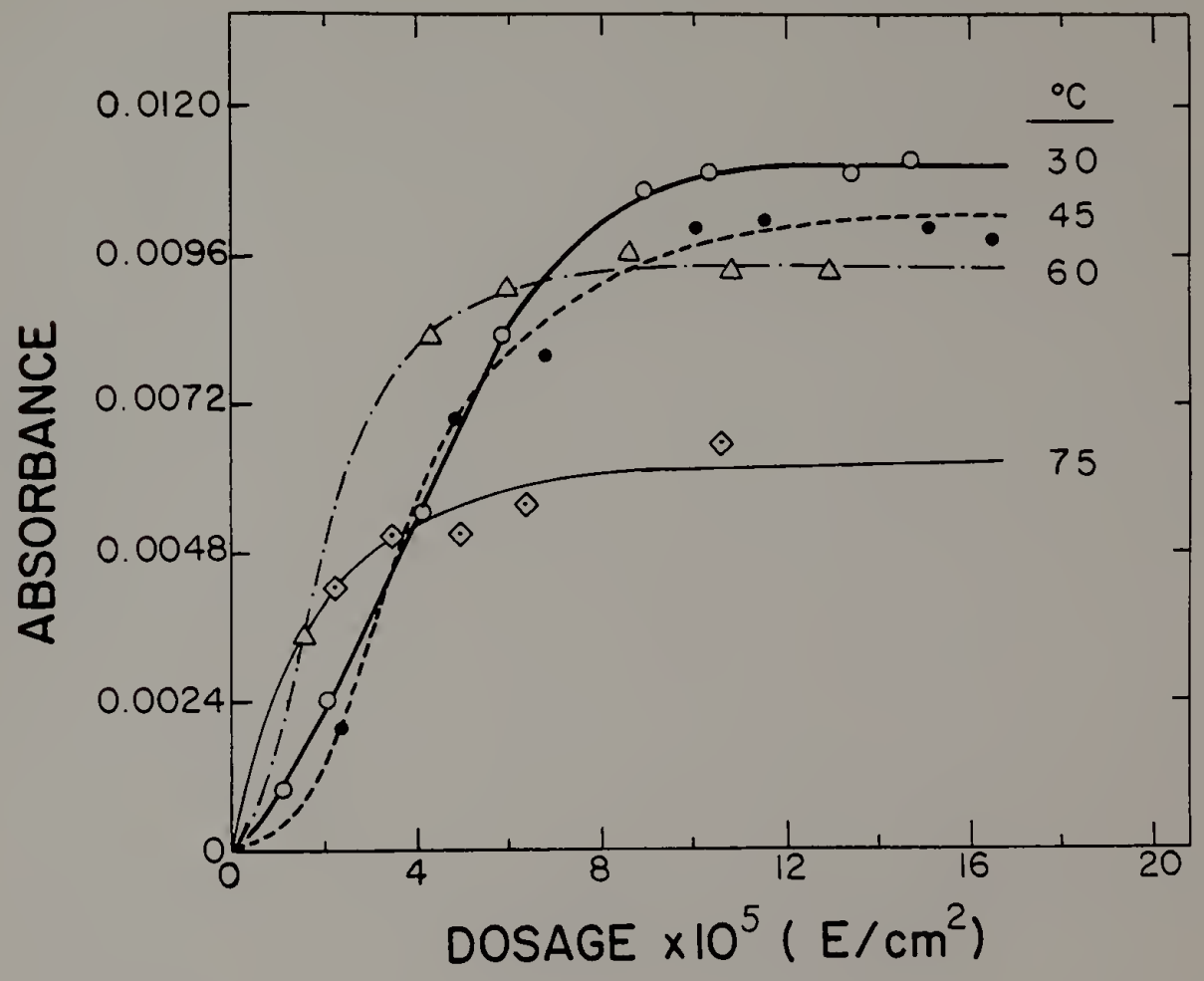
ABSORBANCE
0.0120
0.0096
0.0072
0.0048
0.0024
0
0
4
8
12
16
20
DOSAGE x10^5 (E/cm^2)
°C
30
45
60
75

temperatures. Qualitatively similar results were obtained for the band at 3440cm^{-1}, although the limiting values that were reached were approximately twice that of the 3540cm^{-1} band, and they required 1.3×10^{-4}E/cm^2 to be reached.

Post-Irradiation Treatments

When photooxidized PS was exposed to ammonia or pyridine vapor, a decrease in the 3540 and 3440cm^{-1} bands was detected. This change is partially obscured in the case of ammonia because of the strong ammonium ion band that forms, which is centered at 3180cm^{-1}. The peak intensity lost at 3540 and 3440cm^{-1} was not regained after storage over ferric chloride for three days and the intensity at about 3180cm^{-1} remained somewhat above its initial value. Exposure to pyridine caused a decrease at 3540 and 3440cm^{-1}, and a small increase from 3300 to 3100cm^{-1} (or below). These results are shown in Figure 3.3.

Small decreases in peak intensity at 3540 and 3440cm^{-1} were observed when photooxidized PS was exposed to the mixed vapors of hydriodic and hydrochloric acids and when a film was heated in nitrogen to 145°C. In both cases, the decreases observed were only 10-15% of the initial peak height. However, the mixed acid vapors caused an increase in absorption at about 3200cm^{-1}, whereas the heat-treatment led to a small decrease in this region.

Figure 3.3

Pyridine vapor treatment. Absorbance spectrum of photooxidized PS before (_____) and after (_ _ _ _) exposure to pyridine vapor. Note the decrease in intensity at 3540 and 3440cm^{-1}, and the increase at about 3250cm^{-1}.

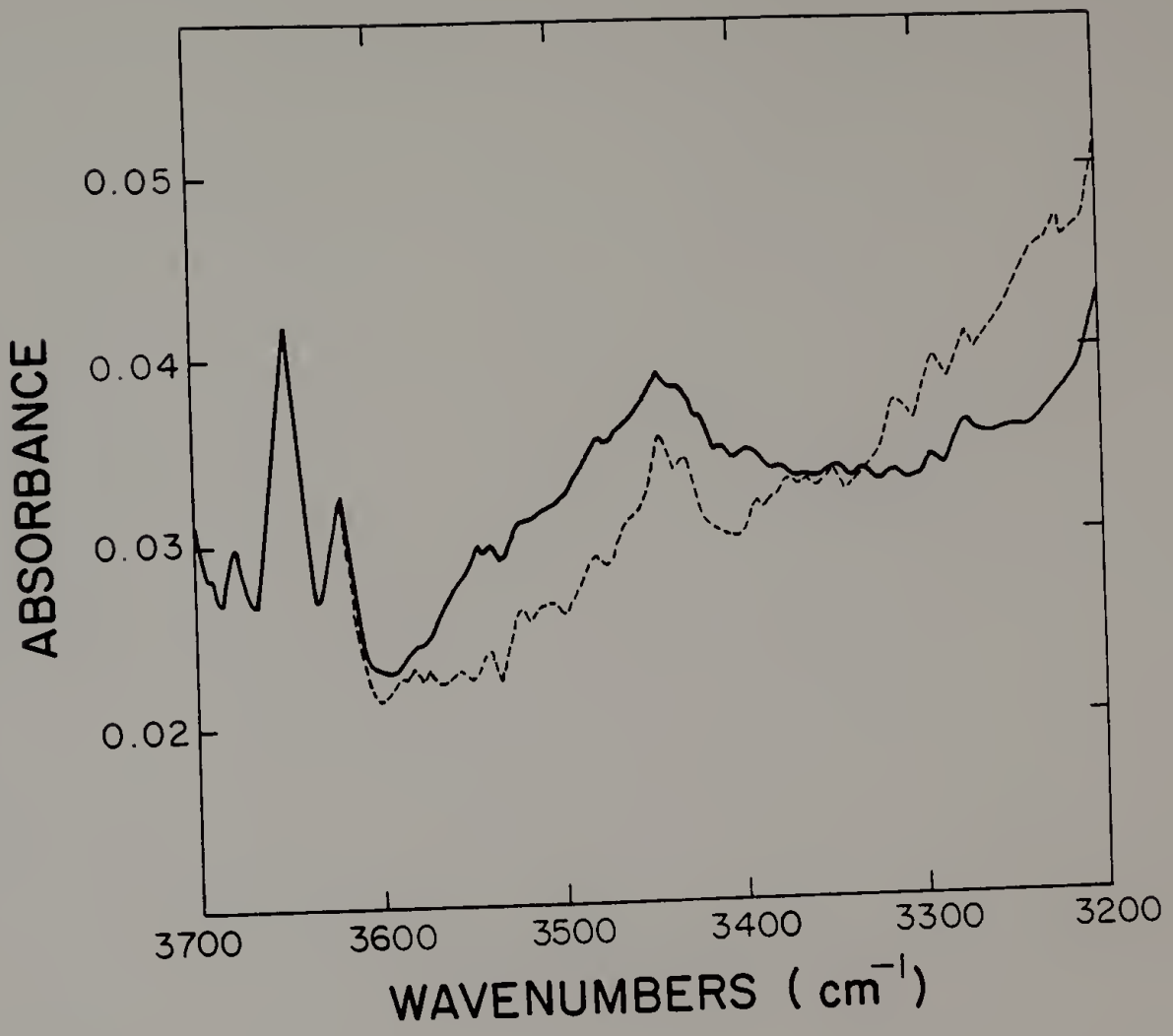
ABSORBANCE
0.05
0.04
0.03
0.02
3700
3600
3500
3400
3300
3200
WAVENUMBERS (cm⁻¹)

Exposing photooxidized PS to sulfur dioxide introduced two new absorption bands into the spectrum at 1331 and 1144cm^{-1}. A broadening of the OH stretch region was observed, with absorption extended to frequencies above 3600cm^{-1}. Spectral subtraction in the carbonyl region revealed two new bands at 1710 and 1620cm^{-1}. These results are shown in Figure 3.4, where the peak at 1331cm^{-1} is also seen.

When acetyl chloride vapor was passed over photooxidized PS, new peaks appeared at 1805 and 1100cm^{-1} (Figure 3.5). A general increase in absorption in the OH stretch region was also detected and it appeared to be centered at 3240cm^{-1}. Storing the film in nitrogen for 15 hours at room temperature eliminated the 1805 and 1100cm^{-1} bands, and returned the OH stretch absorption to its previous strength.

Iodometry

Two determinations were made of the effect of ammonia treatment on the peroxide content of photooxidized PS. It was found that the ammonia treatment decreased the total peroxide content of the films, but this technique did not prove to be very repeatable. In one case, the peroxide content was found to decrease by 34%, while the other determination gave a decrease of only 3% on a per cm^2 of

Figure 3.4

Sulfur dioxide treatment. Difference spectrum showing only the new bands created in photooxidized PS following exposure to sulfur dioxide. The peak at 1331cm^{-1} is due to dissolved SO_2.

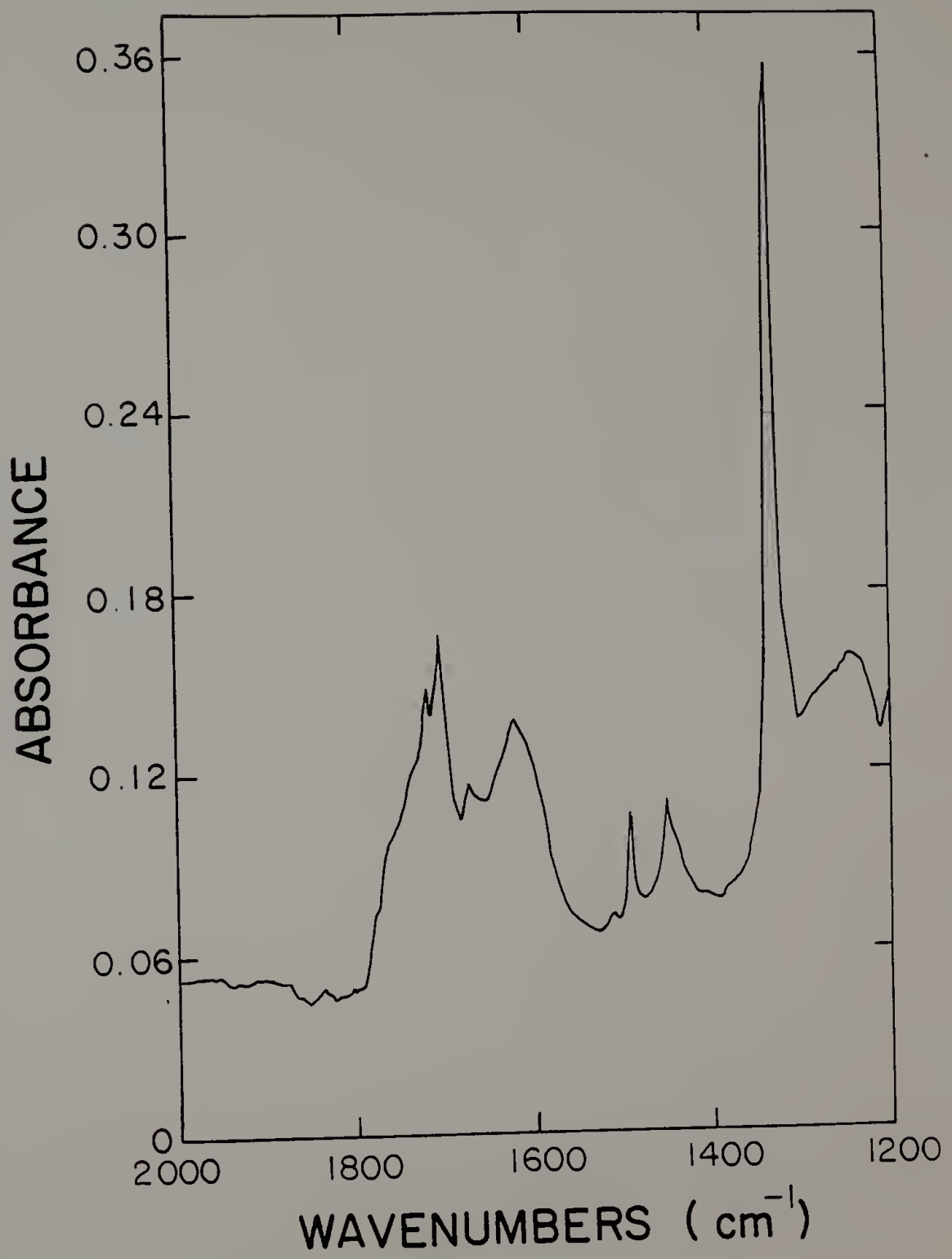
0.36
0.30
0.24
0.18
0.12
0.06
0
ABSORBANCE
2000
1800
1600
1400
1200
WAVENUMBERS (cm⁻¹)

Figure 3.5

Acetyl chloride treatment. Difference spectrum showing dissolved, unreacted acetyl chloride bands at 1805 and 1100cm^{-1} following exposure to acetyl chloride vapor.

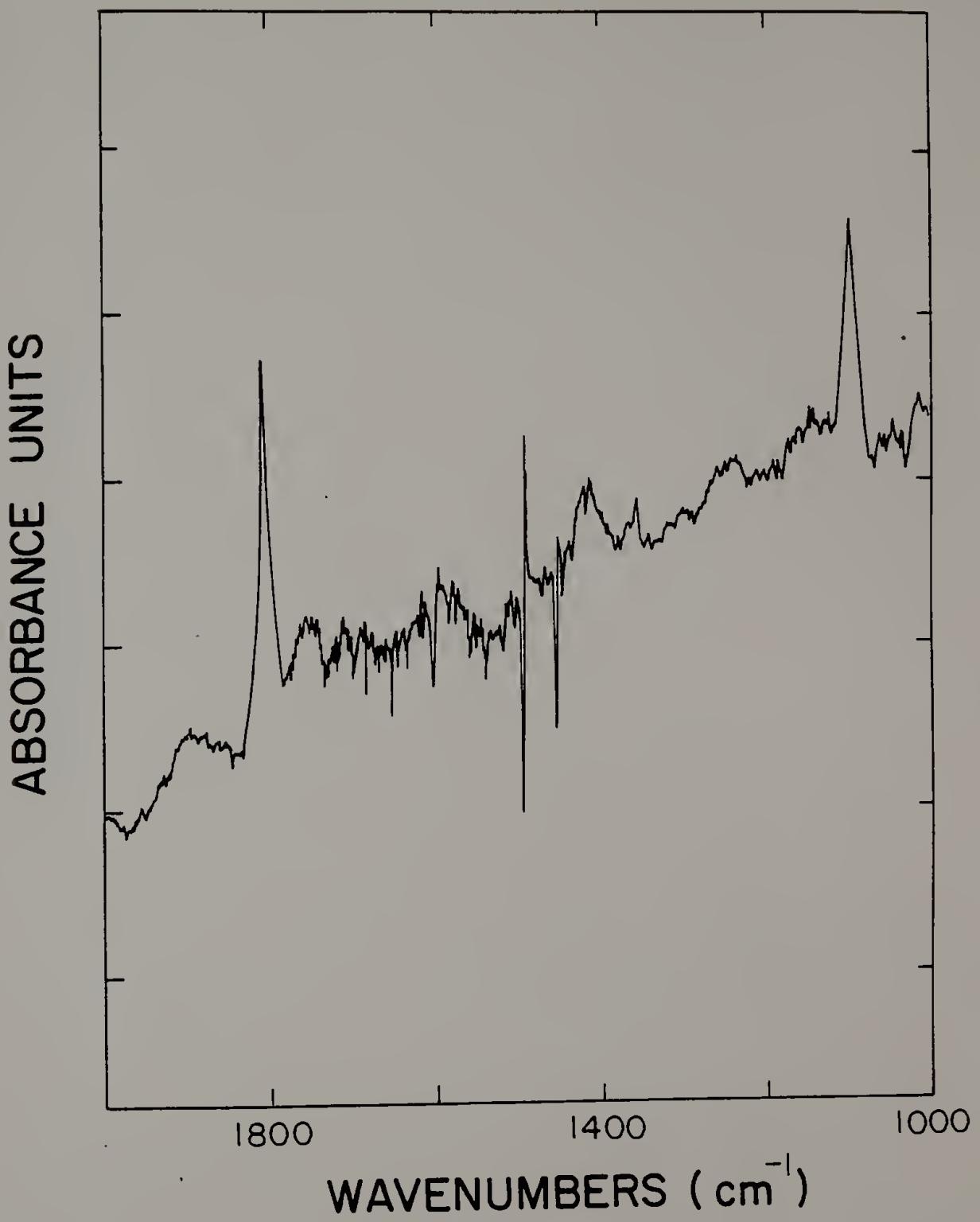
ABSORBANCE UNITS
1800
1400
1000
WAVENUMBERS (cm^{-1})

film basis. It was noticed that the acetic acid/chloroform solvent did not completely dissolve the PS films, and this likely contributed to the lack of repeatability.

Discussion

Infrared Band Shape

As PS is photooxidized, a very broad absorption develops in the OH stretch region of the infrared spectrum. The first band to develop is found at 3540cm^{-1}, and this is consistent with results reported for 365nm UV photooxidation (59). This frequency is appropriate for free (not H-bonded) hydroperoxides (74) and this assignment of the 3540cm^{-1} band is supported by the results discussed below.

The next band to form appears at 3440cm^{-1}, which is a frequency appropriate for H-bonded hydroperoxides (75). This progression, from 3540 to 3440cm^{-1} bands, is probably something to be expected. As the concentration of polar groups increases near the film surface, the opportunity for hydrogen bonding also increases, and this seems to be what is observed in the present case.

The simultaneous development of absorptions at 3250 and the region below 2800cm^{-1} may indicate that they are both produced by the same functional group. This is thought to be the case, with the OH stretch on carboxylic acids

being responsible for these bands. However, the OH stretch from H-bonded alcohols and phenols also reportedly appears near 3300cm^{-1} (67), and it is not known how much they may contribute to this absorption.

Figure 3.2 has shown that the 3540cm^{-1} peak develops more slowly and reaches a higher limiting value when PS is photooxidized at 30°C than at higher temperatures. The slower rate of development at 30°C is consistent with the observation that hydrogen production in vacuum photolysis of PS has a positive temperature coefficient (3) i.e. the initiation of photodegradative reaction proceeds faster at higher temperatures. This, however, cannot be the complete explanation for this behavior because energy transfer to hydroperoxides from excited phenyl rings is reported to produce free radicals much more rapidly than occurs by simple photolysis (10). Thus, some other mechanism is probably responsible for the faster initial growth of the 3540cm^{-1} band at higher temperatures.

Changes in the efficiency of energy transfer processes with temperature may be the reason for the temperature-dependence in the magnitude of the limiting value obtained (Figure 3.2). Although this has not been investigated in detail, it is known that fluorescence intensity generally decreases with increasing temperature (76). This means that at higher temperatures, less of the

UV energy absorbed by the film is lost through photon emission, so that a greater fraction of this energy may be available for photooxidative reactions. Likewise, other photophysical deactivation processes might be activated by increasing temperature, such as transfer to hydroperoxide "energy sinks".

Finally it should be mentioned that it is not evident from infrared spectra alone whether the limiting values reached for the 3540 and 3440cm^{-1} bands reflect steady state conditions or if perhaps that the reaction becomes autoinhibiting. Restated, it is possible that at long exposure times, steady state conditions develop where the loss of water and carbon dioxide removes OH and carbonyl functional groups as quickly as they form. Alternatively, it is also possible that at long exposure times, a highly oxidized layer forms on the surface of the PS film which is chemically stable and that serves as a protective layer to stop photooxidation. This question is investigated in Chapter IV.

Post-Irradiation Treatments

The decomposition of hydroperoxides by amines is well known (77,78), and the reaction of some peroxides with amines is so rapid as to be considered explosive (79). The rapid decomposition of hydroperoxides by ammonia vapor

seems to have occurred in the present study. A decrease in peak intensity at 3540 and 3440cm^{-1} took place rapidly and irreversibly, and this supports the assignment of these bands to hydroperoxides.

Although the 3540 and 3440cm^{-1} bands undergo an irreversible reaction with ammonia, as did the 1775cm^{-1} carbonyl band, it is evident that these OH stretch bands do not represent peracid functional groups. This is because these absorption frequencies (3540 and 3440) are appropriate for hydroperoxides, but are not appropriate for peracids (80) which appear at 3300 to 3280cm^{-1}. Also, the loss of the 1775cm^{-1} band upon heating at 87^{o}C (Figure 2.7) was not accompanied by a decrease in the OH stretch region of spectrum. Therefore, the 3540 and 3440cm^{-1} bands and the 1775cm^{-1} band represent two different functional groups.

The rapid decrease in the 3540 and 3440cm^{-1} bands upon exposure to pyridine vapor at room temperature (Figure 3.3) is interesting. The decomposition of hydroperoxides by pyridine has been reported (81), but this reaction proceeds rapidly for primary and secondary hydroperoxides only. Since tertiary hydroperoxides are reportedly stable with pyridine at 60^{o}C for several hours, it seems that the 3540 and 3440cm^{-1} bands in photooxidized PS are not produced by tertiary hydroperoxides. This is surprising since hydroperoxides are generally thought to form from the

tertiary carbon on the PS backbone (82). Their formation from ring-opening reactions has also been proposed (11), and this idea may be supported by the present results from pyridine exposure.

Small decreases in peak intensity at 3540 and 3440cm^{-1} accompanied exposure to HI/HCl vapors. These mixed acids vapors, however, are reportedly able to decompose relatively stable peroxides (83). This suggests that only a limited quantity of these acid vapors actually entered the PS film under these experimental conditions. The increase in absorption at about 3200cm^{-1} is consistent with the expected formation of alcohol groups following reaction with iodide.

Thermally-induced decomposition of the 3540cm^{-1} band has been reported and this led to its being assigned to hydroperoxides (4). In the present study, heating photooxidized PS to 145^{o}C in nitrogen led to a drop in peak intensity at 3540 and 3440cm^{-1}, as well as in the 3200cm^{-1} region. As with the results from amine and acid vapors, these results support the assignment of the 3540 and 3440cm^{-1} bands to hydroperoxides. The results from the reactive vapors, however, provide the stronger evidence because a decrease in peak intensity upon heating could be due to evaporation. The decrease at 3200cm^{-1} on heating may be due to some decarboxylation process occurring since

there was also a general decrease in band intensity between 1800 and 1680cm^{-1}.

An additional confirmation of the hydroperoxide assignment was sought through the use of SO_2. It has been reported that sulfur dioxide can selectively react with hydroperoxides to form sulfate groups by an insertion reaction into the O-O bond (84). This technique has been used to detect hydroperoxides in photooxidized PS using ESCA (72). The present results, however, call this approach into question since no new bands associated with sulfates were detected. Instead, large quantities of dissolved SO_2 were detected together with what appear to be hydroperoxide decomposition products. These include what is thought to be the free OH stretch of alcohols (ν >3600cm^{-1}), a carbonyl product at 1715cm^{-1} and perhaps another carbonyl product at 1620cm^{-1}. The 1620cm^{-1} band comes at a frequency more typical of olefins, but no new olefin bands could be distinguished in the 1000-700cm^{-1} region. The well-known decomposition of cumene hydroperoxide by SO_2 (88) to acetone and phenol suggests an explanation for the OH stretch and 1715cm^{-1} bands, but not for the 1620cm^{-1} band. Thus, as with the results stated above for pyridine, the SO_2 results may imply that the hydroperoxides in photooxidized PS are not formed off the tertiary backbone carbon.

Finally, acetyl chloride was used in an attempt to react with the OH containing groups at 3540 and 3440cm^{-1}. It was hoped that this would provide additional information about these groups because the expected products (acetates or peracetates) can readily be distinguished in the infrared. It was surprising to see that the acetyl chloride would dissolve in the photooxidized PS film and then evaporate out again with time.

Iodometry

Qualitative confirmation for the amine catalyzed decomposition of hydroperoxides was obtained by iodometric analysis. The experiment was not very repeatable, however, and this was somewhat surprising since this procedure has been used in recent publications (4,10). One obvious problem is that the acetic acid/chloroform solvent used had failed to dissolve the films completely. This could affect the ability of the iodide ion to reach the peroxides. The solubility problems may have been undetected in the published studies if the UV dosages in the present study were greater than the dosages used in these published experiments, as this would affect solubility. Regardless, the present results support the interpretation that a decrease in peak intensity at 3540 and 3440cm^{-1} upon exposure to ammonia is accompanied by a decrease in

peroxide content of the film.

Conclusions

As PS is photooxidized, infrared absorption bands in the OH stretch region appear first at 3540, then at 3440 and finally at 3250, with absorbances down to about 2500cm^{-1}. Band assignment has been made on the basis of absorption frequency and reactivity toward heat and reactive vapor phase reagents. In this way, the 3540 and 3440cm^{-1} bands were assigned to free and hydrogen-bonded hydroperoxides, respectively. Absorptions below 2800cm^{-1} are due to carboxylic acids. The band maximum at 3250cm^{-1} is also thought to be caused by carboxylic acids, although it should include contributions from alcohols and/or phenols if they are present.

Limiting values for peak intensity with irradiation time of the 3540 and 3440cm^{-1} bands were observed. These values were inversely related to the film temperature during photooxidation. The origin of these limits has not been determined, although speculation is offered.

C H A P T E R IV

REACTION SITE AND THE FINAL FILM STATUS

Introduction

In Chapters II and III, experiments were performed to identify the structure and rate of formation of functional groups in PS during photooxidation. New evidence was provided to aid in the assignment of IR bands to particular chemical structures. Two important questions were raised as a result of these experiments, however, and they will be discussed here in Chapter IV. The first concerns the involvement of the phenyl ring in photooxidation reactions. The second concerns the chemical interpretation of the observed limiting values for IR peak intensities such as was seen for hydroperoxide or carbonyl bands.

The first question, that of the importance of phenyl ring reactions, is a central and as of yet unresolved issue. Two general opinions are currently held. One opinion is that the aliphatic polymer backbone is the site of most reactions (5,10,89,90). The other holds that most of the functional groups form from reactions occurring on the pendant phenyl rings (11,15,49).

A number of different low molecular weight compounds have been used to model PS photooxidation. These include cumene, ethyl benzene (91) and 2-phenylbutane (11). In the case of 2-phenylbutane, the resulting photooxidation products were separated chromatographically and were found to contain a number of ring-opened products. This indicates that ring-opening reactions are possible in PS, yet it does not indicate their relative importance. Critics of these experiments argue that PS is a glassy high polymer and that diffusional constraints may determine which processes are dominant in PS (10). This is a very different situation from that found using a well-stirred, liquid model compound. Another general objection to the use of these liquid model compounds is that none allows for the often-described intramolecular reactions such as hydroperoxide decomposition (Figure 1.3) (5,10). This is because none of these compounds possesses the needed alternating arrangement of phenyl rings along an aliphatic backbone.

In this Chapter, the question of phenyl ring reactions is investigated using a polymeric model compound. This model compound is a homopolymer of chain deuterated polystyrene (PSD_3). The importance of ring reactions can be judged with this model polymer because of differences in the infrared absorption frequencies of protium- and

deuterium-containing functional groups. Thus, hydroperoxides that form from ring reactions will absorb at 3540 or 3440cm^{-1} (Chapter III), whereas those forming off the main chain will contain deuterium and will be found at 2600 to 2500cm^{-1} (96).

The second major question approached in this chapter is that of a chemical interpretation of the limiting values reached for IR peak intensities. An example of this is seen in Figure 4.1, which shows the carbonyl band intensity as a function of UV dosage. It is seen here that peak intensity depends only on the UV dosage (rather than light intensity) and that a limiting value is reached after about $5x10^{-4}E/cm^2$.

Two possible explanations exist for the behavior seen in Figure 4.1. One explanation is that the limiting value represents steady-state conditions, where carbonyl containing functional groups are lost as carbon dioxide as rapidly as they are formed (15). Alternatively, it is possible that a highly oxidized layer forms on the surface of the PS film that is more photostable than the pure PS. This would represent a protective layer that causes the reaction to become autoinhibiting.

In order to investigate this question, a more fundamental measure of photooxidation must be used. This involves measuring oxygen uptake by a manometric method

Figure 4.1

Carbonyl intensity vs. dosage. Carbonyl peak intensity at $1725cm^{-1}$ is found to reach a limiting value after about $5x10^{-4}E/cm^2$. Note that peak intensity depends on total UV dosage rather than UV intensity.

● - $1.95x10^{-6}E/cm^2 \cdot hr$, O - $1.23x10^{-5}E/cm^2 \cdot hr$

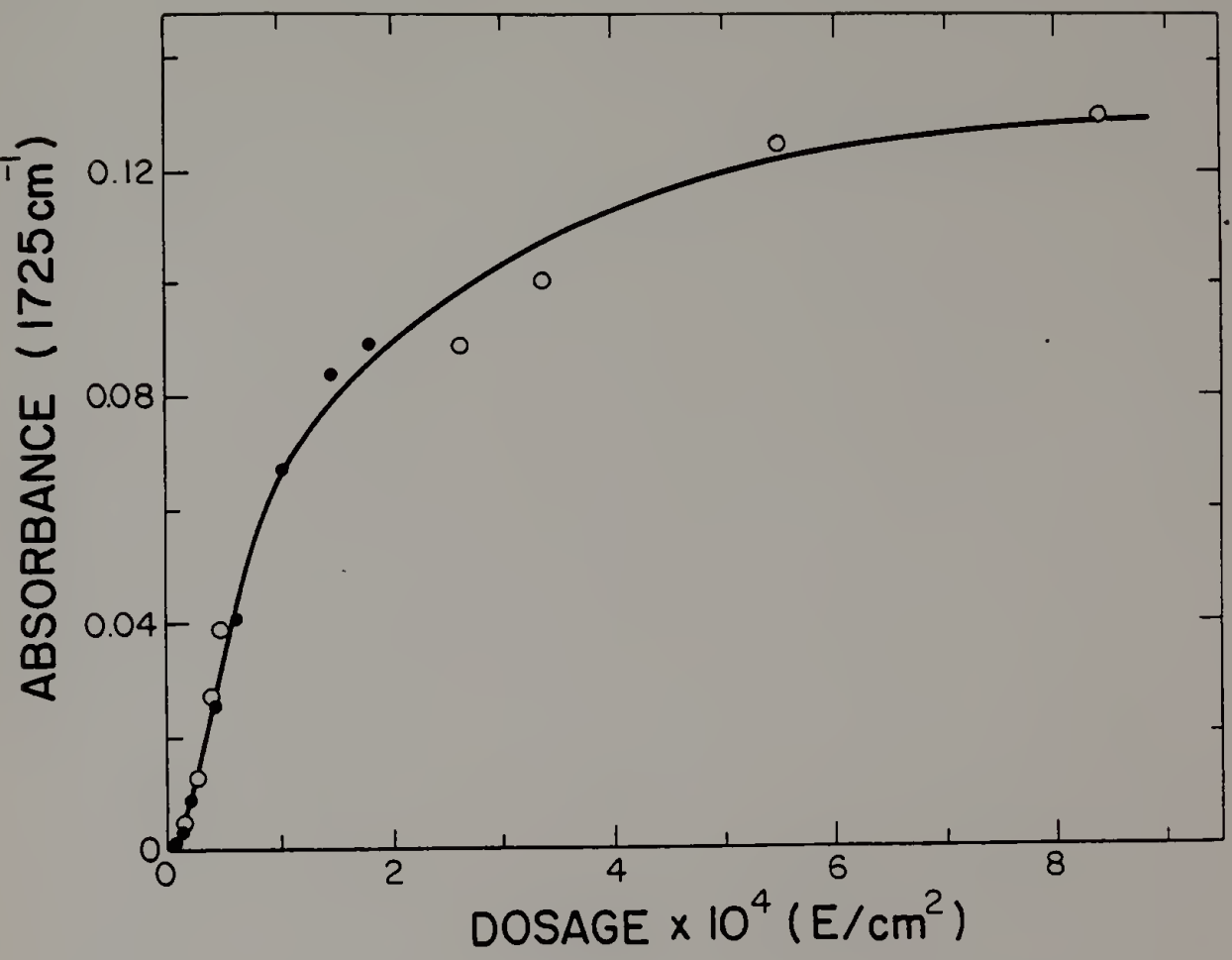
ABSORBANCE (1725cm⁻¹)
0.12
0.08
0.04
0
0
2
4
6
8
DOSAGE x 10⁴ (E/cm²)

similar to that used by Grassie and Weir (58). UV dosages must be greater than $5x10^{-4}E/cm^2$, which is much greater than values typically reported in the literature. The interpretation of this experiment is quite straight-forward. If oxygen uptake proceeds at the same rate above $5x10^{-4}E/cm^2$ as it did below this value, a steady state situation is indicated. Alternatively, if oxygen uptake stops, then a protective layer must have formed.

Experimental

Deuterated Polystyrene

Thin films of chain deuterated polystyrene were cast from dilute chloroform solution and dried under vacuum according to the procedure described for PS in Chapter II. This polymer had been prepared by anionically polymerizing α,β,β-trideuterostyrene (MSD Isotopes of Canada, 99%D) using butyllithium. It had a molecular weight of $\bar{M}n=275,000$, with $\bar{M}w/\bar{M}n=1.89$.

The PSD_3 polymer was further characterized using thermal and spectroscopic methods. It was found using DSC to have the same Tg as the PS used elsewhere in this study. Thus, for PSD_3, Tg is 103°C and for PS Tg is 104°C when scanned at 20°C/min. The PSD_3 was found to have the same UV

absorption spectrum as PS. The quantum yield of fluorescence for films of these two polystyrenes in air was also found to be equivalent, with $\phi_{fl}=0.13\pm0.04$ for PSD_3 and $\phi_{fl}=0.15\pm0.04$ for PS. An aqueous solution of phenol was used as a fluorescence standard (0.000171Molar) (92).

Thin films of PSD_3 ($\sim$15μm) were photooxidized in air using 254nm UV as described in Chapter II. After photooxidation, one film was exposed to ammonia vapors over ammonium hydroxide in a covered Petri dish for 35 minutes. Another film was exposed to ammonia vapors from ND_4OD for 2.5 days. A third film was stored with D_2O vapor in a sealed jar for six days. Finally, another film was heated in nitrogen to 142°C for 2 hours.

Oxygen Uptake

Oxygen uptake in PS photooxidation was measured using the apparatus shown in Figure 4.2. The apparatus was composed of two identical chambers connected by a U-shaped tube (differential manometer) of constant inside diameter. This tube contained dioctyl sebacate, which served as a manometric fluid. The two chambers were sealed with 55/50 quartz cones with flat quartz windows on top. A PS film (0.316 cm^2) was placed in one chamber while the other contained an empty brass sample holder. Both chambers contained 5A molecular sieves to absorb carbon dioxide and

Figure 4.2

Oxygen uptake apparatus. Schematic of the oxygen uptake apparatus. The U-shaped tube connecting the two chambers contains dioctyl sebacate. Gas pressure differences between the two chambers provide a measure of oxygen uptake.

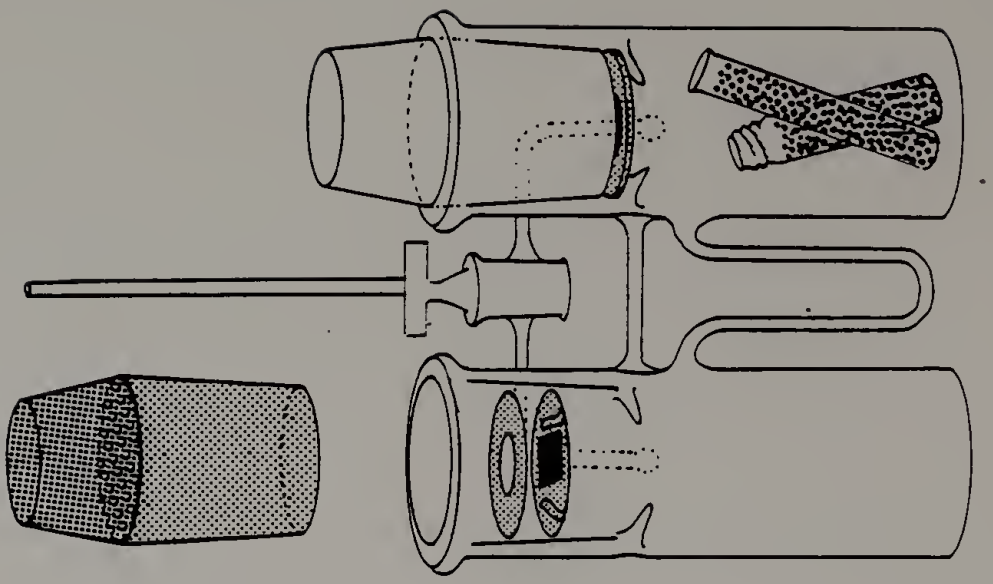

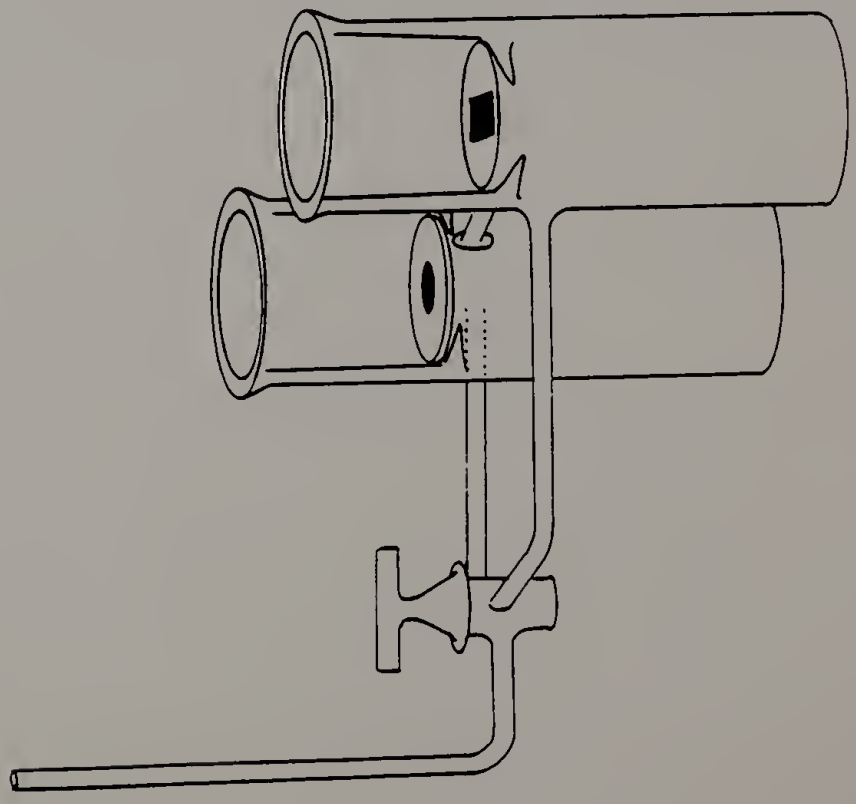

water vapor (10). Each chamber held 375cm^3 of air.

Both chambers were connected by an external glass tube that passed through a three-way valve and into a long, vertical tube. This arrangement made it possible to submerge the chambers in a constant temperature bath, and still have both vented to the atmosphere during a period of thermal equilibration. It was found necessary to vent the chambers for two days in order to achieve long term stability. The first day allowed the apparatus to warm up to 30.0°C and the second day included having the UV lamp (254nm, unfiltered) in operation. For this reason, the vent tube was connected to a trap containing powdered potassium hydroxide at dry ice temperatures to prevent water vapor and carbon dioxide from entering the apparatus. This also meant, however, that the amount of oxygen consumed during photooxidation was measured from the time the three-way valve was closed, rather than from the beginning of UV exposure.

As photooxidation proceeded, oxygen was consumed in the chamber containing the PS film and this led to a gas pressure drop in this chamber. The amount of oxygen consumed was determined using a cathetometer, which could measure the displacement of the manometric fluid in the U-tube.

The stability of the apparatus was checked by

operating it with both chambers containing empty sample holders. Long term stability was confirmed using this procedure.

A test was also made to determine if the molecular sieves had become saturated with carbon dioxide during the course of PS photooxidation. After photooxidizing the PS film, the apparatus was quickly dismantled. The molecular sieves from the PS chamber were placed in a sealed jar and weighed. They were then exposed to dry carbon dioxide gas for 5 minutes followed by a 5 minute exposure to dry air (to displace un-adsorbed carbon dioxide) and were reweighed. The mass difference between these two weighings represented the unused adsorption capacity of the molecular sieves.

Results

Deuterated Polystyrene

The use of FTIR-ATR revealed that as PSD_3 was photooxidized using 254nm UV, a strong OH stretch band was produced (Figure 4.3). This band included peaks at 3540 and 3440cm^{-1}. Spectral subtraction of the PSD_3 bands from the photooxidized PSD_3 failed to reveal any new absorption peaks at 2500cm^{-1}. At longer exposure times, a band maximum developed at 3250cm^{-1} with absorptions extending down to

Figure 4.3

Photooxidized PSD_3. Infrared ATR spectra of PSD_3 before (_ _ _) and after (_____) photooxidation. Note the strong OH stretch band (3600-3000cm^{-1}) and the absence of an OD stretch band (2500cm^{-1}).

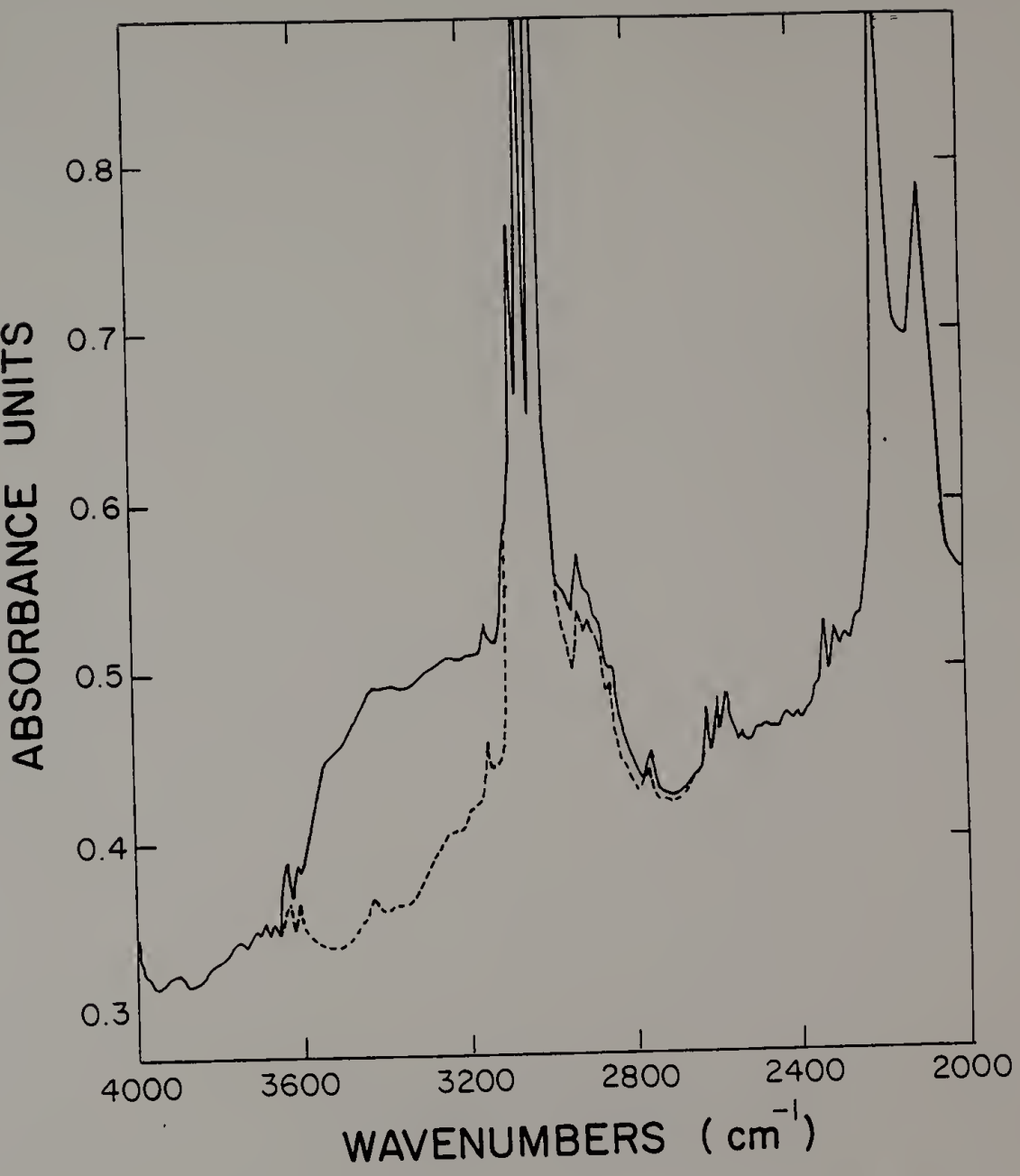
ABSORBANCE UNITS
0.8
0.7
0.6
0.5
0.4
0.3
4000
3600
3200
2800
2400
2000
WAVENUMBERS (cm⁻¹)

about 2400cm^{-1}. This was typical of the results obtained using PS (Chapter III). No evidence was found, however, for a new peak at 2500cm^{-1} in PSD_3. A 43% decrease in the ratio of aromatic to aliphatic C-H stretch peak intensities was observed after $5.5x10^{-4}E/cm^2$. Also detected was a weak peak at 825cm^{-1} (Figure 4.4).

The presence of absorption bands extending down to the 2400cm^{-1} region introduces some uncertainty regarding the possible presence of OD stretch bands. It is desirable, then, to estimate the molar ratio of OH to any OD functional groups by measuring integrated intensities of the OH band and the uncertainty in the OD region. Corrections are made first for differences in ATR depth of penetration and then for differences in molar absorptivities. Molar absorptivities were estimated from methanol and deuteromethanol in chloroform (Appendix C). This calculation indicates that there are at least 90 OH functional groups per OD group after $5.5x10^{-4}E/cm^2$.

Exposing photooxidized PSD_3 to ammonia vapors produced changes in the infrared spectrum that were similar to those produced in photooxidized PS. Thus, the carbonyl band decreased in intensity and carboxylate anion bands formed at about 1575 and 1396cm^{-1} (Figure 4.5). A similar result was found upon exposure to deutero-ammonia vapors, although the ammonium bands appeared at 2500cm^{-1}. As with ammonia

Figure 4.4

Olefin formation in PSD_3. Spectrum A represents the initial spectrum of PSD_3, whereas spectrum B shows the same band after photooxidation. Spectrum C represents the difference between B and A, and it reveals the formation of a peak at $825cm^{-1}$. This new peak is thought to be due to C-H bending of trisubstituted olefins.

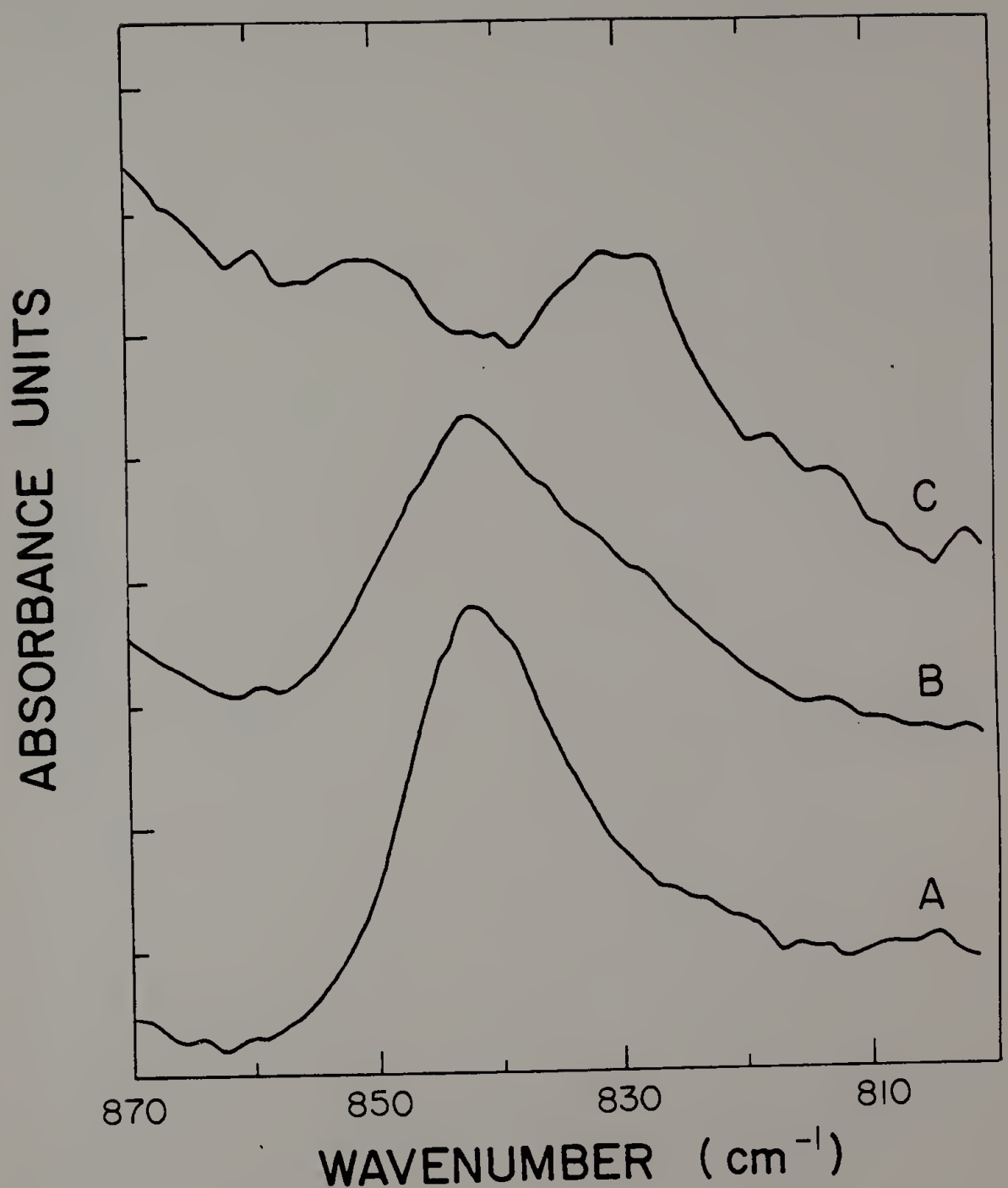
ABSORBANCE UNITS
C
B
A
870
850
830
810
WAVENUMBER (cm⁻¹)

Figure 4.5

Ammonia treatment in PSD_3. Response of the carbonyl band in photooxidized PSD_3 (A) to ammonia vapor (B).

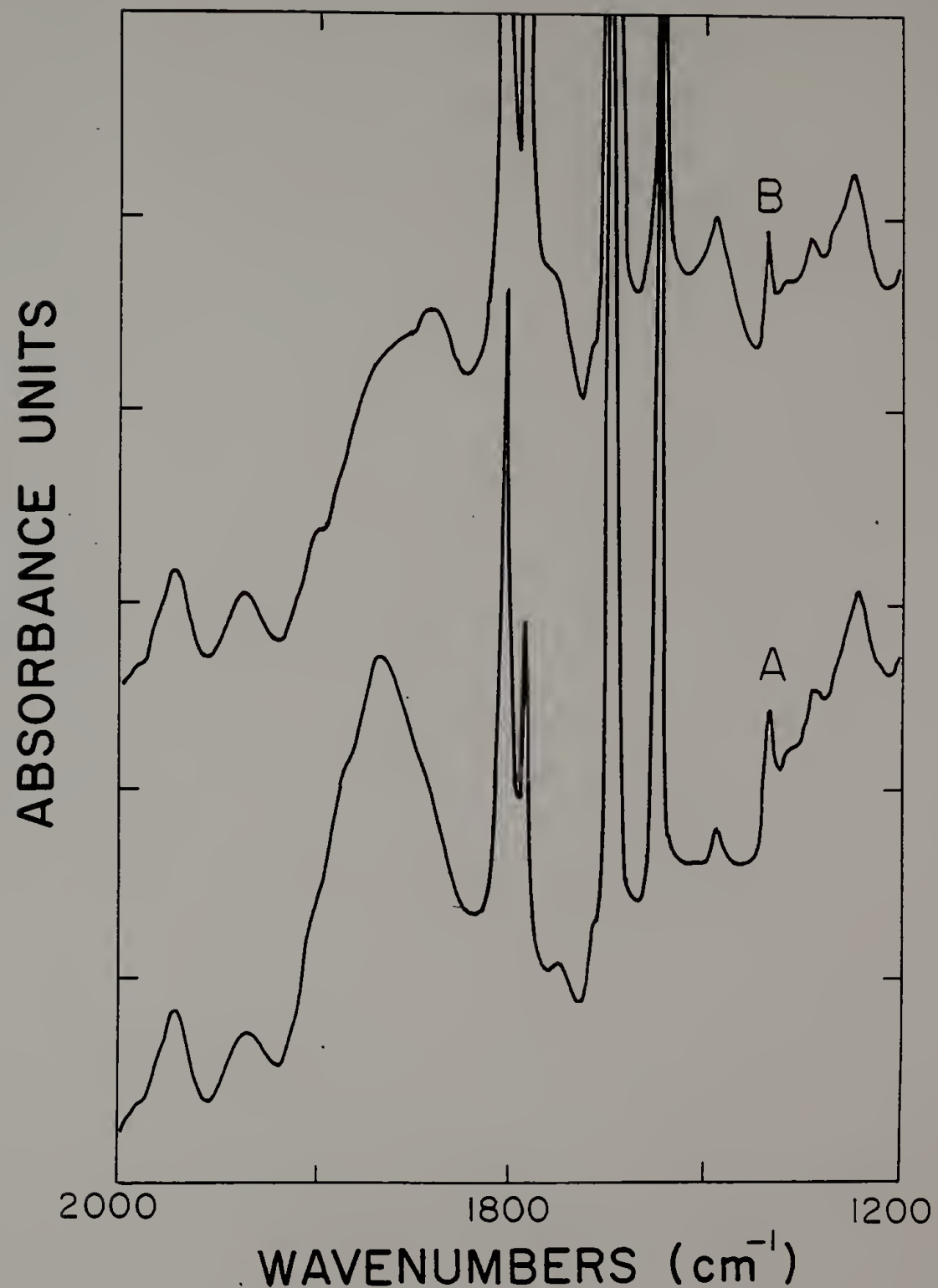
ABSORBANCE UNITS
B
A
2000
1800
1200
WAVENUMBERS (cm⁻¹)

treatment of photooxidized PS, the deutero-ammonia experiment caused a decrease in intensity at 3540 and 3440cm^{-1}. Heating photooxidized PSD_3 to 142°C for 2 hours caused a decrease in peak intensity at 3540 and 3440cm^{-1} of about 50%.

The carbonyl peak intensity in PSD_3 at 1725cm^{-1} was found to be only 56% of the value obtained for PS after an equivalent exposure. Thus, the relative degradation rates were about 2 to 1 (PS to PSD_3).

Oxygen Uptake

The results of the oxygen uptake experiment are shown in Figure 4.6, where they are superimposed on those of Figure 4.1. It is seen in Figure 4.6 that oxygen uptake stops at about the same UV dosage needed to bring the 1725cm^{-1} carbonyl band to its limiting value.

Following this experiment, the molecular sieves were exposed to carbon dioxide and weighed as described. It was found that the molecular sieves were not saturated with carbon dioxide by the PS photooxidation, but could still adsorb about 0.3 gram of the gas. This weight of an ideal gas would occupy about 150cm^3.

Uncertainty in the measurement of oxygen uptake and UV intensity inside the apparatus is moderate. Oxygen uptake is recorded to a given value of ± 0.1 μmoles oxygen. The UV

Figure 4.6

Oxygen uptake. Both oxygen uptake and carbonyl peak intensity (from Figure 4.1) are found to reach limiting values after about $5x10^{-4}E/cm^2 \cdot hr$.

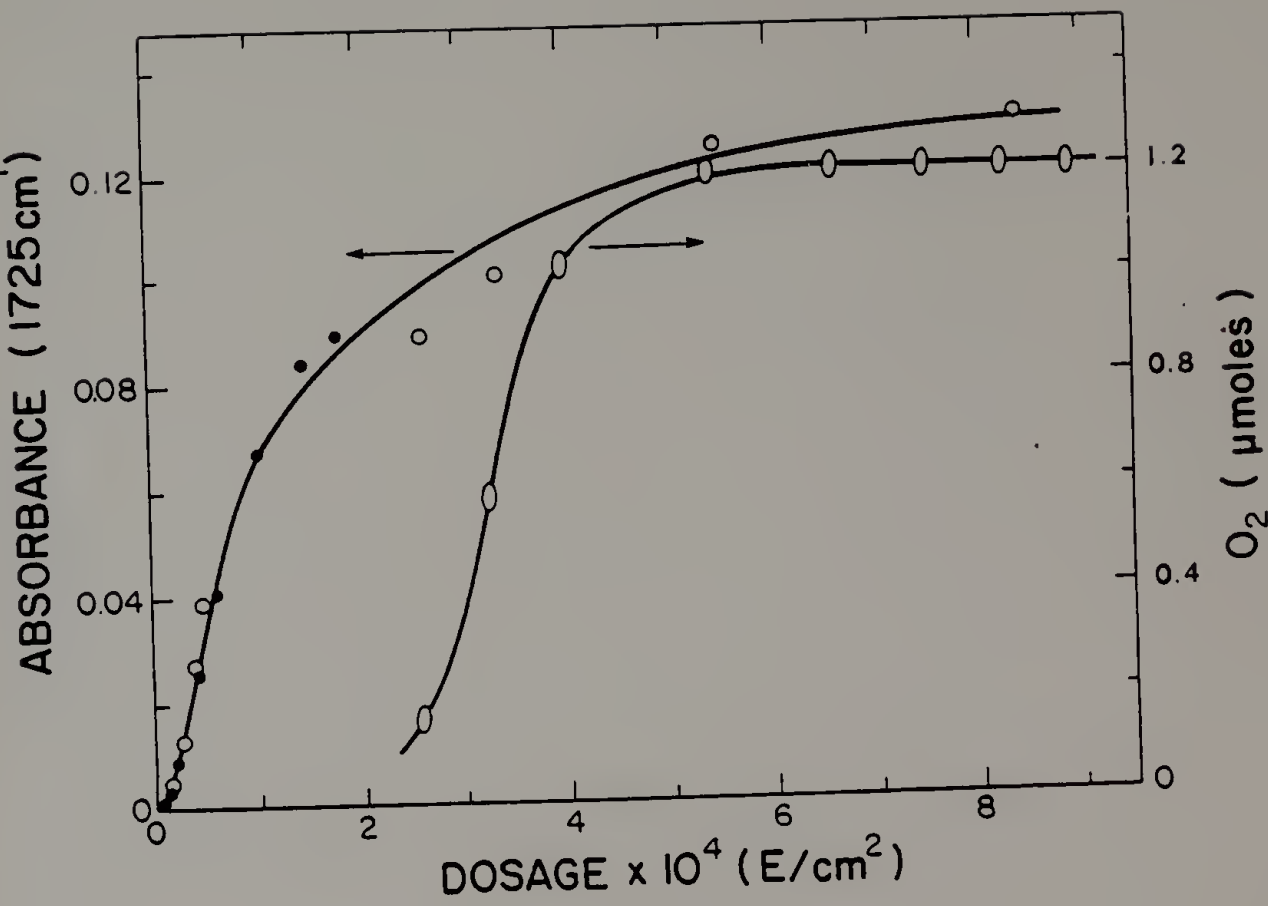
ABSORBANCE (1725cm⁻¹)
0.12
0.08
0.04
0
0
2
4
6
8
DOSAGE x 10⁴ (E/cm²)
1.2
0.8
0.4
0
O₂ (μmoles)

intensity is determined to be $(5.2 \pm 0.7) \times 10^{-6}$ E/cm^2·hr.

Discussion

Deuterated Polystyrene

The results shown in Figure 4.3 and those obtained at longer exposure times show that a strong OH stretch band formed upon photooxidation of PSD_3. As discussed below, this indicates that hydroperoxides and carboxylic acids formed as a result of reactions that take place on the phenyl ring. Thus, the phenyl ring reacts extensively when PSD_3 is photooxidized with 254nm UV. Several points must be considered, however, to clarify this conclusion.

The PSD_3 used in this work was 99% chain deuterated, which means that one percent of the chain hydrogen atoms were protium. This one percent protium, however, could not account for the strong OH stretch band that was produced. Although there is a small difference in the chemical reactivity of the C-H and C-D bonds (8 to 1, or less) (93), there is a large difference in concentrations between chain deuterium and chain protium (99 to 1). This leads to the conclusion that any hydroperoxides formed from the main chain should be predominantly deuterated. The lack of an OD stretch band indicates that phenyl reactions produced the

OH-containing groups found by FTIR.

The fact that differences in the reactivity of C-D and C-H bands is small indicates that PSD_3 is an acceptable model compound for PS. Recently published results (94) suggest that this difference in reactivity in PS is on the order of 4 to 1 (C-H to C-D). Since photooxidation of PSD_3 produced an OH to OD molar ratio of at least 90 to 1, it is evident that PS must also undergo ring reactions during photooxidation with 254nm UV. Although the ratio of ring to main chain OH groups in photooxidized PS need not be 90 to 1 after a similar reaction conversion to PSD_3, it would likely have a high value (perhaps 25 to 1).

It is noteworthy that IR bands formed in PSD_3 at the same frequencies as those in photooxidized PS. For example, free and H-bonded hydroperoxides formed in PSD_3 at 3540 and 3440cm^{-1}. As in PS, these hydroperoxide bands decreased in intensity on heating in nitrogen and exposure to ND_3 vapor. Carboxylate anion bands also formed from ND_3 treatment. This supports the idea that photooxidation reactions in PSD_3 are similar to those in PS.

It is interesting to have found only weak N-D stretch bands at 2500cm^{-1} following 2.5 days exposure to ND_3 vapor. This suggests that only a limited amount of ammonia vapor is present in the film, and that the rate of hydrogen exchange between functional groups in the film is slow. In

fact, the possibility of hydrogen exchange (protium for deuterium) had prompted the experiment of storing photooxidized PSD_3 over D_2O. This was done to learn if protium exchange with atmospheric water vapor could have artificially caused the 9Ø to 1 OH to OD ratio found in photooxidized PSD_3. Similar experiments included photooxidizing PS in air saturated with D_2O, and soaking photooxidized PS in D_2O for six days. In no case did an OD stretch band form in the infrared spectrum. While this may be due to the low solubility of water in PS, it supports the conclusion that the observed OH band in photooxidized PSD comes from phenyl ring hydrogens.

In addition to the IR bands described above, another weak band was found at 825cm^{-1} in photooxidized PSD_3 (Figure 4.4). This band is also found in photooxidized PS, and has been reported to form during PS vacuum photolysis (3), where it was assigned to the out-of-plane C-H bend of a trisubstituted olefin. This absorption frequency is correct for such olefins (67) and if this band assignment is valid in the present case, then this band provides additional evidence for ring reactions in PSD_3 and PS. This would also support the idea that the yellow color in photooxidized PS is caused by ring-opened products such as mucondialdehydes (11) rather than in-chain polyenes (5).

One question clearly remains regarding the

photooxidation of PSD_3, and that question concerns the reason why carbonyl functional groups form at about one half the rate in PSD_3 as in PS. Although it seems likely that the primary photolysis process involves scission of the tertiary C-H bond (94), it is evident that this process becomes trivial when oxygen is present (18). Subsequent reactions may involve attack of the phenyl ring by hydroxy (49) or hydroperoxy radicals (11) to bring about ring opening without producing OD absorption bands. However, secondary kinetic isotope effects are typically on the order of 1.2 to 1 (95), so that these indirect effects (where the C-D bond is not broken) seem unable to explain this difference in the rate of carbonyl formation.

Although it may be difficult to assign a specific reaction mechanism to PS photooxidation at this time, it should be mentioned that the general conclusion of the PSD_3 experiment is consistent with the results seen for PS photooxidation. Evidences for ring-opening reaction products may be inferred from the reactivity of hydroperoxide toward certain derivatizing agents used in Chapter III. As mentioned in Chapter III, the decomposition of hydroperoxides by pyridine (Figure 3.3) is something to be expected with primary or secondary hydroperoxides under the conditions used. Similarly, the reaction products that were produced on exposure to sulfur dioxide (Figure 3.4)

were not completely consistent with those expected from tertiary hydroperoxides. Both of these results suggest the presence of hydroperoxides with properties that could most readily be explained if they formed during ring-opening reactions.

A more direct evidence for ring reactions in PS is obtained directly by considering the peak intensity ratio of the aromatic to aliphatic C-H stretch bands. These results are shown in Figure 4.7, which shows the normalized intensity ratio as a function of UV dosage. It is seen here that there is a significant loss in the aromatic content of the PS film near its surface. This result is not readily seen from absorbance data (Figure 4.7A) but is quite evident from reflectance (ATR) data (Figure 4.7B and C). A similar loss in this aromatic to aliphatic ratio was also observed during PSD_3 photooxidation. These results, together with the OH stretch band formation in PSD_3, provide strong evidence for the importance of ring reactions in PS photooxidation with 254nm UV.

Oxygen Uptake

The formation of a stable, protective layer of highly oxidized PS has been inferred from tensile testing of PS exposed to solar region UV (30). Likewise, it has been reported for PS containing 2,4-dihydroxybenzophenone

Figure 4.7

Aromatic to aliphatic ratio vs. dosage. Aromatic to aliphatic infrared C-H stretch ratio as a function of UV dosage in PS. Although undetectable in absorbance (A), there is a marked drop in this ratio found in reflectance spectra in the top 2.8μm (B) and top Ø.7μm (C) of the film.

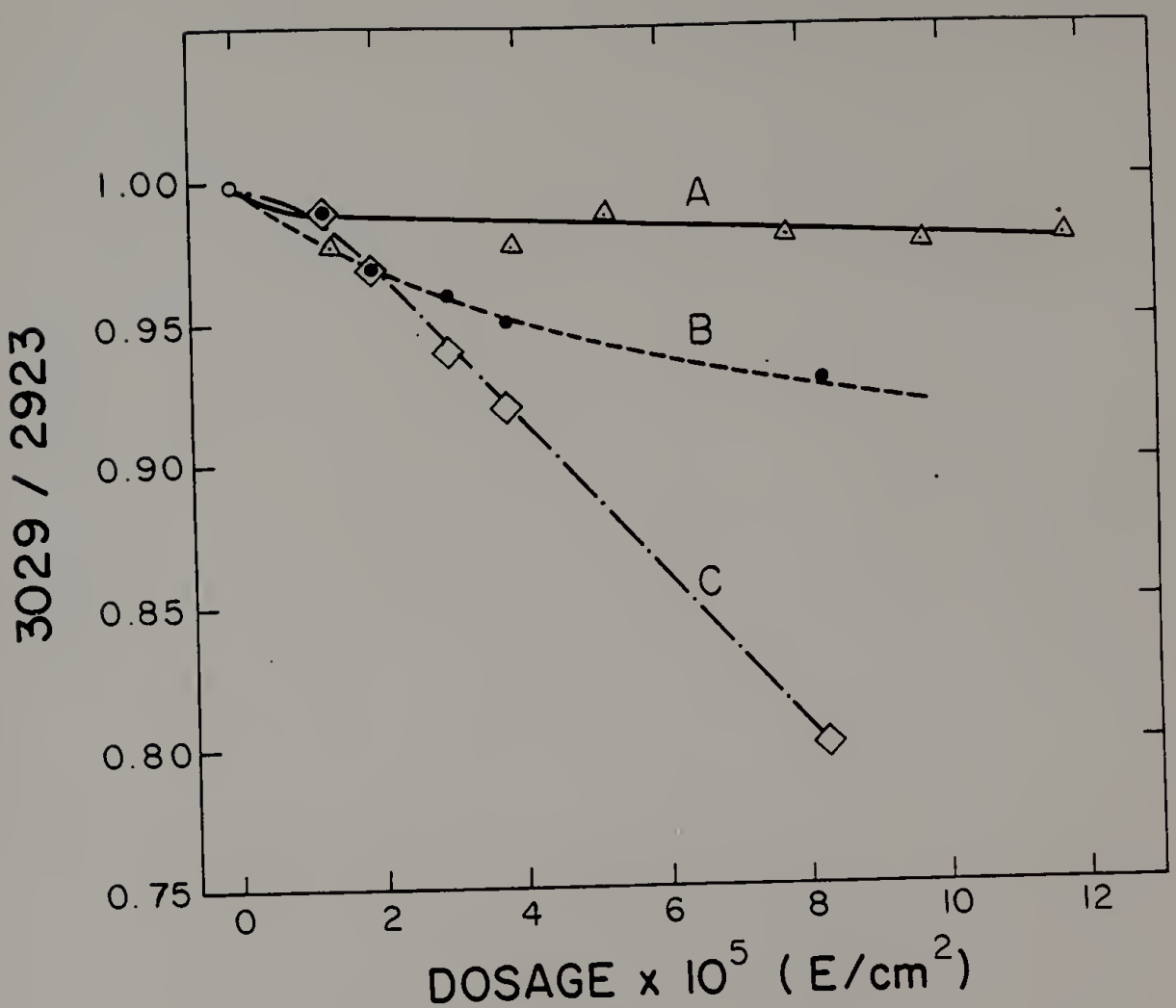
1.00
0.95
0.90
0.85
0.80
0.75
3029 / 2923
0
2
4
6
8
10
12
DOSAGE x 10^5 (E/cm^2)
A
B
C

exposed at 254nm using infrared analysis (59). It was also suggested that a protective layer may form in PS containing 2-hydroxy-4-methoxybenzophenone from oxygen uptake measurements, which showed accelerated photooxidation at 254nm when this "stabilizer" was present (27). Similarly, an ESCA study reported that photooxidation leads to a PS film surface with a stable stoichiometry (15). In none of these cases, however, was autoinhibition proven.

It is seen in Figure 4.6 that PS photooxidation stops after about $5x10^{-4}E/cm^2$. This indicates that the infrared carbonyl band intensity reached a limiting value because the reaction became autoinhibiting at large UV dosages. Evidently the highly oxidized surface region of the film was more photostable than the pure PS.

It is interesting to note that the hydroperoxide peaks had reached limiting values at much lower UV dosages than had the carbonyl band (see Figures 3.2 and 4.6). The 3540 and $3440cm^{-1}$ peaks required about $6x10^{-5}E/cm^2$ and $1.3x10^{-4}E/cm^2$ to reach limiting values, respectively. These dosages are, on average, about 20% of the value needed for the carbonyl band to reach its limiting value. This result is in qualitative agreement with the results of Peeling and Clark (15) who used ESCA to study PS photooxidation. This is consistent with the view that the protective layer that forms is extensively oxidized.

Conclusions

Chain deuterated PS was used to learn if the phenyl ring of the PS repeat unit reacts during 254nm UV photooxidation. The development of a strong OH stretch band in the infrared and the lack of any detectable OD stretch band indicated that the phenyl ring reacts extensively during photooxidation. The functional groups that form in PSD_3 appear to be the same as those produced in PS. These results indicate that reaction mechanisms proposed in the literature that describe ring-opening reactions should be given further consideration.

At large UV dosages, the PS film surface is highly oxidized and the infrared carbonyl band intensity reaches a limiting value. This limiting value has been judged by an oxygen uptake experiment to correspond to the formation of a photostable protective layer. This protective layer prevents further photooxidation from occurring, so that the reaction becomes autoinhibiting.

C H A P T E R V

PHOTOOXIDATION WITH SOLAR REGION UV

Introduction

In the preceding chapters, much attention has been given to identifying the functional groups that form as PS is photooxidized and to determining if the phenyl ring reacts under 254nm UV. Photooxidation was carried out under controlled conditions using pure PS and 254nm UV, which is absorbed directly by the phenyl ring. The photooxidation process, including initiation reactions, is therefore controlled by the properties inherent to pure PS.

As discussed in Chapter I, pure PS does not absorb solar region UV (λ>300nm) and yet it is rapidly photodegraded outdoors. The initiation of photooxidation reactions is likely, then, to be caused by impurities that will absorb these wavelengths of UV. Therefore, the initiation of PS photodegradation with solar UV will proceed by a reaction sequence that is different from that with 254nm UV. The types of products formed may also be quite different from those produced using 254nm UV. It is therefore of interest to learn if the observations made in the preceding chapters can be applied to PS photooxidized with solar region UV.

In the present chapter, a study is made of the products and possible ring reactions in the solar region photooxidation of PS. This is done using suitable photosensitizers added to PS or PSD_3 films. Since acetophenone-type end groups are thought to be prominent in the initiating process (43), acetophenone or trideuteroacetophenone are used as sensitizers. A comparison is also made with PS containing anthracene, which is a common atmospheric pollutant in urban areas.

Experimental

PS and PSD_3 films were prepared as described in Chapter II. Additionally, one film was cast from a chloroform solution containing traces of anthracene. This film was dried in the same way as other films.

Following preparation, one film of PS was exposed to acetophenone vapor in a sealed jar for five hours. This introduced acetophenone into the film. Similarly, the three PSD_3 films were exposed to α,α,α-trideuteroacetophenone (MSD Isotopes, Canada; 99.1%D) for several hours. The acetophenone content of these films, and the anthracene content of the film containing anthracene were determined using UV photometry. The PS/acetophenone film contained 0.14 molar acetophenone, the PSD_3/D_3-acetophenone films

contained Ø.49 to 2.8 molar deuterated acetophenone and the PS/anthracene contained Ø.Ø3 molar anthracene.

Films containing acetophenone or anthracene photosensitizers were photooxidized for one month using a 365nm broadband UV source. This lamp emitted UV over the entire range of 3ØØ to 4ØØnm, with its maximum output at 365nm. The output of the lamp was estimated using potassium ferrioxalate actinometry at $7.3x1Ø^{-7}$ E/cm^2·hr. As before, a slow, steady stream of air was passed through the irradiation chamber, which was held at 3Ø°C. Another film of pure PS was also exposed under these conditions.

Changes in the films were detected using FTIR and UV/Visible spectroscopies and with gel permeation chromatography. Spectra were recorded using the solid films, whereas the GPC traces were recorded in THF solution.

Following photooxidation, films were exposed to ammonia vapors over ammonium hydroxide in a covered dish for 3Ø minutes. Infrared spectra were recorded before and after exposure to ammonia.

In order to learn if the ammonia treatment caused chain scission, one film of photooxidized PSD_3 was cut in half and one half was exposed to ammonia vapor for 45 minutes. The other half of the film served as a control. Both films were stored over $FeCl_3$ for three days and were

then analyzed by GPC to look for changes in molecular weight.

Results

The initial and final UV absorption spectrum of PS/acetophenone is shown in Figure 5.1. The spectrum of the starting material in Figure 5.1 shows the weak absorption at 319nm caused by the presence of acetophenone. After exposure for one month, the film was photooxidized and the UV absorption in the solar region increased. The film acquired a faint yellow color, which was caused by the UV absorption extending into the visible region beyond 400nm.

Molecular weight changes are shown in Figure 5.2. It was found that the number average molecular weight decreased from 233,000 to 58,800, and the molecular weight distribution broadened from $\bar{M}_w/\bar{M}_n \leq 1.06$ to a value of 3.12.

Infrared spectra revealed bands forming at 3540 and 3450cm^{-1}, as shown in Figure 5.3. A carbonyl band formed that was similar in shape to that found using 254nm UV, except for a strong decrease in absorption seen at 1690cm^{-1} (Figure 5.4). Decreases in absorption at about 1780 and 1730cm^{-1}, and increases near 1560 and 1390cm^{-1} were introduced upon exposure to ammonia vapor. Ammonia vapor also caused a decrease in peak intensities at 3540 and

Figure 5.1

UV absorption spectrum of PS/acetophenone.

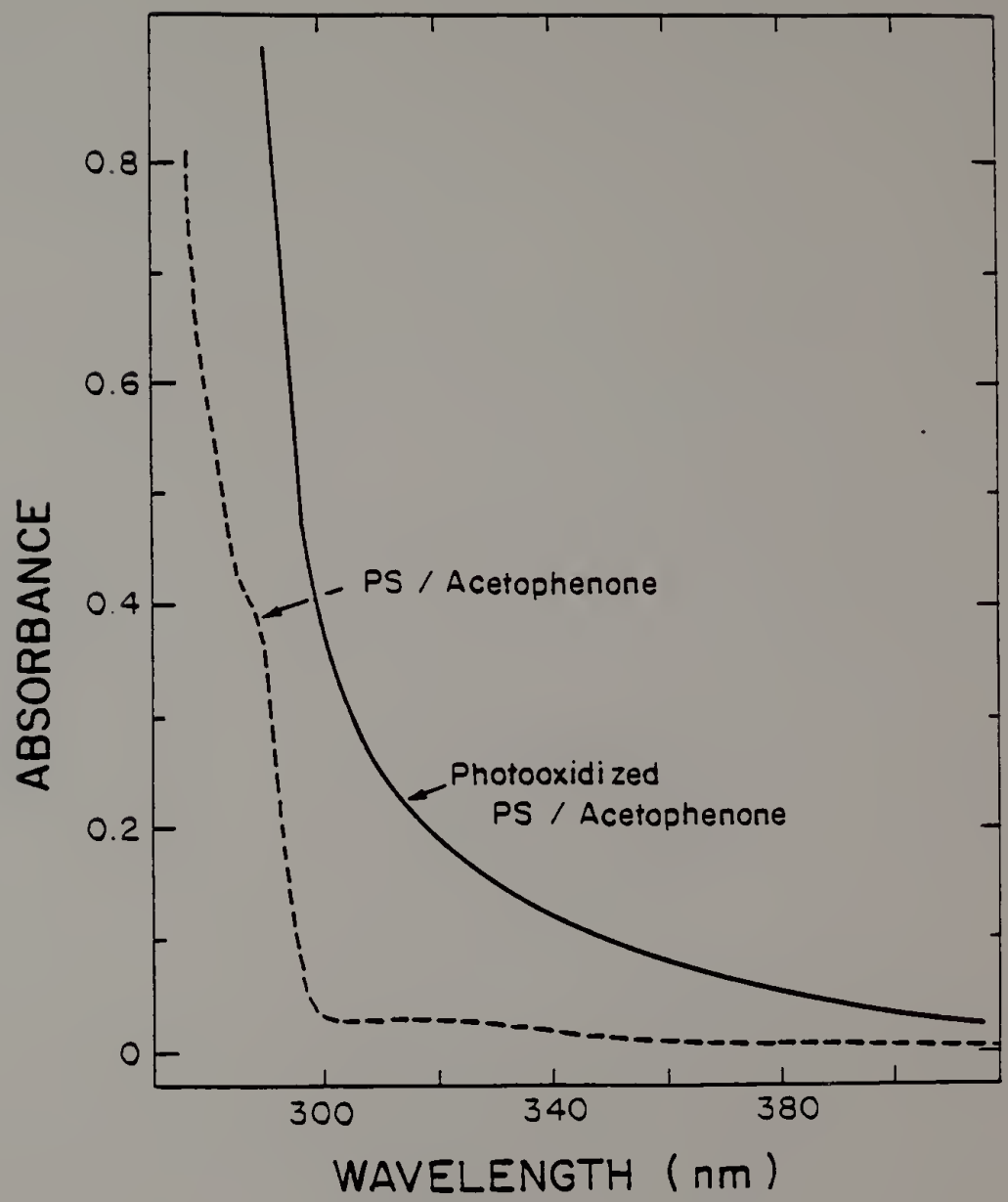
ABSORBANCE
0.8
0.6
0.4
0.2
0
PS / Acetophenone
Photooxidized
PS / Acetophenone
300
340
380
WAVELENGTH (nm)

Figure 5.2

Molecular weight changes in PS/acetophenone. The dotted line is from the original PS whereas the solid line is obtained following 30 days exposure (areas not normalized).

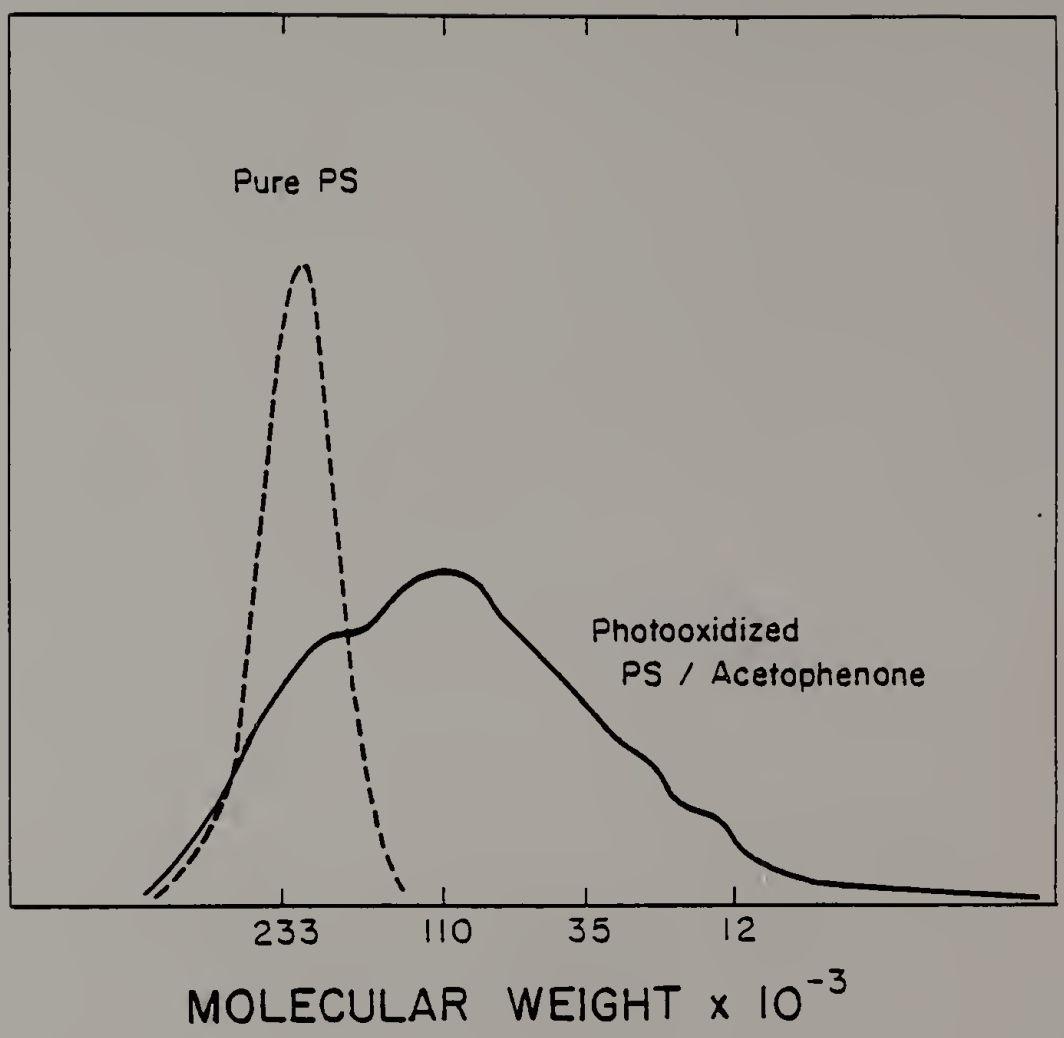
Pure PS
Photooxidized
PS / Acetophenone
233
110
35
12
MOLECULAR WEIGHT x 10^{-3}

Figure 5.3

Hydroperoxide infrared bands in photooxidized PS/acetophenone.

D = exposure time in days

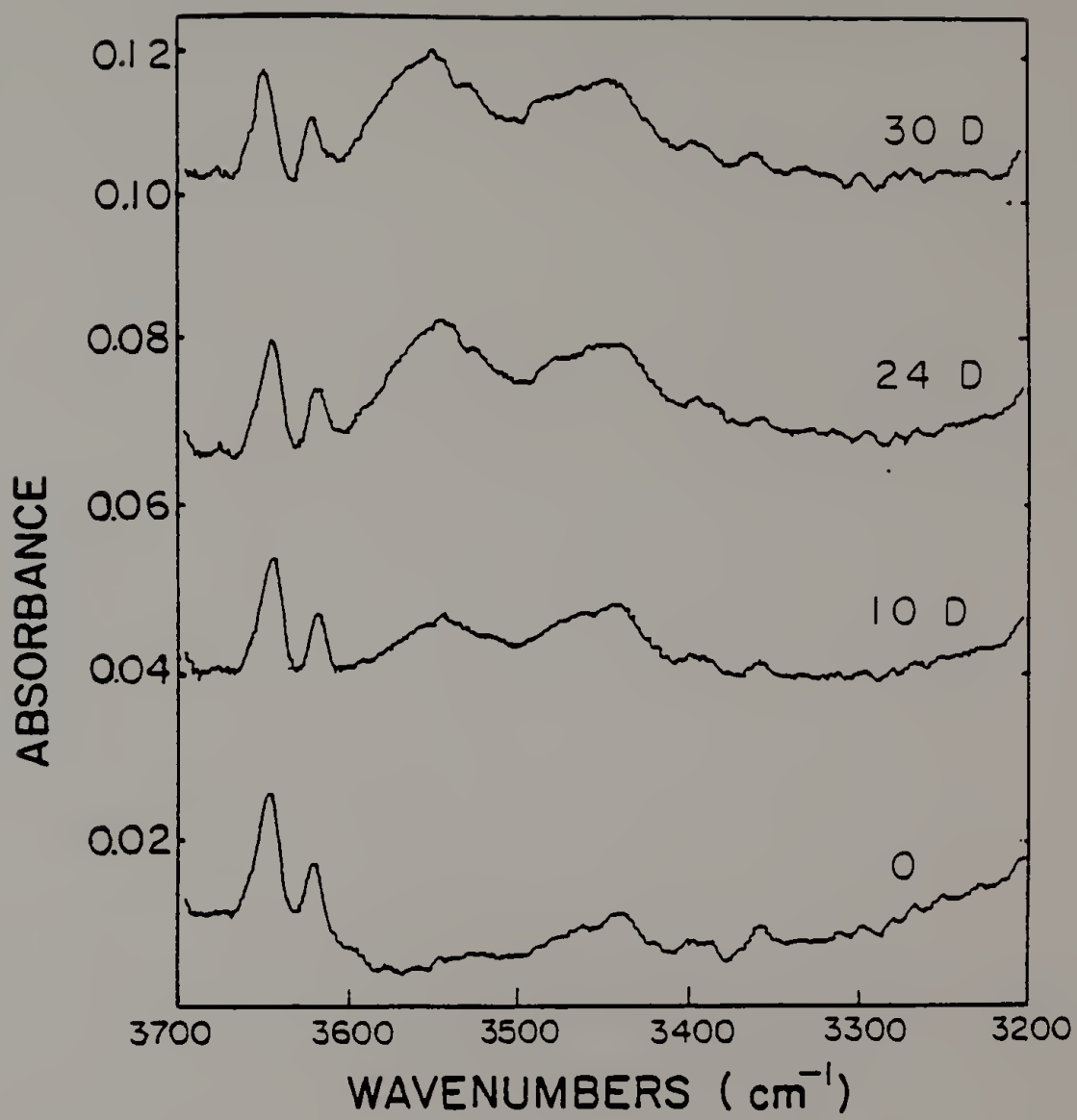
0.12
0.10
0.08
0.06
0.04
0.02
ABSORBANCE
30 D
24 D
10 D
0
3700
3600
3500
3400
3300
3200
WAVENUMBERS (cm⁻¹)

Figure 5.4

Infrared carbonyl absorption in photooxidized PS/acetophenone. This spectrum represents the difference between spectra collected before and after photooxidation.

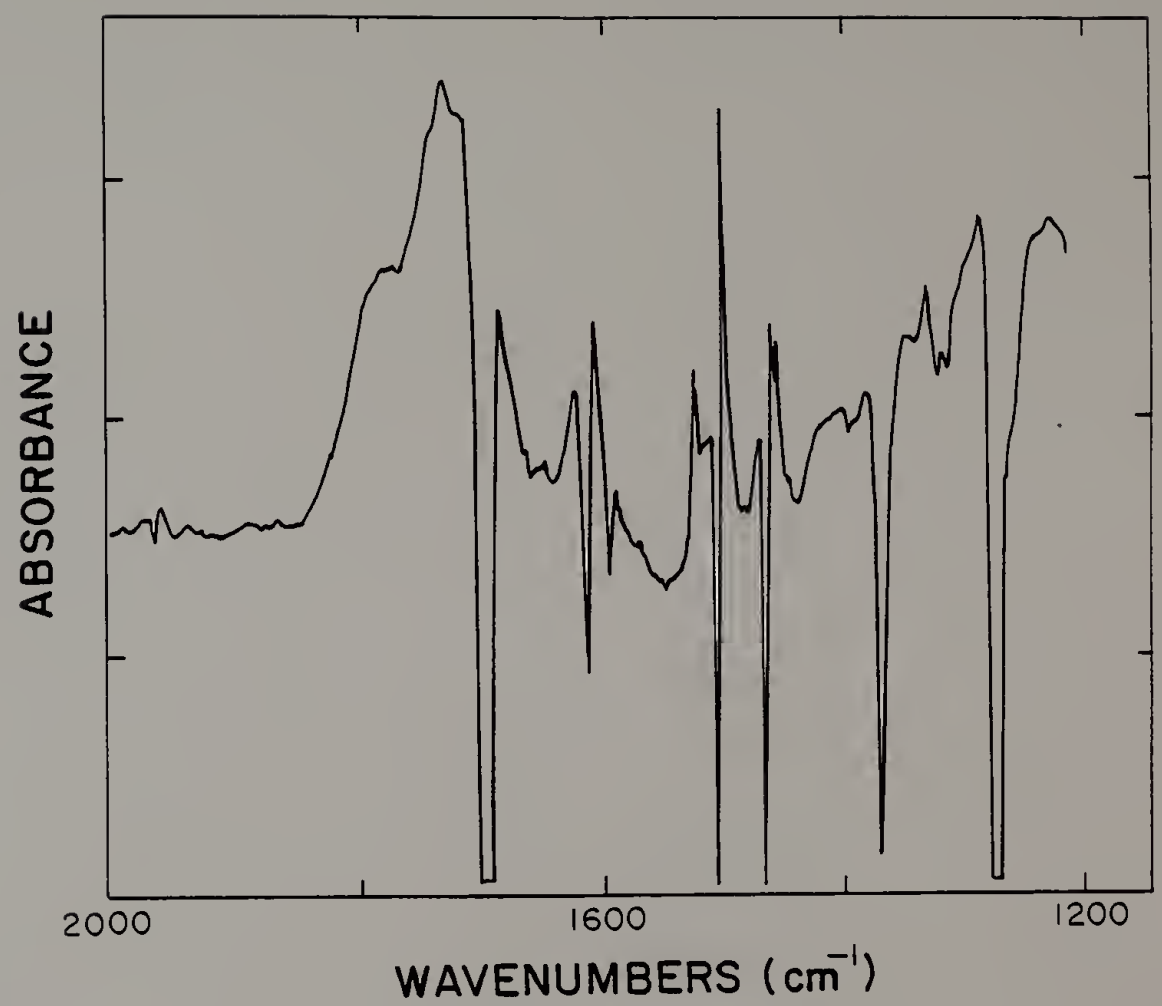
ABSORBANCE
2000
1600
1200
WAVENUMBERS (cm⁻¹)

3450cm^{-1}.

The photooxidation of PSD_3/D_3-acetophenone led to the formation of IR bands at frequencies typical of those found in PS/acetophenone. Figure 5.5 shows the appearance of bands at 3540 and 3440cm^{-1} and also shows the lack of any new bands at 2500-2600cm^{-1} in the film containing 2.8 molar D_3-acetophenone. Integrated intensities of the total OH stretch band and the experimental uncertainty in the OD stretch region leads to the conclusion that at least 40 OH functional groups form for any one OD containing group that may be present. Similar results were obtained with the films containing less D_3-acetophenone, although the extent of photodegradation was not as great.

Molecular weight changes in the PSD_3/D_3-acetophenone took place during photooxidation and these changes were detected using GPC. For the film containing 2.8 molar D_3-acetophenone, the molecular weight and MWD changed from their initial values of $\bar{M}_n$=275,000 and $\bar{M}_w/\bar{M}_n$=1.89 to values of $\bar{M}_n$=35,000 and $\bar{M}_w/\bar{M}_n$=2.33. It was also found that exposing a photooxidized film to ammonia vapor caused no changes in the polymer molecular weight. The film exposed to ammonia vapor had number- and weight-average molecular weights of 57,000 and 110,000 respectively, compared to the control sample with values of 58,000 and 110,000 respectively.

Figure 5.5

Hydroperoxide infrared bands in photooxidized PSD_3/D_3-acetophenone. The absorption at 3360cm^{-1} is an overtone of the D_3-acetophenone carbonyl band.

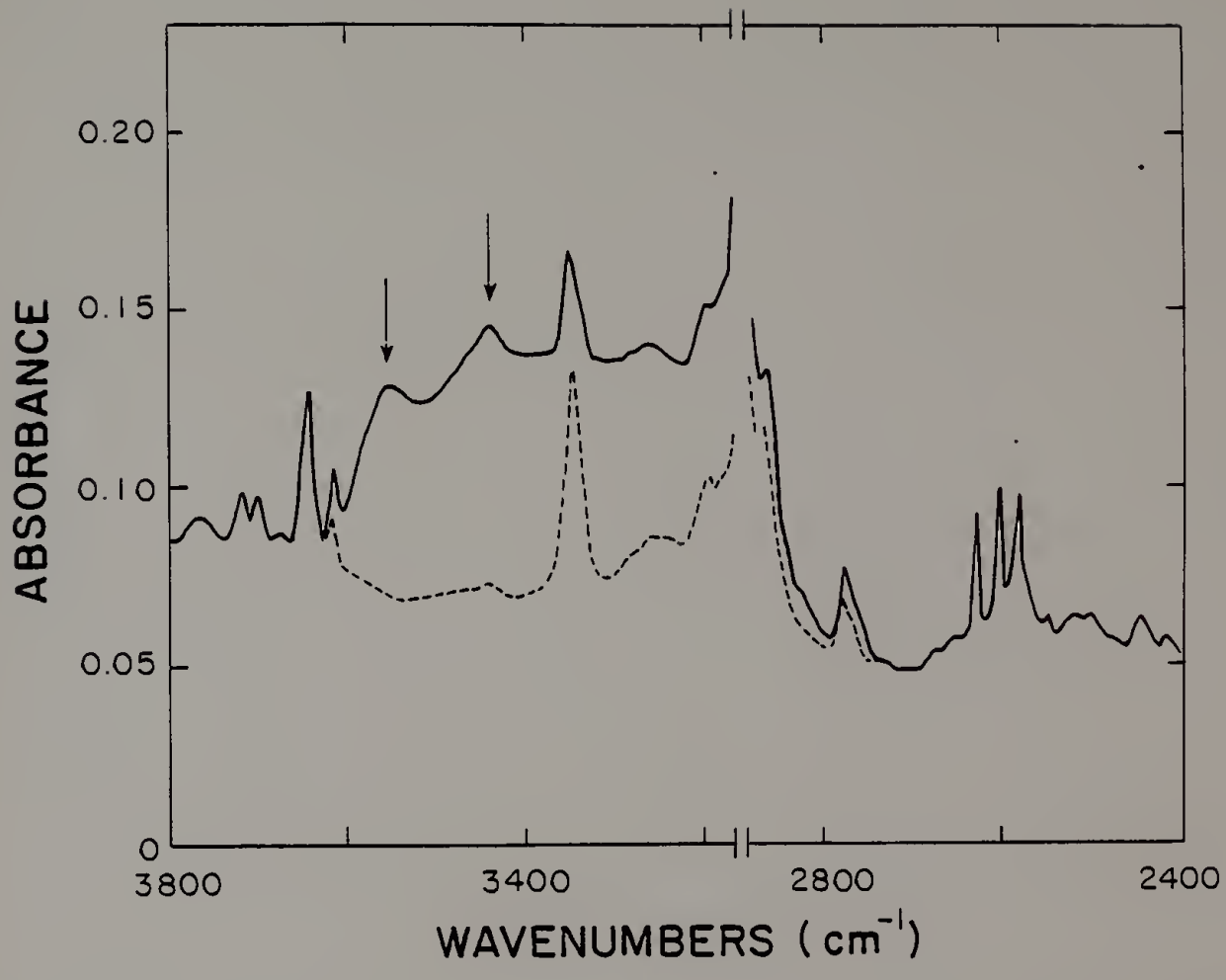
ABSORBANCE
0.20
0.15
0.10
0.05
0
3800
3400
2800
2400
WAVENUMBERS (cm⁻¹)

Photooxidizing PS/anthracene brought about a marked decrease in the UV absorption spectrum of the anthracene that was in the film. As seen in Figure 5.6, the strong absorption bands associated with anthracene decrease in intensity and the absorption tails off into the visible region as the film becomes yellow.

Molecular weight changes are also detected during PS/anthracene photooxidation, as shown in Figure 5.7. In this case, however, it is plain that crosslinking reactions play a significant role in photooxidation, as the molecular weight decreased only somewhat from $\bar{M}_n$=233,ØØØ to 148,ØØØ, while the molecular weight distribution broadened from $\bar{M}_w/\bar{M}_n \leq$ 1.Ø6 to a value of 3.95.

Along with increases in the infrared absorption at about 354Ø and 344Øcm^{-1}, a band also formed in the carbonyl region. The carbonyl band, shown in Figure 5.8, is quite different in appearance from those produced using 254nm UV, as it contains a number of weak shoulders and maxima. Major bands are found at 1775 and 1735cm^{-1}, and weaker shoulders appear at 1788, 1722, 1691, 1677, 1665, and 1634cm^{-1}. Also shown in Figure 5.8 is the carbonyl band following exposure to ammonia vapor. It is seen here that ammonia vapor caused a decrease in absorption bands near 178Ø and 1735cm^{-1}, and increases near 168Øcm^{-1}. Very weak intensity increases could also be seen near 156Ø and 139Øcm^{-1}.

Figure 5.6

UV absorption spectrum of PS/anthracene.

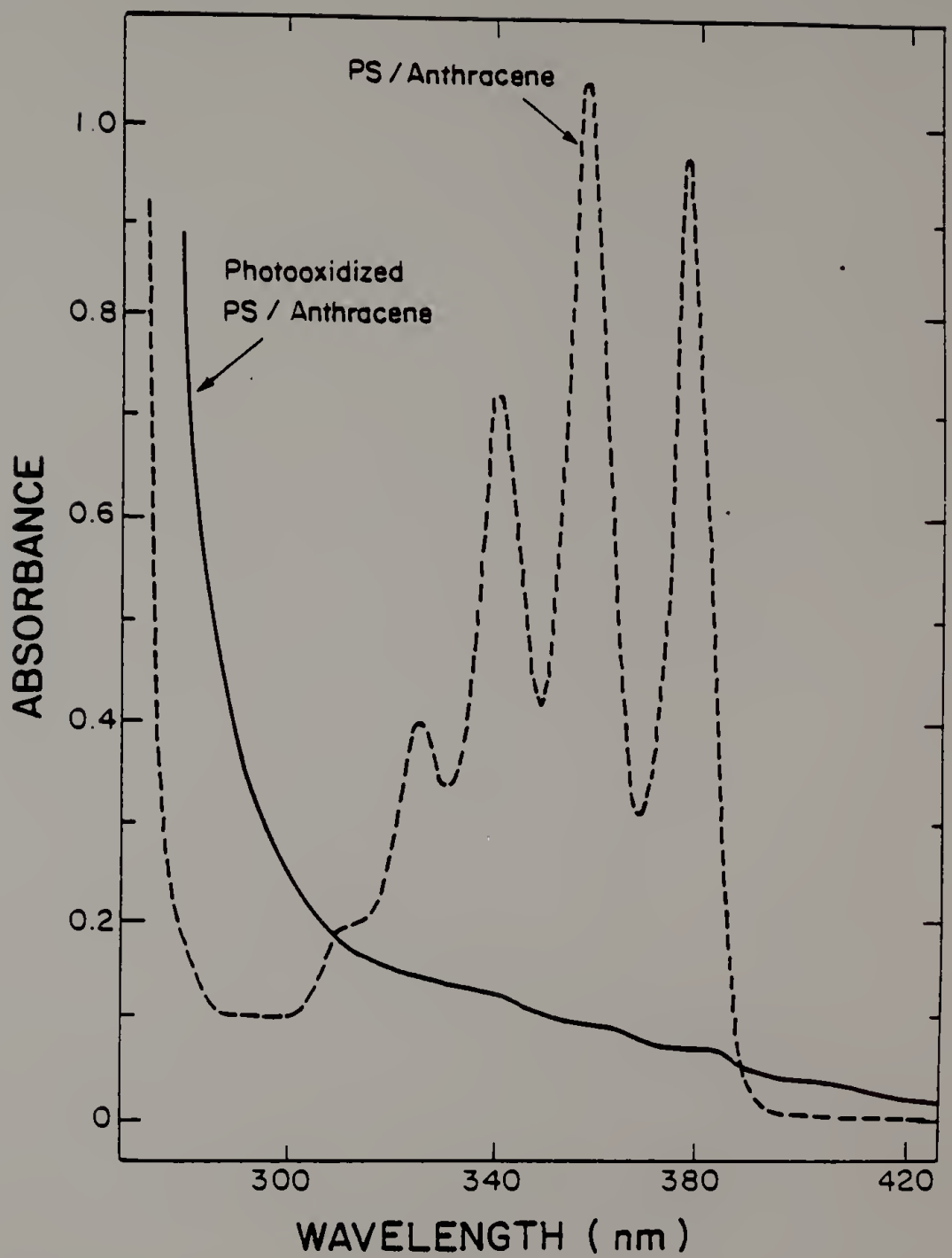
PS / Anthracene
Photooxidized
PS / Anthracene
ABSORBANCE
1.0
0.8
0.6
0.4
0.2
0
300
340
380
420
WAVELENGTH (nm)

Figure 5.7

Molecular weight changes in PS/anthracene (peak areas not normalized).

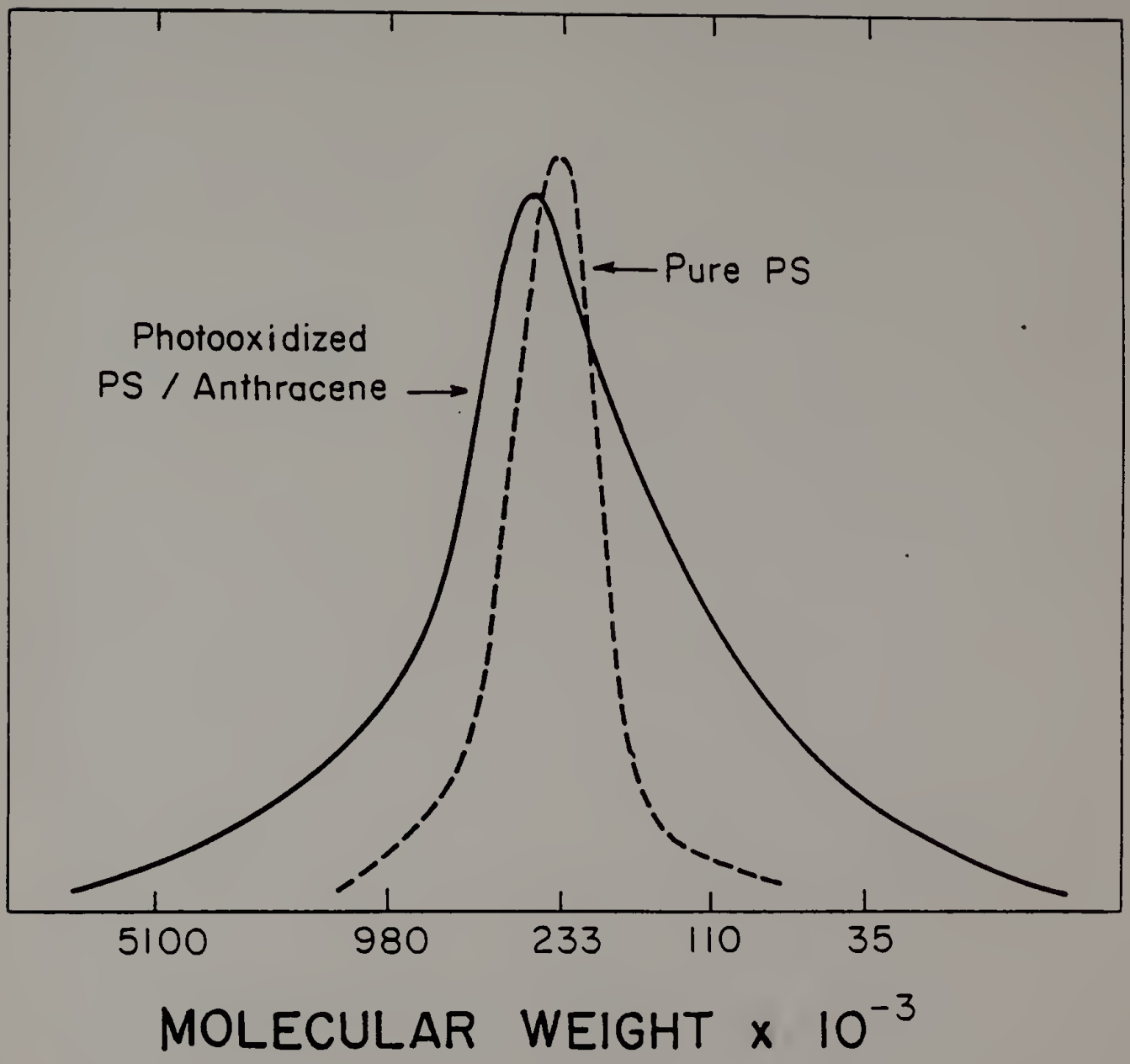
Pure PS
Photooxidized
PS / Anthracene
5100
980
233
110
35
MOLECULAR WEIGHT x 10^{-3}

Figure 5.8

Infrared carbonyl absorption in photooxidized PS/anthracene. These spectra represent difference spectra of photooxidized PS/anthracene minus the unoxidized PS/anthracene spectrum (A). Spectrum B is the same as A after exposure to ammonia vapor.

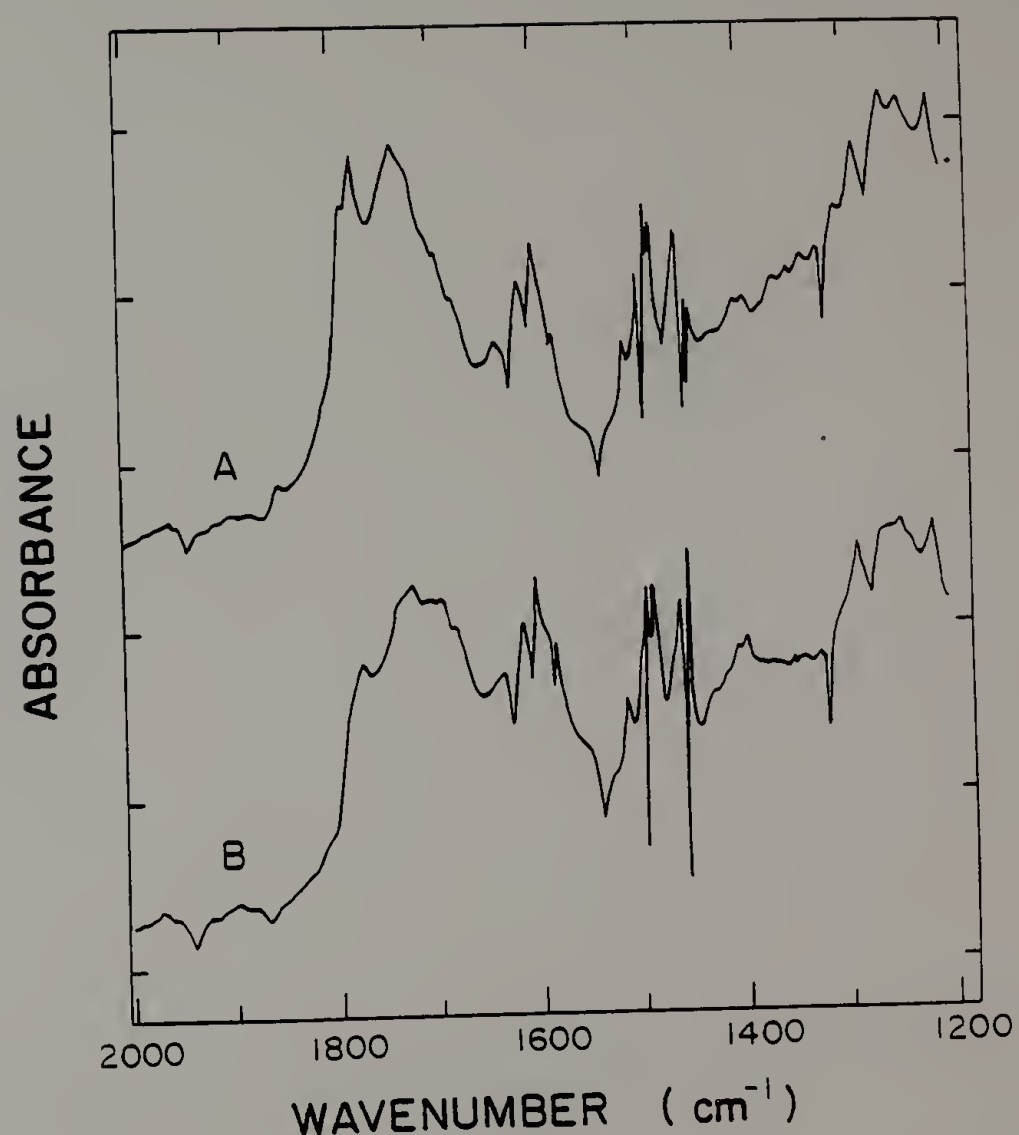
ABSORBANCE
A
B
2000
1800
1600
1400
1200
WAVENUMBER (cm⁻¹)

Discussion

PS/Acetophenone

The presence of 0.14molar acetophenone in a PS film produced only a weak absorption above 300nm (Figure 5.1). It is clear, however, that the acetophenone provided a means of initiating photooxidation because exposing pure PS to the solar region UV lamp for one month produced no changes in the infrared spectrum. It is also evident from Figure 5.1 that photooxidation causes an increase in the UV absorption above 300nm and this eventually leads to the much-discussed yellow coloration of PS. This increase in UV absorption also indicates that new chromophores are being produced, in addition to the acetophenone that was present initially. The structure and chemistry of these chromophores, however, is not known for certain (82), but they too may initiate photooxidation reactions.

The decrease in molecular weight shown in Figure 5.2 is consistent with the molecular weight changes reported for PS containing benzophenone (52). In the present case, Figure 5.2 serves as proof that acetophenone initiated PS photooxidation. It is plain from these results that the PS had undergone photodegradation and that the acetophenone had not simply been consumed within an inert PS matrix.

The products of photooxidation from PS/acetophenone

using solar region UV are qualitatively similar to those formed in pure PS with 254nm UV. As seen in Figure 5.3, IR absorption bands are produced at 3540 and 3440cm^{-1} and, as in Chapter III, they are assigned to free and H-bonded hydroperoxides, respectively. Unlike the case of 254nm photooxidation, however, these groups are produced as the UV light is absorbed diffusely through the PS film. Thus, the appearance of these two distinct absorption bands is likely caused by the physical isolation of hydroperoxides from one another within the polymer matrix. Completely isolated groups lead to the free OH stretch band. As hydroperoxides decompose, other polar functional groups can form, including more hydroperoxides, and this would produce the H-bonded absorption band.

PSD_3/D_3-Acetophenone

Figure 5.5 is typical of those obtained with the three deuterated films examined in this chapter. Peaks at 3540 and 3440cm^{-1} are caused by free and H-bonded hydroperoxides. The peak at about 3360cm^{-1} is an overtone of the D_3-acetophenone carbonyl band, while the absorption at 3250cm^{-1} and below includes carboxylic acid bands. The strong OH stretch band and the lack of any detectable OD stretch band indicates that the hydroperoxides detected in the film formed from reactions on the phenyl rings. This

indicates the importance of the phenyl ring in solar region photooxidation when acetophenone endgroups are the initiators.

These results serve to underscore the importance of oxygen in determining the course of photodegradation in PS. The primary photolysis process of PS containing an aromatic ketone is thought to be the abstraction of hydrogen from the PS by the triplet state ketone (18). Such an abstraction reaction would seem likely to occur at the tertiary position on the PS backbone. A peroxy radical would then form on the PS main chain, becoming a hydroperoxide, if oxygen were present (Figure 5.9). If these hydroperoxides form, they must decompose and allow heavy water to leave the film, as it is evident that such hydroperoxides form only in a very low steady-state concentration. The hydroperoxides detected in the infrared formed from the phenyl ring since they contained protium. The alcohols formed by the photoreduction of the aromatic ketones in Figure 5.9 would also contain deuterium and these were not detected either.

One possible mechanism for the occurrence of ring-opening reactions involves the addition of molecular oxygen to a resonance structure of the tertiary radical (Figure 5.1Ø) (47). This process was thought to lead to quinomethine formation, which would be very yellow in

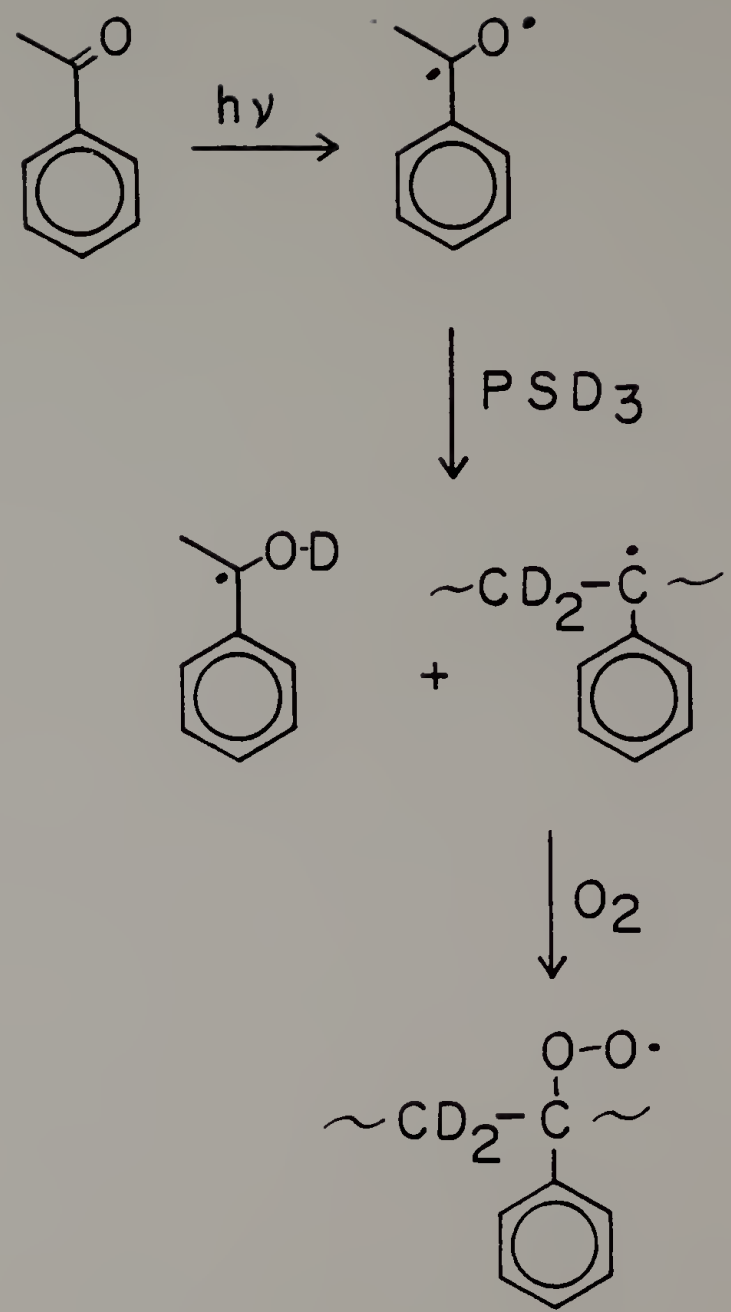

Figure 5.9

Generally-held photoinitiation process with aromatic ketones.

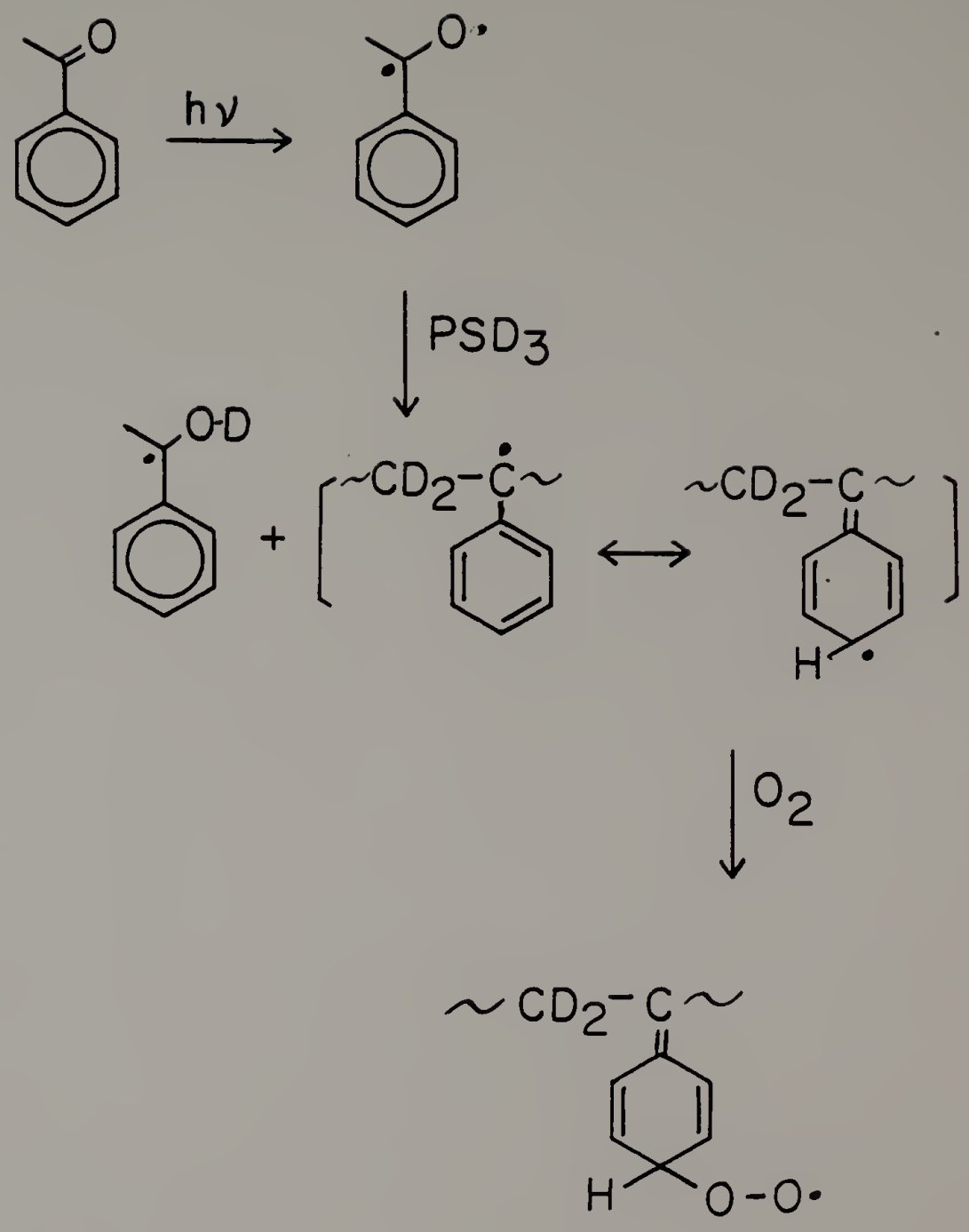

Figure 5.10

One possible mechanism of phenyl ring reactions.

color. Quinones are known to initiate PS photodegradation if oxygen is present (99), so that continued reactions are likely once the phenyl ring starts to react. It should also be mentioned that hydroxyl radicals reportedly add to the phenyl ring of toluene or benzene (100), providing another way of initiating ring reactions. In addition, singlet oxygen may attack the ring directly (82), although the role of this reaction in PS photooxidation has not been clearly demonstrated (101). Once olefinic groups have formed, singlet oxygen would likely contribute to the photodegradation process. Finally, the observation that phenyl rings react in solar region PS photooxidation is consistent with recent ESCA studies in this field (102,103).

The large changes in PS and PSD_3 molecular weight indicate that main chain reactions do take place. Therefore, the GPC data was analyzed to learn if there might be a correlation between molecular weight changes and the infrared carbonyl absorption. These results are described later in this chapter.

PS/Anthracene

Anthracene absorbs UV strongly in the solar region. It has been proposed that the excited state anthracene is quenched by oxygen, and the resulting singlet oxygen

attacks the PS (104). As seen in Figure 5.6, the initially strong absorption bands of anthracene are lost by exposure to solar region UV and oxygen. Because of its low volatility, this suggests that the anthracene has been consumed during the photooxidation process. As with acetophenone, however, molecular weight changes in the PS show that PS photooxidation had been initiated by the anthracene, and this is consistent with results reported for PS/anthracene in solution (104).

Figure 5.8 shows the carbonyl region of the photooxidized PS/anthracene film. This absorption band contains a number of peaks not normally seen in photooxidized PS. These peaks can be assigned to the various quinones and hydroxyquinones that are produced when anthracene is photooxidized (105,106,107). This shows that anthracene is consumed as it initiates PS photooxidation and does not serve only to form singlet oxygen. This further indicates that anthracene would not serve as a suitable photosensitizer in the PSD_3 experiment since protium from the anthracene would likely be found in the reaction products. However, quinones are thought to initiate PS photooxidation by a singlet oxygen mechanism, since they only degrade PS when oxygen is present (99). This suggests that singlet oxygen may play an important role in PS photooxidation when anthracene is present.

Chain Scission

Suitable equations have been reported that can describe the extent of crosslinking and chain scission from GPC data (108). The integrated intensity of the entire infrared carbonyl band was used to calculate the number of carbonyl groups per cm^2 of film, based on the absorptivity of acetone. As with other carbonyl peaks (e.g. Fig. 2.4A), the carbonyl band was assumed to pass smoothly through the "negative" peak at 1690cm^{-1}, where acetophenone had been lost.

The ratio of carbonyl groups to chain scissions/cm^2 film was 4.1 for PS/acetophenone, 0.37 for PSD_3/D_3-acetophenone and 24 for PS/anthracene. No obvious correlation is established by these experiments and yet this is not surprising, as discussed below.

As seen in Figure 5.4, negative peaks appear at 1690, 1380 and 1260cm^{-1} and these are caused by the loss of acetophenone. Whether it is caused by chemical reaction, evaporation or both, this loss of acetophenone is a complicating factor for all films containing this compound. Acetophenone absorption bands overlap PS bands and also contribute to the carbonyl band. The loss of acetophenone, therefore, changes both the background peak intensities and the carbonyl band shape. This introduces a large experimental uncertainty into these calculations.

Anthracene possesses a low vapor pressure and infrared absorption bands that do not extensively overlap the carbonyl region. As a result, changes in carbonyl absorption can be more accurately determined. Unfortunately, the anthraquinone products that form during anthracene photooxidation contribute to the total carbonyl absorption. Nevertheless, the high value obtained for carbonyl groups to chain scissions is expected since carbonyl groups can form from the reacted phenyl ring. Clearly a low concentration of a non-volatile photosensitizer is needed to best compare carbonyl formation and chain scission.

Conclusions

Pure PS does not absorb solar region UV. However, the use of acetophenone and anthracene as photoinitiators has allowed solar region PS photooxidation to be studied. In the case of acetophenone, infrared spectra of the hydroperoxide and carbonyl products formed, and their response to ammonia vapor, qualitatively resemble those obtained from pure PS photooxidized with 254nm UV. In the present case, however, the UV light is diffusely absorbed, so that these products are distributed uniformly through the PS film.

The occurrence of reactions involving the phenyl ring in solar region UV photooxidation has been demonstrated using chain-deuterated PS with trideuteroacetophenone. These experiments showed that the hydroperoxides detected in the infrared spectrum contained hydrogen atoms that came from the phenyl ring rather than the main chain. Molecular weight changes were also observed, indicating that main chain reactions also take place. Losses of acetophenone and deuteroacetophenone during photooxidation, however, prevented making a meaningful comparison between the carbonyl band intensity and the number of chain scissions observed in these two experiments.

Anthracene was photooxidized to anthraquinones while it initiated PS photooxidation. Since excited state anthracene, quinones and aromatic ketones (e.g. acetophenone) are quenched by oxygen to form singlet oxygen, the present results are consistent with published mechanisms describing the direct singlet oxygen attack of the phenyl ring. Other reactions are also possible and, indeed, some must also occur to account for the molecular weight changes that were observed.

C H A P T E R VI

SUMMARY AND FUTURE WORK

The Introduction mentioned that PS photooxidation represents a complex assortment of photophysical and photochemical processes. The reactions that take place during photooxidation quickly change in character from those of the PS repeat unit to those involving the products of photooxidation reactions. In order to guide mechanistic studies, it is first necessary to identify the various reaction products that form. Therefore, the work undertaken in the present study has focused on characterizing the products of PS photooxidation.

The first formed products detected with infrared spectroscopy during PS photooxidation with 254nm UV were free hydroperoxides and carbonyl products. Continued exposure quickly produced H-bonded hydroperoxides and more of the carbonyl products. The hydroperoxides were identified by their appropriate IR absorption frequencies and the decrease in absorption intensity upon exposure to reactive vapors. These vapor reagents were ammonia, methyl amine, pyridine and HI/HCl vapors. In addition, heating a photooxidized film in an inert atmosphere decreased the peak intensities, confirming their assignment to hydroperoxides.

The carbonyl products formed were found to include simple ketones such as acetophenone-type end groups and carboxylic acids. Additionally, a volatile compound and an unknown structure were found to be major contributors to the carbonyl absorption band, and both were found to react irreversibly with ammonia vapor. Minor components were also detected by their reaction with methyl amine, although their structure is not certain. Eventually, though, the OH stretch and carbonyl infrared bands of the carboxylic acids became very strong, indicating their prominence in highly photooxidized PS.

In order to learn if the phenyl ring in the PS repeat unit reacts during photooxidation, chain deuterated PS was used in a model compound study. Photooxidizing chain deuterated PS produced hydroperoxides and carboxlic acids containing protium rather than deuterium. This indicated that the phenyl ring reacts extensively during photooxidation. Additional evidences include the marked drop in the infrared aromatic-to-aliphatic C-H stretch ratio observed on PS photooxidation and the drop in aromatic C-H to aliphatic C-D ratio in chain deuterated PS. These results show that reaction mechanisms that propose phenyl ring reactions should be given further consideration.

The photooxidation products were located within the

top few micrometers of the film surface. Using ATR it was found that these products are distributed along a concentration profile resembling the UV absorption profile. At large UV dosages, this highly oxidized surface region forms a photostable protective layer so that the reaction becomes autoinhibiting. This conclusion was reached on the basis of infrared and oxygen uptake data which showed autoinhibition after about $5x10^{-4}E/cm^2$. At this point, the surface region contains a high proportion of carboxylic acids which must dissipate the UV energy photophysically.

In order to learn if the observations made using 254nm UV could be extended to solar region photooxidation, PS films containing sensitizers were photooxidized using a broadband UV source having an output of 300 to 400nm. Photooxidation initiated with acetophenone led to the production of free and H-bonded hydroperoxides and a carbonyl band that resembled the one formed with pure PS and 254nm UV. These results, however, could not be readily quantified because acetophenone was lost during photooxidation and this influenced the shape and intensity of the observed carbonyl band. As with 254nm UV exposure, phenyl ring reactions in solar region photooxidation were found to be important by the use of chain deuterated PS plus trideuteroacetophenone.

The presence of 0.03 molar anthracene initiated PS

photooxidation and led to the rapid photooxidation of the anthracene to anthraquinones. These anthraquinones gave the PS film a yellow color. This result serves to underscore the importance of low levels of photoactive impurities and the need to test polymers in the presence of such common pollutants as may be found in the end-use environment. It should also be mentioned that all films exposed to solar region UV remained completely soluble in tetrahydrofuran. This stands in marked contrast to 254nm UV, which produced an insoluble product. This difference in solubillity, however, may have been due to the diffusely-absorbed solar region UV producing fewer crosslinks per chain, i.e. the reaction had not proceeded as far with the solar region UV. It is evident, then, that UV wavelength can determine which chemical processes dominate, so that this aspect of exposure environment is also critical in testing polymers.

Several questions have been raised by the observations described in the present study and they suggest possible future work. The most surprising result is that the phenyl ring reacts extensively using either 254nm UV or wavelengths longer than 300nm. The lack of any detectable deuterated hydroperoxides in chain deuterated PS indicates that they are never present in large quantities, perhaps due to their decomposition and loss as heavy water. It would therefore be of interest to learn the fate of

hydroxyl radicals in PS. Although originally done by Weir with PS and hydrogen peroxide, the photolysis of D_2O in PSD_3 with 313nm UV would be informative. Infrared spectroscopy of the PSD_3 and mass spectroscopy of the evolved water vapor would show what happens to the OD radicals.

Throughout the present work, reactive vapors were used to aid in correlating infrared absorption bands with chemical functional groups. While other reactive vapors may also give informative results, it should be possible to solvent extract the low MW carbonyl product ($1775cm^{-1}$) to clearly identify its structure. Perhaps mildly degrading solutions could also be used together with classical derivatizing solutions to isolate and identify fragments of the degraded chains.

Another area of interest is characterizing the protective layer formed on PS after high dosages of 254nm UV. This would likely require the use of a number of techniques, such as absorption and emission spectroscopies and perhaps pyrolysis-mass spectroscopy.

Somewhat ambiguous results were obtained (Appendix E) when a plasticizer was added to PS to test the influence of the glassy matrix on photodegradation. Nevertheless, the influence of the glassy matrix could be further investigated by the use of PS oligomers. Oligomers of PS

range from the liquid state of ethyl benzene, to viscous liquids of DP=6, to glassy solids of DP=10 at room temperature. A series of each of these materials could be photooxidized above or below their Tg. Thus, it may be possible to distinguish effects of the glassy matrix from those brought about by changes in environmental temperature. Difficulties with analyzing the insoluble photooxidized product would undoubtedly be reduced by this approach.

R E F E R E N C E S

1. K. Kato; J. Appl. Polym. Sci. 13 599 (1969).
2. G. Geuskens, et al.; Eur. Polym. J. 14 299 (1978).
3. N. Grassie and N.A. Weir; J. Appl. Polym. Sci. 9 975 (1965).
4. J. Lucki and B. Ranby; Polym. Deg. Stab. 1 1 (1979).
5. N. Grassie and N.A. Weir; J. Appl. Polym. Sci. 9 999 (1965).
6. R.B. Fox and T.R. Price; in: D.L. Allara and W.L. Hawkins, eds. Adv. Chem. Ser. 169, ACS, Wash. D.C. 1978 p. 103.
7. G. Geuskens and C. David; Pure Appl. Chem. 51 2385 (1979).
8. J. Lucki and B. Ranby; Polym. Deg. Stab. 1 165 (1979).
9. G. Geuskens et al.; Eur. Polym. J. 18 387 (1982).
10. G. Geuskens et al.; Eur. Polym. J. 14 291 (1978).
11. J. Lucki and B. Ranby; Polym. Deg. Stab. 1 251 (1979).
12. J.F. Rabek and B. Ranby; J. Polym. Sci.-Polym. Chem. Ed. 12 273 (1974).
13. B. Ranby and J.F. Rabek; Photodegradation, Photo-oxidation and Photostabilization of Polymers; John Wiley and Sons N.Y. (1975) p. 278.
14. T. Shiono, E. Niki and Y. Kamiya; Bull. Chem. Soc. Japan 51 3290 (1978).

15. J. Peeling and D.T. Clark; Polym. Deg. Stab. 3 97 (1980-81).

16. F. Sondheimer, D.A. Ben-Efraim and R. Wolovsky; J. Am. Chem. Soc. 83 1675 (1961).

17. G. Geuskens and C. David; in: G. Geuskens ed.; Degradation and Stabilization of Polymers; John Wiley and Sons N.Y. 1975 pp. 113-135.

18. G. Geuskens and Q. Lu-Vinh; Eur. Polym. J. 18 307 (1982).

19. G. Geuskens and C. David; Pure Appl. Chem. 51 233 (1979).

20. Y. Okamoto, et al.; Chem. Ind. (London) 2004-6 (1961).

21. K. Kato; J. Appl. Polym. Sci. 15 2115 (1971).

22. R.B. Fox; Pure Appl. Chem. 30 87 (1972).

23. R.F. Cozzens, W.B. Moniz and R.B. Fox; J. Chem. Phys. 48 581 (1968).

24. G.E.K. Branch and M. Calvin; The Theory of Organic Chemistry, An Advanced Course; Prentice-Hall, Inc.; N.Y. 1941 p. 161.

25. J. Peeling, M.S. Jazzar and D.T. Clark; J. Polym. Sci.-Polym. Chem. Ed. 20 1979 (1982).

26 L.A. Matheson and R.R. Boyer; Ind. Eng. Chem. 44 867 (1952).

27. N. Grassie and N.A. Weir; J. Appl. Polym. Sci. 9 987 (1965).

28. C.A. Brighton, G. Pritchard and G.A. Skinner; Styrene Polymers: Technology and Environmental Aspects; Applied Science Publishers, Ltd. London 1979 p. 146.

29. M.J. Reiney, M. Tryon and B.G. Achhammer; J. Res. Nat. Bureau Std. 51 155 (1953).

30. G. Geuskens, P. Bastin, Q. Lu-Vinh and M. Rens; Polym. Deg. Stab. 3 295 (1980-81).

31. G.A. George and D.K.C. Hodgeman; J. Polym. Sci. Pt. C. 55 195 (1976).

32. G.A. George; J. Appl. Polym. Sci. 18 419 (1974).

33. W. Klopffer; Eur. Polym. J. 11 203 (1975).

34. R.W. Lenz; Organic Chemistry of Synthetic High Polymers; Interscience Publishers, N.Y. 1967 p. 720.

35. J.B. Lawrence and N.A. Weir; J. Polym. Sci.-Polym. Chem. Ed. 11 105 (1973).

36. R.C. Hirt, N.Z. Searle and R.G. Schmitt; SPE Trans. 1 21 (1961).

37. G.G. Cameron and I.T. McWalter; Eur. Polym. J. 18 1029 (1982).

38. G.A. George and D.K.C. Hodgeman; Eur. Polym. J. 13 63 (1977).

39. J.R. MacCallum and D.A. Ramsey; Eur. Polym. J. 13 945 (1977).

40. J.G. Calvert and J.N. Pitts; Photochemistry; John Wiley and Sons; N.Y. 1966 p. 247.

41. N. Yamamoto, S. Akaishi and H. Tsubomura; Chem. Phys. Lett. 15 458 (1972).

42. W. Schnabel and J. Kiwi; "Photodegradation" in: Aspects of Degradation and Stabilization of Polymers, H.H.G. Jellinek ed. Elsevier Scientific Pub. Co. N.Y. 1978.

43. P.J. Burchill and G.A. George; J. Polym. Sci.-Polym. Lett. Ed. 12 497 (1974).

44. J. Kubica and B. Waligora; Eur. Polym. J. 13 325 (1977).

45. L.A. Wall, M.R. Harvey and M. Tryon; J. Phys. Chem. 60 1306 (1956).

46. G. Zaitoun; Chem. Abs. 57 3626i.

47. B.G. Achhammer, M.J. Reiney and F.W. Reinhart; J. Res. Nat. Bur. Std. 47 116 (1951).

48. M. Tryon and L.A. Wall; J. Phys. Chem. 62 697 (1958).

49. N.A. Weir; Eur. Polym. J. 14 9 (1978).

50. R.B. Fox, T.R. Price and D.S. Cain; in: Adv. Chem. Ser. 87 ACS, Wash. D.C. 1968.

51. B.G. Achhammer, M.J. Rieney, L.A. Wall and F.W. Reinhart; J. Polym. Sci. 8 555 (1952).

52. C. David et al.; Eur. Polym. J. 14 501 (1978).

53. H.C. Beachell and L.H. Smiley; J. Polym. Sci. A-1 5 1635 (1967).

54. L.A. Matheson and J.L. Saunderson; in: Styrene: Its Polymers Copolymers and Derivatives, R.H. Boundy and

R.F. Boyer eds., ACS Monograph Series, Part II, Reinhold Pub. Co. 1952, p. 532.

55. K.E. Wilzbach, J.S. Ritscher and L. Kaplan; J. Am. Chem. Soc. 89 1031 (1967).

56. B. Wandelt, J. Brzezinski and M. Kryszewski; Eur. Polym. J. 16 583 (1980).

57. H. Kambe; in: Aspects of Degradation and Stabilization of Polymers; H.H.G. Jellinek, ed.; Elsevier, N.Y. 1978.

58. N.Grassie and N.A. Weir; J. Appl. Polym. Sci. 9 963 (1965).

59. S.A. Curran; PhD Thesis; Dept. of Chemistry, Univ. of Massachusetts, Amherst, Mass. 1981.

60. M. Ito and R.S. Porter, J. Appl. Polym. Sci. 27 4471 (1982).

61. C.G. Hatchard and C.A. Parker, Proc. Royal Soc. A 235 518 (1956).

62. N.J. Harrick, Internal Reflection Spectroscopy, Interscience, N.Y., (1967).

63. F.M. Mirabella, J. Polym. Sci.-Polym. Phys. Ed. 21 2403 (1983).

64. H.G. Tomkins, Appl. Spectros. 28 335 (1974).

65. D.J. Carlsson and D.M. Wiles, Macromolecules 4 174 (1971).

66. L.H. Cross and A.C. Rolfe, Trans. Faraday Soc. 47 354 (1951).

67. R.M. Silverstein et al., Spectrometric Identification of Organic Compounds, John Wiley and Sons, N.Y., 1974.

68. L.J. Bellamy, The Infrared Spectra of Complex Molecules, John Wiley and Sons, N.Y., 1958.

69. A.G. Davies, Organic Peroxides, Butterworths, London, (1961).

70. J.C. Masson, in Polymer Handbook 2nd Ed., J. Brandrup and E.H. Immergut (eds.), John Wiley and Sons, N.Y. (1975).

71. D. Dolphin and A. Wick, Tabulation of Infrared Spectral Data, Wiley-Interscience, N.Y. (1977).

72. D.T. Clark and H.S. Munro; Polym. Deg. Stab. 8 213 (1984).

73. D.K. Banerjee and C.C. Budke, Anal. Chem. 36 792 (1964).

74. J.C.W. Chien, in: Degradation and Stabilization of Polymers, G. Geuskens (ed.), John Wiley and Sons, N.Y., 1975.

75. H.R. Williams and H.S. Mosher, Anal. Chem. 27 517 (1954).

76. Perkin-Elmer Corporation, "Instructions: Models MPF-43 and MPF-44 Fluorescence Spectrophotometers", Norwalk, Conn. 1975.

77. N. Kornblum and H.E. DeLaMare, J. Am. Chem. Soc. 73 880 (1951).

78. C.W. Capp and E.G.E. Hawkins, J. Chem. Soc. 4106 (1953).

79. A.V. Tobolsky and R.B. Mesrobian, Organic Peroxides, Interscience, N.Y. (1954).

80. D. Swern, in: Organic Peroxides Vol. 1, D. Swern (ed.), Wiley-Interscience, N.Y. (1970).

81. O.L. Mageli and C.S. Sheppard, in: Organic Peroxides Vol. 1, D. Swern (ed.), Wiley-Interscience, N.Y. (1970).

82. N.A. Weir, in: Developments in Polymer Degradation-4, N. Grassie (ed.), Applied Science Publ. London (1982).

83. R.M. Johnson and I.W. Siddiqi, The Determination of Organic Peroxides, Pergamon Press, N.Y. (1966).

84. J. Mitchell and L.R. Perkins, in: Weatherability of Plastic Materials, Appl. Polym. Symp. 4, M.R. Kamal (ed.), John Wiley and Sons, N.Y. (1967).

85. C.A. Parker, Proc. Royal Soc., A 220 104 (1953).

86. G.D. Cooper and B.A. DeGraff, J. Phys. Chem. 75 2897 (1971).

87. L.J. Heidt and H.B. Boyles, J. Am. Chem. Soc. 73 5728 (1951).

88. J.D. Holdsworth, G. Scott and D. Williams, J. Chem. Soc. 4692 (1964).

89. J.Kowal, M. Nowakowska and B. Waligora; Polymer 19 1313 (1978).

90. R.B. Fox, L.G. Isaacs, F.E. Saalfeld and M.V. McDowell; NRL Report 6284, U.S. Naval Research Laboratory, Wash. D.C. 1965.

91. R.B. Seymour and H.S. Tsang; Texas J. Sci. 23 (2) 187 (1971).

92. G.G. Guilbault; Practical Fluorescence, Marcel Decker, N.Y. 1973.

93. J.H. Espenson; Chemical Kinetics and Reaction Mechanisms, McGraw-Hill, N.Y. 1981.

94. N.A. Weir, J.K. Lee and J. Arct; Polym. Deg. Stab. 14 249 (1986).

95. L. Merlander and W.H. Saunders; Reaction Rates of Isotopic Molecules, John Wiley and Sons, N.Y. 1980.

96. O. Bain and P.A. Giguere; Can. J. Chem. 33 527 (1955).

97. J.K. Sears and J.R. Darby, The Technology of Plasticizers, John Wiley and Sons, N.Y. 1982, p. 50.

98. A. Torikai, et al., Polym. Deg. Stab. 14 367 (1986).

99. J.F. Rabek and B. Ranby, J. Polym. Sci.-Polym. Chem. Ed. 12 295 (1974).

100. W.C. Schumb, C.N. Satterfield and R.L. Wentworth, Hydrogen Peroxide, Amer. Chem. Soc. Monograph Ser., Reinhold Pub. Co. NY 1955 p. 411.

101. J.R. MacCallum, in: Developments in Polymer Degradation-1, N. Grassie (ed.) Applied Science Pub., London 1977.

102. D.T. Clark and H.S. Munro, Polym. Deg. Stab. 9 63 (1984).

103. H.S. Munro, D.T. Clark and J. Peeling, Polym. Deg. Stab. 9 185 (1984).

104. G. Ramme and J.F. Rabek, Eur. Polym. J. 13 855 (1977).

105. G.W. Cowell and J.N. Pitts, J. Am. Chem. Soc. 90 1106 (1968).

106. E. Voyatzakis, et al., Anal. Lett. 5 (7) 445 (1972).

107. Sadtler Research Laboratories, Inc., Phila. PA (1973) Standard Grating Spectra 635K, 279K, 18454K, 29706K.

108. C. David and D. Baeyens-Volant, Eur. Polym. J. 14 29 (1978).

A P P E N D I X A

UV ABSORPTIVITY OF POLYSTYRENE

The absorptivity of PS at 254nm was determined using four PS films of different thicknesses. Absorbance measurements at 254nm were made using a Beckman ACTA MVI UV/Vis spectrophotometer set at 254nm with a 2nm slit width. Film thicknesses were determined interferometrically from infrared spectra according to the following equation:

$$b(cm) = \frac{N}{2n\,(\nu_1 - \nu_2)}$$

where N = number of interference fringes between ν_1 and ν_2

n = 1.59, the PS refractive index

ν_1, ν_2 = frequency in wavenumbers

Results are given in Table A.1.
Applying Beer's Law to the data in Table A.1, we obtain:

$$A = (ac)b = 0.223b \qquad b=\text{micrometers},\ \mu m$$

Table A.1

UV Absorbance vs. Film Thickness

Film Thickness, μm	Absorbance
3.3	Ø.632
6.Ø	1.28Ø
8.7	1.5Ø1
12.1	2.697

A P P E N D I X B

UV LAMP INTENSITY

The intensity of the low pressure mercury arc source used in the present study was determined using a chemical (potassium ferrioxalate) actinometer. This method provides a description of the lamp output in Einsteins per cm^2 hour, where one Einstein equals one mole of photons. Details of the use of this actinometer are available in the literature (61,85,86).

The output of the low pressure mercury arc lamp was determined with a 10nm bandpass filter fitted in front of the lamp to isolate the 254nm line at 30°, 45°, 60° and 75°C. These results are shown in Table B.1. It is seen that the output of the lamp is affected by its temperature during use, increasing to 45°C and then decreasing at 60°C and again at 75°C. This trend is typical of low pressure mercury arcs (87), although as seen here, it causes only a small variation in intensity. This, however, must be included as a correction factor in determining the photon dosage delivered to the film at a given temperature.

Table B.1

UV Intensity vs. Temperature

Temperature, ^{o}C	Output, $E/cm^2 \cdot hr$	Relative Output
30	1.95×10^{-6}	1
45	2.36×10^{-6}	1.21
60	1.95×10^{-6}	1
75	1.44×10^{-6}	0.74

The output of the low pressure mercury arc lamp was also determined with a quartz plate substituted for the 10nm bandpass filter. The intensity was found to equal $1.25 \times 10^{-5} E/cm^2 \cdot hr$.

A P P E N D I X C

INFRARED ABSORPTIVITIES

Infrared integrated intensity absorptivities were determined for one PS band, for methanol OH and OD stretch bands and for the carbonyl band of acetone. A Beer's Law analysis was performed for PS using five films of differing thickness; film thickness was determined interferometrically. Absorptivities for OH, OD and carbonyl groups were determined in chloroform solution using a liquid cell of 11 m path length. Integrated absorbance intensities are expressed in terms of units of absorbance times frequency ($A \cdot cm^{-1}$). PS molar absorptivities are based on a 10.1 molar repeat unit concentration.

Table C.1

PS Absorbance at 1950cm^{-1}

Path Length, μm	Integrated Intensity, $A \cdot cm^{-1}$
5.5	0.882
8.7	1.29
12.4	1.40
17.6	----
24.9	2.12

This gives an integrated intensity absorptivity of 59.4 $Acm^{-1}/cm \cdot molar$.

Table C.2

Acetone Carbonyl Absorbance

11 μm path length; chloroform solution

Concentration, molar	Integrated Intensity, $A \cdot cm^{-1}$
Ø.169	2.ØØ
Ø.338	4.7Ø
Ø.676	8.79
1.35	19.3
2.71	38.6

This gives an integrated intensity absorbtivity for the carbonyl band of $1.31x1Ø^4$ A $cm^{-1}/cm \cdot molar$.

Table C.3

Methanol OH Stretch Absorptivity

11 μm path length, chloroform solution

Concentration, molar	Integrated Intensity*, Acm^{-1}	
	Free & H-bonded	H-bonded
Ø.617	13.6	11.2
1.23	27.Ø	24.5
2.47	63.6	61.2
4.94	183.Ø	181.Ø
Absorptivity, A $cm^{-1}/cm \cdot molar$	36,4ØØ	36,4ØØ

* The OH stretch band is composed of a sharp, "free" OH band and a broad, H-bonded band. Including the free OH band does not change the absorptivity within experimental error.

Table C.4

Deuteromethanol* OD Stretch Absorptivity

12 μm path length, chloroform solution

Concentration, molar	Integrated Intensity, Acm^{-1}	
	Free & D-bonded	D-bonded
Ø.615	4.64	4.1Ø
1.23	12.7	11.7
2.46	3Ø.4	29.3
4.92	72.4	71.4
Absorptivity, Acm^{-1}/cm-molar	13,2ØØ	13,1ØØ

* Sigma Methyl Alcohol-d (99.5% atom percent D).

A P P E N D I X D

IODOMETRY

The iodometric method used to analyze photooxidized PS for total peroxide content was the spectrophotometric procedure of Banerjee and Budke (73). This procedure determines the total I_2 liberated when the peroxide reacts with an excess potassium iodide.

$$ROOR + 3I^- + 2H^+ \longrightarrow I_3 + ROH + ROH + 2H_2O$$

A calibration curve was prepared by dissolving Ø.1150g I_2 in a mixture of 2:1 (vol.) acetic acid/chloroform, diluting to 100ml and preparing standard solutions. These standards contained Ø, 1, 2, 3, 4, 5ml aliquots of this iodine stock solution in 25ml of acetic acid/chloroform solution. Absorbance was recorded at 470nm, Ø.5nm slit width. The results are given in Table D.1. The molar absorptivity equals 843 A·l/cm·mole. A value of 845 is reported by Banerjee and Budke.

Table D.1

Iodine Calibration Curve

Solution, meq/25ml	Absorbance
Ø.Ø	Ø.Ø41
Ø.ØØ453	Ø.192
Ø.ØØ9Ø6	Ø.327
Ø.Ø1358	Ø.5Ø2
Ø.Ø1811	Ø.653
Ø.Ø2264	Ø.798

A P P E N D I X E

PLASTICIZED POLYSTYRENE

As mentioned in Chapter I, the rigidity of the glassy PS matrix is thought to influence the course of photooxidation reactions (19) and the formation of in-chain peresters was explained in these terms (10). As the temperature approaches Tg, free volume increases as do local molecular motions and this may affect the likelyhood of a given reaction taking place. Another method of influencing molecular mobility is to add a plasticizer to the film. This was done using phenyl ether as the plasticizer and the results are described in this appendix.

Four PS films were cast from chloroform solution, three of which contained phenyl ether. After drying, these films were analyzed using UV photometry to determine their phenyl ether content and also by DSC to measure Tg. These results are given in Table E.1, and are consistent with reported values for plasticized PS (97). These films were photooxidized using 254nm UV at 70°C for 11 hours ($\sim 1.4 \times 10^{-4}$ E/cm^2). After this exposure, IR spectra were recorded. The UV absorbance values were measured at 300nm (0.5nm slit width) and are given in Table E.2.

Table E.1

Properties of Plasticized Films

Film	Wt.% Phenyl Ether	Tg, °C*
Pure PS	Ø.Ø	1Ø4
A	1.Ø	91
B	2.4	82
C	3.2	79

* Second scan, 2Ø°/min.

Table E.2

UV Absorbance at 3ØØnm

Film	Absorbance
Pure PS	Ø.54
A	Ø.5Ø
B	Ø.48
C	Ø.48

These data show that as the plasticizer content increased, the extent of photodegradation decreased. The shape of the resulting IR carbonyl absorption band was also affected by the presence of plasticizer. This is shown in Figure E.1 where it is also seen that the carbonyl absorption band is smaller for the plasticized film C than for pure PS.

These results are surprising in light of the increase

Figure E.1

Photooxidized PS/Phenyl Ether. Difference spectrum A represents the carbonyl band obtained with pure PS after photooxidation (photooxidized PS minus pure PS spectrum). Difference spectrum B shows the smaller carbonyl band obtained when phenyl ether was present at 3.2wt% (photooxidized PS/phenyl ether minus pure PS/phenyl ether).

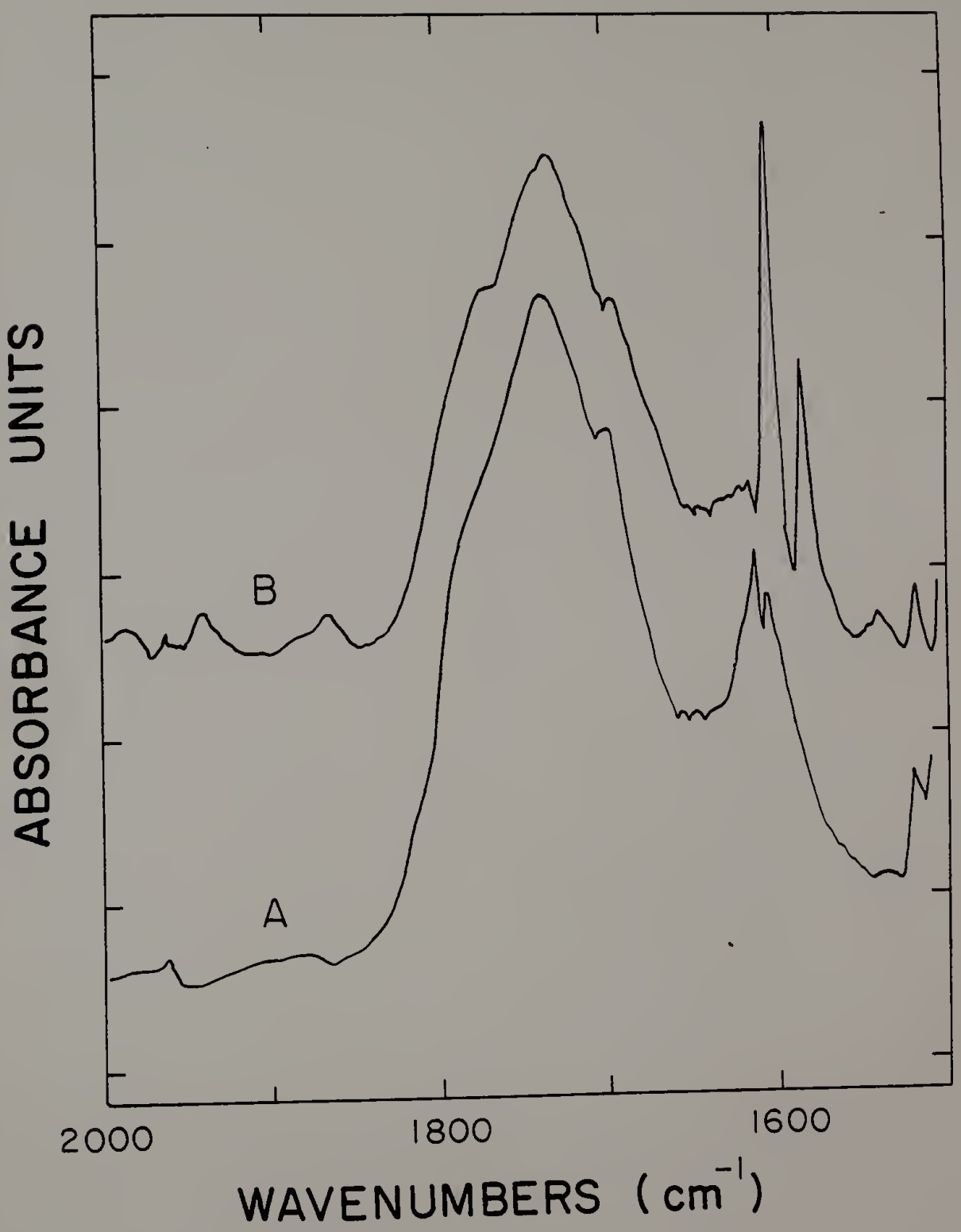
ABSORBANCE UNITS
B
A
2000
1800
1600
WAVENUMBERS (cm⁻¹)

in photooxidation rate with temperature described in Chapter II. An increase in photooxidation rate was also reported as exposure temperature approached Tg, as well as a change in the reaction product composition (98). Seemingly this increase in reaction rate is not due to increased free volume with increased temperature, or else the plasticizer would have a similar effect. Thus, the phenyl ether could be affecting the reaction in some way other than by simply increasing free volume in the film.

An examination of the UV absorption spectrum of phenyl ether may provide an explanation for the stabilizing influence of this plasticizer. Phenyl ether possesses two strong absorption maxima, which are found at 248 and 280nm, and a minimum at 254nm. This means that the phenyl ether will absorb very little of the incoming 254nm UV; 4% or less in the present case. But it also means that phenyl ether possesses a low energy excited state (the 280nm band) compared to the PS absorption band. This may provide an energy transfer mechanism, so that phenyl ether quenches the excited PS phenyl rings and photophysically dissipates the energy.

As described in Chapter II, higher temperatures during photooxidation lead to a greater proportion of the product absorbing at 1775cm^{-1}. Similar results are obtained in the present case where the plasticizer is present, increasing

the free volume in the PS film. This serves as further evidence opposing the idea that this band is caused by in-chain peresters that form because of the rigidity of the PS matrix. It is also possible, though, that the phenyl ether reacts and its degradation products contribute to the observed infrared spectrum. This possibility suggests, then, that a better approach to studying the effects of the glassy matrix might be to use very low molecular weight polystyrenes. This would allow Tg to be lowered to room temperature without significantly changing the chemistry of the polymer.